Republic of Iraq
Ministry of Higher Education
and Scientific Research
University of Babylon
College of Materials Engineering
Department of Polymer Engineering and Petrochemical Industries

Investigation of Tribological and Rehological Properties of a Self-Lubricant Polymeric Composite

A Thesis

Submitted to the Council of the College of Materials Engineering, University of Babylon in Partial Fulfillment of the Requirements for the Master Degree in Materials Engineering\ Polymer

By

Enas Talib Sahib Ouda

(B. Sc. in Materials Engineering\Polymer, 2017)

Supervised By

Assist. Prof. Ammar Emad Al-kawaz (Ph.D.)

2021 A.M 1442 A.H


بسم الله الرحمن الرحيم
الله لا إله إلا هو الحي القيوم لا تأخذه
سنة ولا نوم له ما في السموات وما في الأرض
من ذا الذي يشفع عنده إلا بإذنه يعلم
ما بين أيديهم وما خلفهم ولا يحيطون
بشيء من علمه إلا بما شاء وسع كرسيه السموات
والأرض ولا يؤوده حفظهما وهو العلي العظيم

Dedication

To the one raining me with his blessings .To the one who I rely upon in my life. .....To GOD

To our great prophet Mohammad and his relatives

(peace and blessings of Allah be upon him and them)

To whom without them, every step in my life will seem meaningless.
To whom I had no will in choosing them, but if I had I will chose no other than them.

.....To the soul of my mom and dad

To my redemption, who have bewitched me body and soul, I never wish to be parted form you. Step by step we'll be walking during every journey of our lifetime

.....To my husband

For those who are our livers. I will continue to give you the strength to dispel the obstacles of eternity for a better world

....To my children

To the troublemakers, I hope to become someone you all look up to and set an example

.....my brothers and sisters

Acknowledgments

First of all, I would like to express my utmost thanks to our almighty God ***Allah*** *whom blessed me with this opportunity, encompasses us with his mercy and gave us more than we asked for .*

I would like to thank the ***Dean*** *collage of material engineering and the* ***Head*** *department of polymer engineering and petrochemicals industries, the* ***staff*** *of polymer engineering department and collage for their support and help and for offering this chance to get this degree.*

I would like to express my sincere gratitude for my supervisors, ***Dr. Ammar Emad*** *for his incredible support, gaudiness, dedication and patience throughout this year.*

I would like to express my deepest gratitude for my ***Friends*** *who've been good company throughout these years.*

I would like to thank my ***family*** *whom showed great support and patience throughout the years endured everything to make me the person who I am today and I hope I can payback even if small part if it one day.*

Researcher

Enas Talib al-Zubaidy

Abstract:

In order to provide a long lubricating life span, it must be ensured that the solid polymer or polymer compound provides self-lubrication and at the same time, it must provide adequate interface contact pressure, which is the most important factor with self-lubricating compounds so that the polymeric compound is able to support the dynamic stresses of the applied load and pressures .

In this study, a poly methyl methacrylate (PMMA) self-lubricating compound was synthesized with solid lubricants and multi-walled carbon Nano tube and selected as the self-lubricating approach. Calcium stearate, polyethylene wax and beeswax were selected as solid lubricants that have the ability to migrate to the surface of the polymer during its service life. Using in situ polymerization of free radicals with the following parameters: PMMA (100% MMA + 0.9 wt% BPO) / solid lubricant (0.05 , 0.1 , 0.2 , 0.5 wt.%), PMMA / MWCNT (0.05 ,0.1 ,0.2 , 0.5 wt.% Via sonication) , hybrid compound ((50 % PMMA : 50 % Beeswax) (0.05 , 0.1 , 0.2 , 0.5 wt.%) + PMMA).

Fourier transform infrared (FTIR) was used to verify the identity of solid lubricants after in situ polymerization of free radicals and multiwalled carbon nanoparticles. On the tribological behavior of the surface of polymers reinforced with solid lubricants and nano-fills after wear test, using optical microscopy (OM) the flow is verified using a capillary pressure gauge (SR20) and a contact angle test was conducted to verify the effectiveness of solid lubricants and nano-fills in increasing the susceptibility of the polymer Hydrophobic.

The PMMA sheets produced are characterized by relatively round shapes, with an average diameter of 15 cm and a thickness of about 2 mm. The results of the tests for both friction and abrasion proved a higher efficiency up to (9.4 %) and a friction coefficient (0.8 %) for the sample filled with Beeswax much more than the

rest of the solid lubricants, which confirms the transfer of particles to the surface and reduces the amount of interfacial shear stress during dry friction, and by increasing Over time and loads applied at a constant speed, friction negatively affects the overall wear rates and impairs the internal structure and thus the mechanical properties. The self-lubrication system works successfully and this is confirmed by the scratch test results of the samples that showed the deformation behavior of pure polymer plastic and elastic deformation of the polymer filled with beeswax and the results were consistent with the results of friction and wearing. This was evident from the residual effect after scratching, which is characterized by a very smooth area in the contact area with little contact stress and surface scratch flexibility and plays an important role in reducing the interfacial shear stress up to (0.8 %). Flow resulted in PMMA / solid lubricant by weight %capillary rheometer and PMMA / reinforcing fillers wt.% showed that shear viscosity decreases with increasing shear rate and shear stress increases with increasing shear rate. Increasing the shear stress cuts the polymeric chain and reduces the viscosity with an increase in temperature, the migration to the surface increases, which helped to postpone the extrusion process and reduce the amount of the total melting fracture. Shear stress plays an important role in indicating surface quality , it is clear that the determination of the critical region is necessary to be able to change the surface quality and its relationship to pressure, shear stress and shear rate.

Table of contents

Abbreviations

Abbreviation	Definition
2D-LINS	**Two-dimensional inorganic nanomaterials**
AFM	**Atomic force microscope**
ASTM	**American Society for Testing and Materials**
CNT	**Carbon Nano-tube**
COF	**Coefficient of friction**
Cp	**Specific heat Capacity**
DSC	**Differential scanning calorimetry**
DPH	**Diamond Pyramid hardness**
FTIR	**Fourier-transform infrared spectrometer**
HV	**Vickers hardness**
IFRP	**In-Situ Free Radical Polymerizaton**
KBr	**Potassium bromide**
MMA	**Methyl methacrylate**

MWCNT	**Multi-wall Nanotube**
OM	**Optical microscope**
PBO	**Benzoyl Peroxide**
PH	**Potential of hydrogen**
PCs	**Polymeric composites**
PEEK	**Polyether ether ketone**
PTFE	**Poly tetrafluoroethylene**

List of Symbols

Symbol	Description	Unit
$\dot{\gamma}_{app}$	Apparent shear rate	s^{-1}
$\tau_{app.}$	Apparent Shear Stress	MPa
$\eta_{app.}$	Apparent shear viscosity	Pa*s
σ_b	Bending Stress	MPa
Tc	Crystalline temperature	c°
E	Elastic Modulus	Gpa
Tg	Glass transition temperature	c°
ΔP	Pressure Difference	N/m^2
Rpm	Rounds per minute	mm/min

τ	Shear stress	MPa
τ_w	Shear stress at the wall	MPa
$\dot{\gamma}_w$	Shear rate at the wall	s^{-1}
Tm	Melting temperature	c°
Q	Volume flow Rate	m^3/s
σ_w	Wall shear stress	MPa

List of Figures

List of Tables

CHAPTER ONE

Introduction

1 . 1 Introduction

The concept of self-lubricating polymer-based composites has occupied increasing interest in recent times due to their excellent wear parameters and excellent self-lubricating properties. However, with all the radical developments witnessed by modern science technology, the obstacles represented by high coefficients of friction and wear for high-performance tribological applications remain. It is worth noting, there are widespread methods in the past, which can reduce friction and wear to approximate limits, leaving unimaginable consequences, including the widespread use of lubricant fluids such as oil to achieve an inter-separation of sliding surfaces with a film of low shear strength. to filters, pumping and cooling systems; (I) environmental damage due to frequent cleaning operations to dispose of used lubricating oils (II) due to leakage and emission of gases or particles; (III) Contamination in products, such as foods and textiles, during the manufacturing process [1]. Self-lubricating materials have witnessed a wide development, especially in the period 2018-2019, and it covered multiple aspects including: superlubrication, lubrication theory, new lubricating fluids and additives, modern hard coatings, and precise measurement techniques. Recent studies have reported that the surface science known as tribology has moved To a broad newly developed field, for example, super lubrication, bio lubrication, and molecular lubrication. Green lubrication, lubricants with low viscosity, and lubricants for harsh environments (high temperatures, ultra-low temperatures, vacuum, high pressure, etc.), have been of interest to researchers over the past few years [2]. The work of lubricants in contemporary technology, such as the optical and thermal control surfaces used in spaceships, is fraught with obstacles as the oils of the external system tend to migrate and volatilize as well as condensate in these extreme conditions. This applies to aircraft engines, where external lubricating oil evaporates, oxidizes and

degrades when average temperatures increase and negatively affects the cost and efficiency of the mechanical system as a whole. In the late 1970s, reviews of crude oils and lubricants were restricted, and research and studies confirm the feasibility of oils themselves not very effective for aiding in advanced tribological applications. Then there was a trend towards hard lubricants such as boric acid (H_3BO_3) and hexboron nitride (hBN)[3]. Lubrication has a pioneering role in developing energy efficiencyLubrication has a leading role in the development of energy efficiency. In addition, lubrication engineering improves machine operation and reduces unwanted noise and sounds from moving contact sites. Therefore, lubrication engineering continues the process diligently in the background to support, install and highlight civilized technology. Followers of applied sciences communicate the importance of lubrication engineering but may not take it seriously, as a subject of extensive discussion and field research, and this is due to the fact that lubrication is an advanced technology and not an objective of applied science, and the correct methods must be followed in the application of basic sciences that lead to success New Research and Development Methods Because lubricants are produced from a range of different materials, the understanding of lubricant chemistry properties appears to be an understatement, lubricant chemical parameters are provided without exact details and descriptions, due to the complexities of routine procedures and commercial issues. Many tribologists refer to the importance of chemistry parameters in tribology and describe them as a "black box" [4]. Different types of fillers are added to polymer compounds as inorganic particles to develop the mechanical properties of polymers, and the hardness of the resulting compound depends on the size of the reinforcement particles particle [5]. However, researchers did not report priority in ordering additives, and their research was the beginning of the Renaissance with lubricants whose properties could be chosen in accordance with the base materials. There are many hypotheses that take into account

the mechanism of border lubrication, but there are some issues related to the use of various forms of solid lubricants that are still in ongoing discussion circles [6,7]. Solid lubricant have many characteristic like: good lubrication in vacuum and very low vapor pressure (eg: transition metal dicalkogenides), Relative strength to extreme stresses, They operate at both low and high temperatures; Low heat generation due to shearing, Some of them equip excellent electricity , it was relatively affected by nuclear weapons, it has excellent wear performance at slow speeds through friction [8]. The fairly wide variety of self-lubricants in their formulations underlined their applicability in harsh corrosive environments, high temperatures and environments with high load characteristics. However, the compatibility of self-lubricating composites is unreliable. For example, glass fibers with MoS_2 (fiber / MoS_2) and glass with PTFE (glass / PTFE) in short, the process is to disperse the cut glass fibers in a polymer matrix to enhance a certain property. It would be fair here to point out the presence of MoS2 with the selected glass fibers, which enhances its corrosion resistance. However, this cannot actually be done: much greater fiber/MoS_2 corrosion is observed than that of composite glass/PTFE by a factor of about 2 [9]. Hence, this requires the completion of a comprehensive analysis of the appropriate application of self-lubricants prior to implementation. The emergence of self-lubricating materials had a correlation with the actual applicability to a variety of forms of bearing materials, but In the early 1990s, it was selected to begin operating under harsh environmental conditions and extended to include space applications [10]. Lubrication occupies a critical position for operational safety in industry and processing and industrial manufacturing reliability. Cylinder bearings, magazine bearings, and gears can be mentioned which demonstrate effective lubrication reliability in dissipating friction heat, prolonging fatigue life, and reducing friction.

And wear [11]. Despite the reliability of synthetic lubricating oil or mineral oil, which is difficult to use in some areas such as pharmaceutical and food industries due to potential product contaminations [12]. Certain polymers provide a low coefficient of friction ($\mu < 0.2$) and a low wear rate ($k < 10{-}6$ mm^3/Nm) without external lubrication of the contact area [13–15].

Aims of this study

•Study the effect of adding variety types on self-lubricant behavior on the tribological and mechanical properties on PMMA polymer.

•Study the the role of solid lubricant material on Rheological behavior of PMMA polymer during self-lubricant behavior .

CHAPTER TWO

Theoretical background & Literature Survey

2 . 1 Introduction

Lubricants are materials used to improve the flow and cure properties of polymers. There is a variety of different materials that can significantly improve material mixing, flow and straightening. Internal lubricants are among the types of additives that work to modify the viscosity of the material. Today's trend is towards the use of value-added internal lubricants that can modify properties and be more cost-effective. Slippery additive is also a kind of internal lubricant that generates the ability to better treat internal friction and viscous polymer, to reduce surface friction of the polymers[16].

Solid lubricants are more promising with these requirements than other lubricants. This is due to the difference in bonds, crystal structure, base material, type of coating process, inclusion of lubricants in the substrate. Early research related to solid lubricants led to multiple ideas for the formation and inclusion of self-lubricants .The main basic principle remains the same in all the different technologies. Among the benefits that can be mentioned with regarding self-lubricating bearings include the ability to withstand high pressures. It is characterized by the small size of the bearings, which helps them reduce the size of the adjacent members and reduce the size and weight of other components, which leads to lower manufacturing costs [17].

The main function of solid lubricants is: to reduce friction rates, improve wear performance and increase efficiency in bearing loads. They are typically run as coatings, powders, or as matrix-diffusing additives. As additives, solid particles can be easily and conveniently inserted into moving interfaces via lubricant oil. Graphite and MoS_2 are common additives to lubricants that have been studied for decades [18–20] .

Lubricant additives are designed to enable a specific feature of lubricant parameters, such as viscosity, effectiveness at certain temperatures, support

pressures in extreme conditions, and friction and reduce corrosion, oxidative stability [21]. Conventional oils and greases are subject to severe deterioration and contamination at elevated temperatures (~250°C), while when available in the solid state, More capable of operating in high temperature environments [22].

2 . 2 Self-lubricant polymeric composite

For the work of polymeric compounds suppose the existence of many reasons for this. One of these reasons is to increase the bearing capacity of polymers, such as the use of fibers or particles to reinforce the polymeric matrix. Clear differences can be distinguished, for example, fiber compounds have superior durability over particulate compounds. Self-lubricating polymeric compounds can be produced by including lubricating additives to enhance their capabilities in reducing friction coefficients and wear rates. Extensive studies should be conducted before embarking on the use of these additives, since they can be a cause of reducing the load bearing capacity because the added lubricants have easy slip paths. When ultra-high load capacity and excellent lubrication are needed ,composite materials are often produced by incorporating reinforcing fibers and lubricating additives into the substrate matrix, or incorporating a mixture of both non-lubricated and lubricated fibers. The fibers can be used by cutting them into short pieces at random [23]. The main function of lubricant is to controlling friction, cooling the contact, cleaning the contact. Lubricants come in a variety of forms including liquid, semi-solid (grease), or solid (including particle and coating) greases. It was noted that the repetitive cleaning and cooling functions need a smooth flow of grease and solid lubricants that can be applied to the machine components where heat and pollution cannot play a serious role [24].

2 . 2 . 1 Why self-lubricant material?

The use of liquid or greasy lubricants in tribological applications because they combat and inhibit friction and corrosion ,Fig.(2.1 a). The role of lubricants is to facilitate the relative movement of solid bodies by reducing friction and corrosion between opposite surfaces[25]. A lubricant is a layer that has low shear resistance between two contact surfaces and is less than the surface shear resistance between sliding surfaces ,Fig.(2.1 b). Therefore, low shear strength reduces friction between surfaces and no rough crosses form at all depending on the thickness of the lubricant and the test condition [26–28].

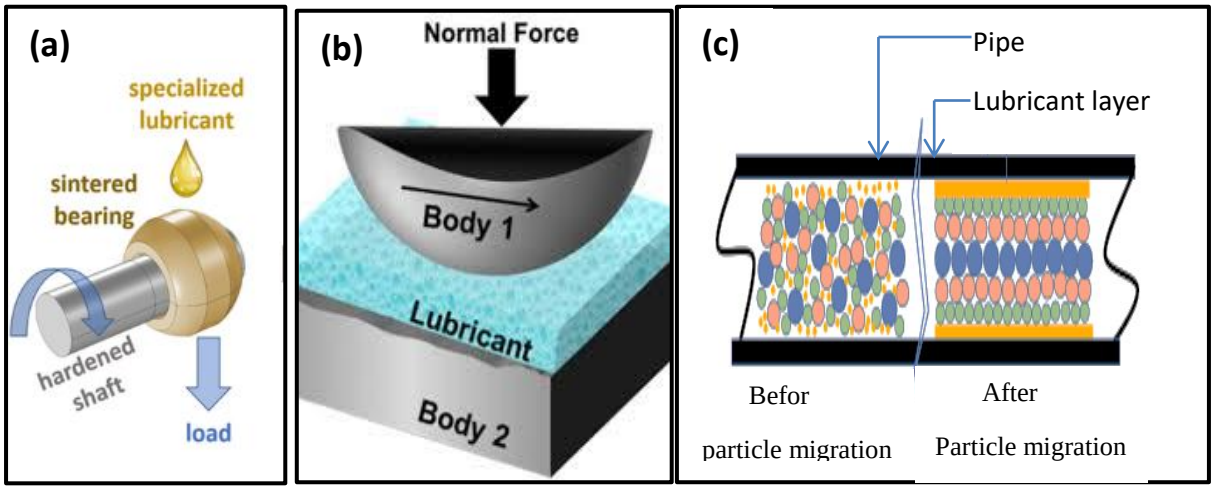

Figure 2.1 : (a) Greasy lubricants[29] **(b)Lubricating coating**[25] **,and, (c) Particle migration** [31]**.**

Evolutionary innovation ensures that solid lubricants are prepared for insertion as reinforcement into the matrix of a sliding component. A self-lubricant is one whose composition or structure provides a reduction in friction and wear coefficients. These materials are receiving increasing attention as the world becomes more aware of their environmental impact and our use of energy. An important factor in manufacturing is cost, energy consumption, and self-lubricants have the ability to effectively raise energy efficiency through operating system components more flexibly. The matrix of self-lubricating compounds consists of metals, ceramics and polymers as assembly materials. Self-lubricating metal matrix

compounds (SLMMCs) are processed using casting or powder metallurgy. Self-lubricating compounds have been used extensively by the industry to eliminate friction and wear problems in a variety of slip, roll and turn applications. It is possible for self-lubricating compounds to eliminate the use of liquid lubricants knowing that the lubricant film is absent at the beginning, and with migration to the surface after a period of time , Fig.(2.1 c) . Self-lubricating film is formed by surface wear and subsurface deformation, self-regenerating by solid lubricant particles embedded inside the matrix [32, 33].

2 . 2 . 2 Self-lubrication of polymers transfer film, and migration

Polymer self-lubricants have one common feature: it is the ability to form self-lubricating friction transfer films on the friction surface. Solid lubricants are applied either as surface coatings or as fillers in self-lubricating composites. The lubrication mechanism follows the principle of arrangement of the additives (as a filled system), the components comprising them, the matrix of the compounds, the topography of the surface, the materials of the antibody-containing body, the operating conditions of the interface, etc. A predictive picture of that along with friction and wear, particle transport eventually alters the corresponding body surface and thus has the obvious influence on the wear mode [34]. A polymer was taken as a host or a polymer mixture that contains a host polymer and combine additives chemically identical or compatible with the host polymer and the polymer or other polymers compatible with the host polymer to impart the changing surface properties due to spontaneous surface separation or due to flow-induced migration. The additives must be in the form of a branched molecule of low molecular weight, and an optional nucleus or final groups must be present. Potential migrating chemicals include plasticizers, antioxidants, thermal and slip stabilizers ,Fig(2.2 a , b) . For compounds and monomers ,therefore, one of the reasons for the migration to the surface of monomers and additives is exposure to high temperatures during processing [35].Lubricating agent migration is a meth-

od for obtaining a specific surface property and characteristic in a host polymer or a mixture of a host polymer with other polymers by blending the host polymer or polymer mixture with 0.1 to 10 wt% of low molecular weight additives') chemically identical to the host polymer on condition The presence of one or more cores so that the nuclei are chemically linked with linking points with branches that have functional end groups as well as the chemistry of the core, and / or the physical shape of the heart in this case, the transfer of properties to the surface of the host polymer or polymer mixture and for a period of time or storage [36] . Migration contributes to a decrease in clumping, and this decrease may be due to the method of formation, the extraction process and the restriction of movement. Recent studies have contributed to the synthesis of a polymer with a controlled structure, and additives may contribute to agglomeration because the addition of migrating additives and incomplete mixing exposes the plasticizers to the problem of clogging [37] .

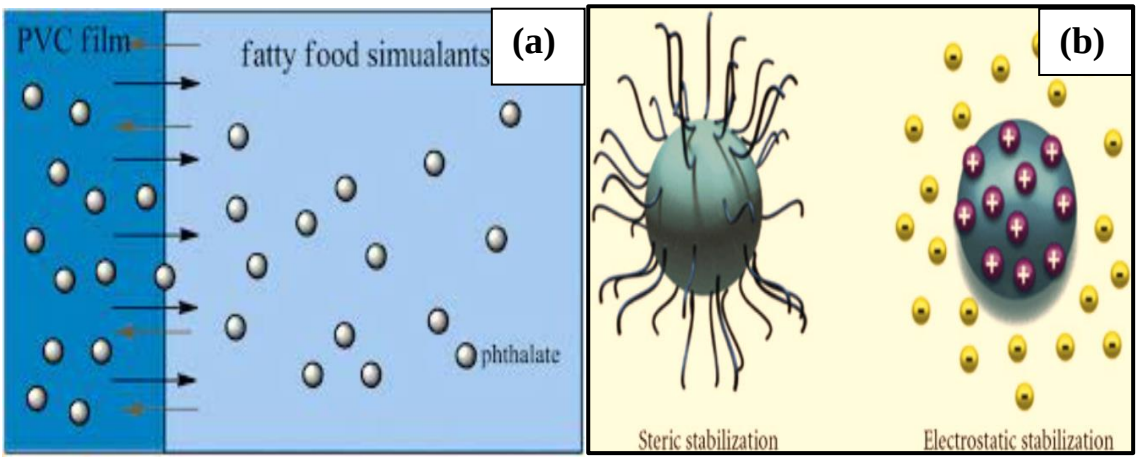

Figure 2.2 : (a) Potential migrating chemicals[38]**, (b) plasticizers**[39]**.**

2 . 2 . 3 Criteria of self-lubricating technology

Relatively stiffer and more flexible, friction and wear properties can be obtained after determining the properties during surface contact by film layer, homogeneity, hardness, lubrication, and adhesion. Some of the criteria that must be met to enhance the performance of a solid lubricant film coating or a lubricant incorporated into the self-lubricating compound matrix are as follows:

- Determine the minimum shear force for adhesion between opposite surfaces to maintain desired border lubrication.
- Maintaining the internal cohesion of the film large enough to prevent the film from disintegrating during friction.
- Provide less adhesion between particles and layers in the shear direction that is as small as possible to keep the friction resistance low [40].

2 . 2 . 4 Lubrication Types

1. Solid Self-lubricating

Solid lubricant technology has conquered distinguished positions that deserve the attention of designers of machines and devices that operate under normal and harsh environment conditions. Machine parts are designed with hard film lubricants to enhance solid lubrication reliability and wear life. Solid lubricants are incorporated either as a surface coating on the substrate surface or as fillers within the substrate or so-called self-lubricating compounds. Tribological interactions (friction and abrasion) with solid lubricating coatings result in the transfer of a thin layer of material from the coating surface to the surface facing friction, and it is called the (trilayer) transfer film. Various chemicals, various microstructures, and crystal textures can emerge from corroded surfaces from what is originally in the loose paint due to surface chemistry interactions with the environment. As a result, solid lubricant coatings may be damaged. They provide agents for reducing friction

and long anti-corrosion service life in one environment and cannot continue in different environments. The primary mechanism on which friction depends is the dry interfacial slip Fig(2.3), which occurs between the worn coating and the transfer film,[41].

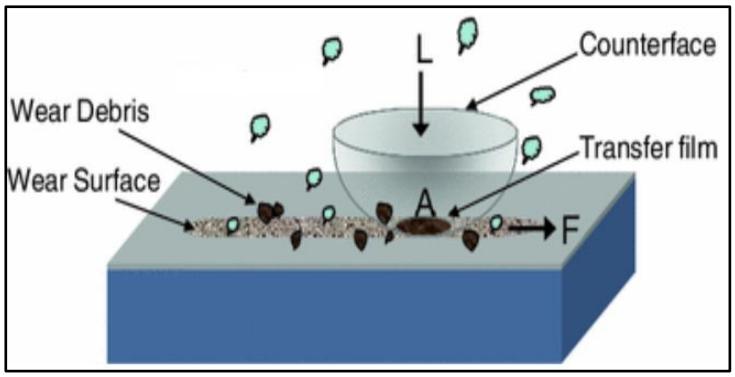

Figure 2.3 : Primary mechanism of the dry interfacial slip [41] **.**

2. Capsulations self- lubricating

The process of encapsulating a specific phase of materials (solid, liquid, and gaseous) contained in a chemically inert substance to give protection and to secure opportunities to isolate it from the surrounding environment, The preservative is called by the shell and the substance included in the core. The resulting substance appears as shown in Fig.(2.4) mentioned as a microcapsule [42]. The size ranges of the microcapsules are (1-1000 μm) and they are spherical, and here it turns out that the microcapsules are not microscopic because the two systems are in a different situation between them, for the microcapsule, the polymer shell surrounding the active liquid or solid material without engaging in any chemical reaction Because it plays the role of repositories only, while the microsphere occupies the sites of a matrix of compounds as a matrix that is either dispersed or dissolved in it. In the event of friction, the pellets are damaged and the lubricant is released in the contact area, which leads to a reduction in the friction coefficient and reduced wear [43].

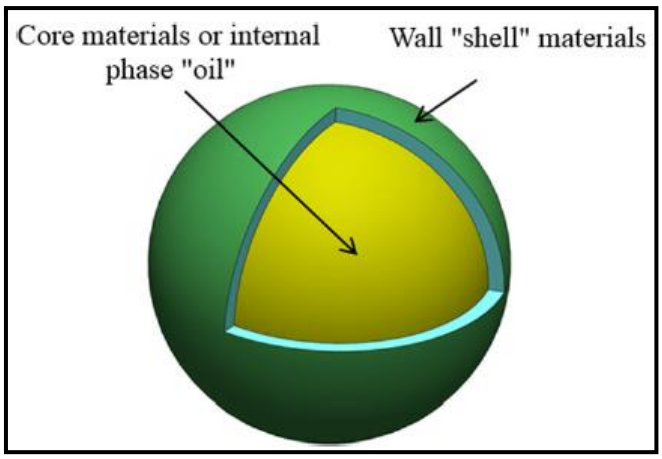

Figure 2.4 : Microcapsules with its constitutes shell and wall [42]**.**

2 . 3 Lubrication and lubricant additives

Lubricant additives are divided into three main gatogries (1) Organic additives, (2) In-Organic , And (3) Hybrid additives

1. Organic additives

Ionic liquids and hydrogels are two of the most popular organic additives of recent times. Whereas ionic liquids are widely used as industrial lubricants or as additives to lubricating oil, while hydrogels show remarkable biocompatibility, their use is increasing for bio-lubrication [44–46].

1 . 1 Ionic liquid lubrication

ILs have excellent stability and low friction. Including different molecular structures, different lubricating properties. Due to its high thermal stability and promising bonding properties, it has aroused more interest. Studies have reported the result of factors affecting the lubrication and flow characteristics of an ionic liquid by simulating molecular dynamics. The interaction between IL molecules and the solid wall is observed due to the main driving force controlling the behavior of molecules for ionic fluids in the gap. A phase transition is defined from dense liquids to ordered and solid ionic liquids under loading and the nor-

mal shear is unstable. The effect of water on the structure and properties was confirmed of ionic liquids near solid surfaces [47].

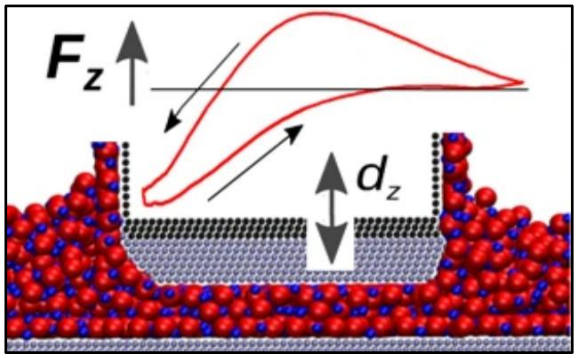

Figure 2.5 : Ionic liquid lubrication[47]**.**

1 . 2 Oil-based lubrication

Lubricating oil occupies the first place in the field of lubrication. This is what many researchers aspire to for effective lubrication and lower viscosity. Oil lubrication is observed to have very low friction that is attributed to the decomposition and oxidation of the substrate arising from friction, and a repulsive force appears between the OH end and the solid surface [48].

Figure 2.6 : Oil-based **lubrication**[49]**.**

1 . 3 Wax-based lubrication

Candles are environmentally friendly and functionally used in many applications, they can be used on almost any surface in industry. Wax enhances the surface tribology and improves its properties, including: improving slip in harsh

environmental conditions, resistance to clogging due to pollution, water repellency by increasing the hydrophobic properties of the surface, and abrasion resistance, Fig.(2.7) [50] .

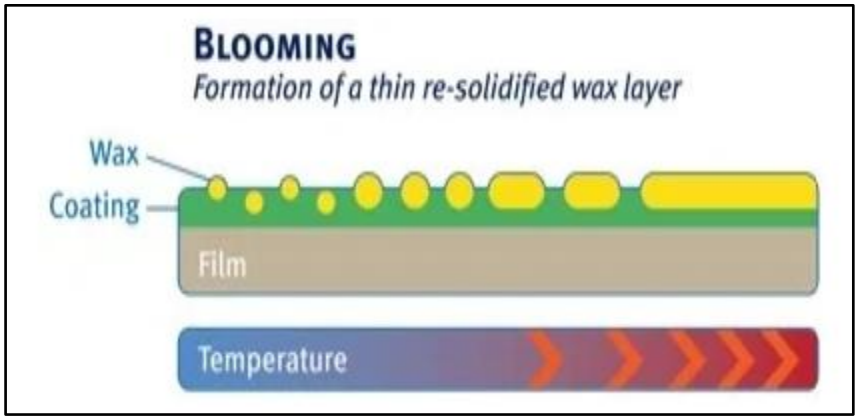

Figure 2.7 : Wax-based lubrication[50]**.**

1 . 4 Carbon Nano-Tube lubrication

The researchers' interest was centered on the development of organic Nanomaterials for many applications due to their unique properties such as semiconductors, as catalysts, optical properties, friction reduction, and reduced magnetism [51], Lubrication of moving parts, system cleaning, anti-wear and improved performance and engine cooling ,Fig.(2.8) [52].

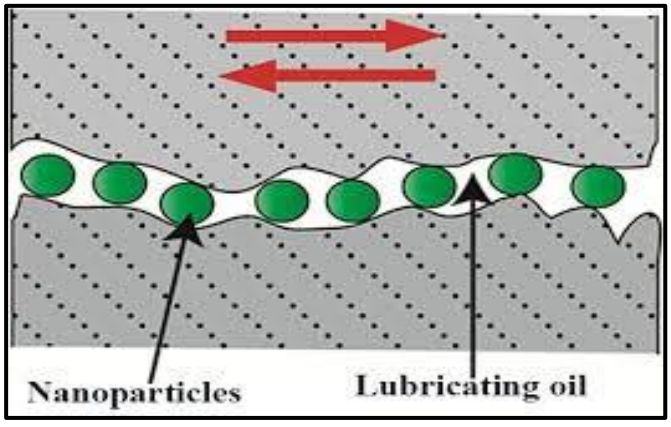

Figure 2.8 : Carbon Nano-Tube lubrication [52]**.**

1 . 5 Graphite-based lubrication

The graphite achieves extremely low friction between surfaces in relative motion under dry slip conditions. Its high-performance effect, including structural super lubrication, and super lubrication through its control of normal force, and contact activation, in addition to the accompanying processes of thermal lubrication and liquid super lubrication, are noted, Fig. (2.9) [53].

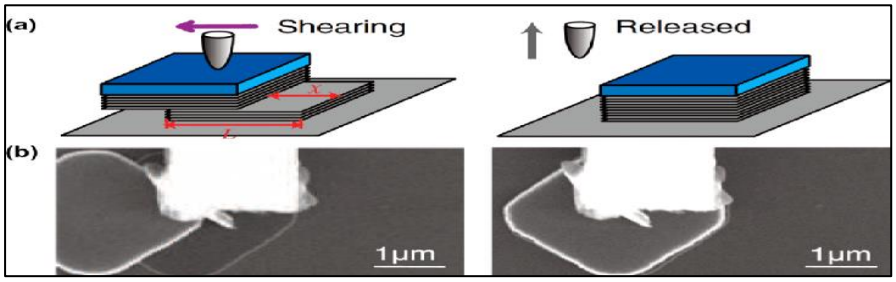

Figure 2.9 : (a)Graphite-based lubrication under dry slip,(b) SEM image[53] **.**

1 . 6 Graphene-based lubrication

Super self-lubrication was obtained between the graphene layers under high loading. Using graphene-coated microspheres (GMS) the coefficient of friction was enhanced to extremely low values (0.0025) at a local contact pressure of approximately (1 GPa), as a result of non-contact the stoichiometric provided by randomly oriented graphene Nano-crystals ,Fig(2.10)[54].

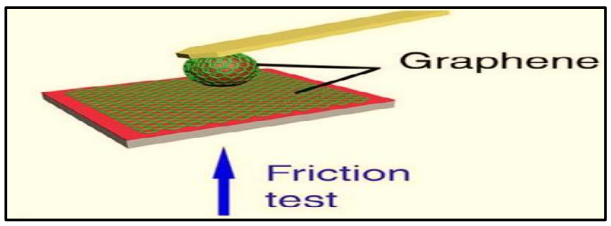

Figure 2.10 : Graphene - based lubrication under dry slip[54]**.**

1 . 7 PETF-based lubrication

PTFE sample showed a significant improvement in the rates of wear and friction by transferring the entire chain during the corresponding friction of the PTFE . Its particles under shear separating the C-C bonds to the metal surface to form

perfluoroalkyl radicals during sliding [55,56]. Carboxyl groups (R-COOH) formed in humid environments (formation of carboxylic acids) indicate that PTFE chemistry has a clear effect on the tribological performance[57].

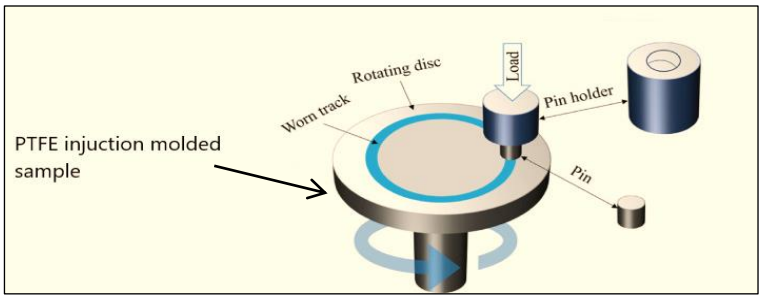

Figure 2.11 : PETF - based lubrication under dry slip[58]**.**

2. Inorganic additives

Common inorganic nanomaterials are: 2D materials and they mainly include, boron nitride [59], MoS_2 [60], and other 2D materials [61–63]. Other materials include metallic or non-metallic nanoparticles [64, 65], metallic oxides or non-metallic aggregates [66, 67], and inorganic nanocomposites [68]

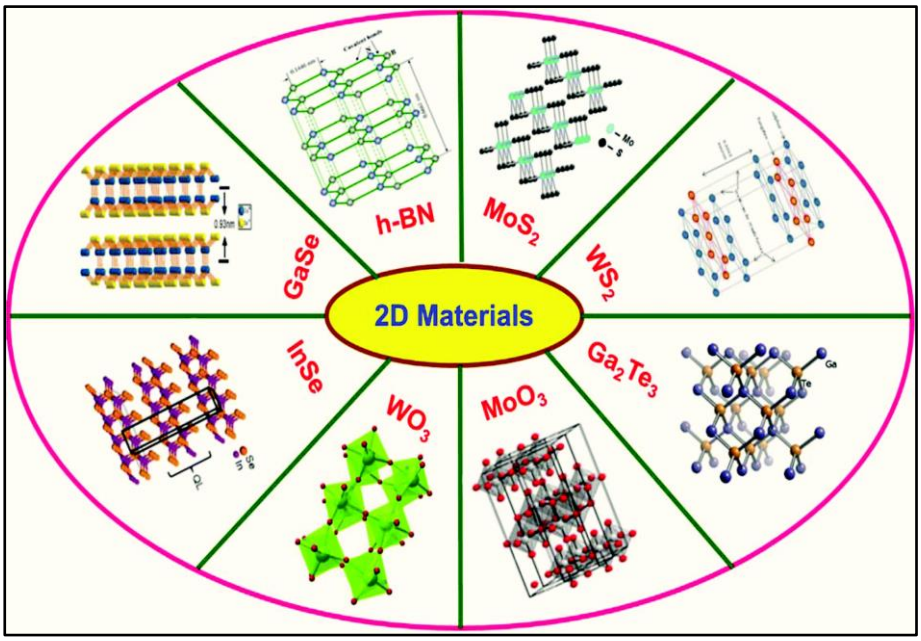

Figure 2.12 : 2D layered inorganic nanomaterial[69]**.**

3. Hybrid additives

Hybrid compounds are materials that are manufactured by combining two or more different types of materials within one common matrix. There are several definitions of hybrid compounds for hybrid compounds describing them as a strengthening material incorporated in a mixture of different matrices or as a material that is strengthened by incorporating it into two or more additives and packaging materials present in one matrix. Hybrid compounds occupy a more advanced position than fiber-reinforced compounds and have a wide range of desirable applications. An accurate description of the performance of the hybrid compounds is the sum of the individual components with a more consistent balance between the inherent advantages and disadvantages. Hybrid compounds can supplement the benefits of one type of properties lacking in the other type[70].

2 . 4 Polymerization of methyl methacrylate:

PMMA polymerization is carried out through free radical polymerization of MMA (polymerase chain via the double bond of the MMA monomer),Fig. (2.13). It is the most common method and it is either homogeneous (mass or solution polymerization) or heterogeneous (suspension polymerization or emulsion). The radical scavenger is oxygen and it is necessary to completely remove it. From polymerization by heating and absolute dehydration is not necessary, as oxygen is considered one of the reasons for ending the polymerization of free radicals. Thermal polymerization of MMA is classified as bulk polymerization, solution polymerization, suspension polymerization, and emulsion polymerization. The application of the final polymer plays an important role in choosing the type of polymerization, we find that in situ polymerization with free radicals of MMA is the dominant method for producing high-quality acrylic glass, and solution polymerization from MMA to produce adhesives, coatings resins and additives. As for the emulsion polymerization of MMA, it is for the production of

resin, coating and paper processing agents, as well as additives and textile binders [71]. In situ polymerization consists of chemical reactions that generate stages of stiffening at the micro level and the compound is dynamically stable within the anatomy of the matrix, where the nanoparticles or the solid lubricant are dispersed using ultra sonication in a liquid monomer and the addition of the initiator with the use of a suitable heat [72].

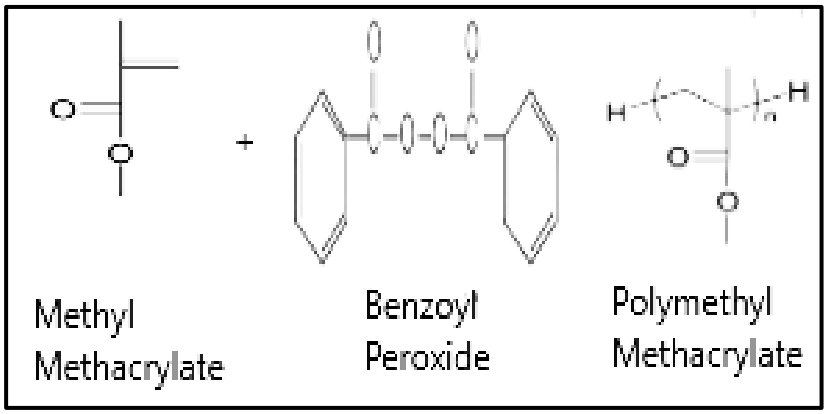

Figure 2.13 : Free radical polymerization [72].

Among the advantages of an in situ polymer are: thermodynamic compatibility within the matrix reinforcement interface , features non-polluting reinforcing surfaces allowing for a stronger matrix chit bond to be reinforced. Facilitates the preparation of insoluble and thermally unstable polymer compounds, which poses obstacles during treatment with solution or even treatment with melting. Used to prepare MWCNT with high loading, it gives very good mixing with almost all types of polymers[73].

2 . 5 Tribological Behavior

Tribology is the science that deals with the study of surfaces in contact in a sliding motion. Its origins can be traced back to the Greek word tripos, meaning (to rub). One of the important parameters of tribology is wear and friction, and the lubricating effect between them is very important. Moreover, it can be considered as an interfacial phenomenon with multiple properties, and folds under its folds the physics parameters, chemistry parameters, mechanics, thermodynamics and materials science of both reactants under dry slip conditions, Fig (2.14) [74].

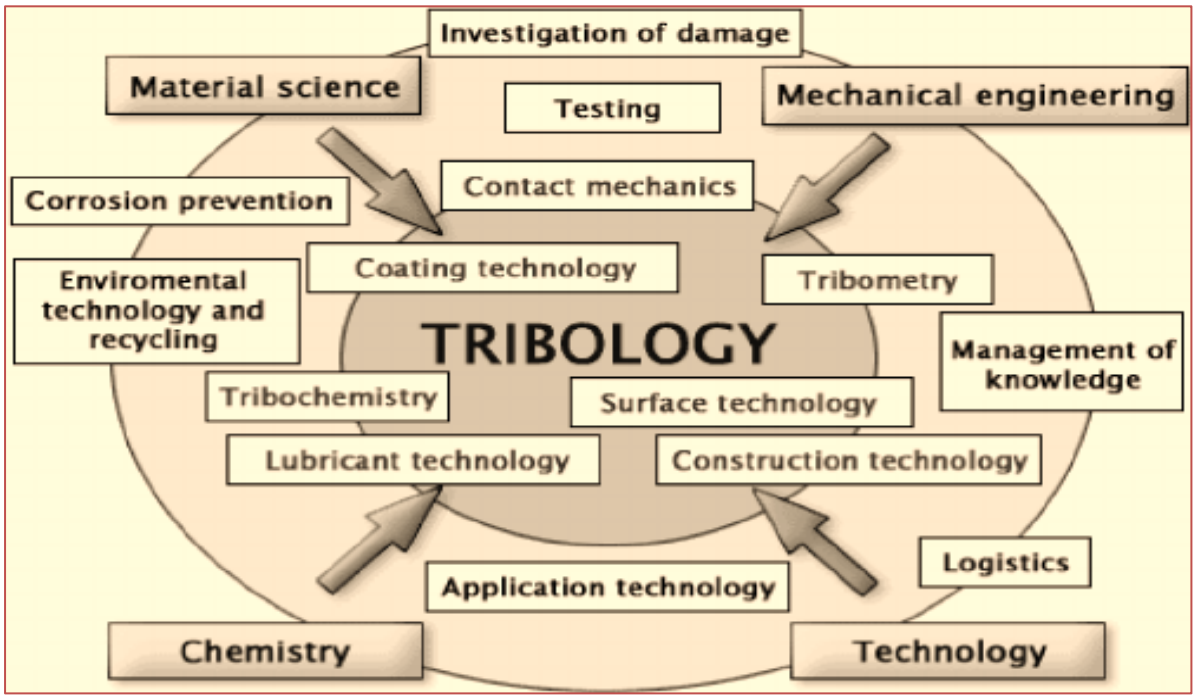

Figure 2.14 : Graphic description of tribology interacting with other sciences [75] **.**

Here comes the role of polymers, occupying advanced positions in bonding applications, due to their flexibility, and their adaptation to shock loading, with low friction and less wear. However, there are differences between the tribology of polymers and metals for several reasons. Polymers are characterized by their flexibility, viscosity and time reliability. It has a great absorbency for external lubricants, The main objective of material tribology is to work to minimize physical damage or damage or increase its resistance [76]. Undoubtedly, the in-

clusion of many transparent polymers in many applications such as optical lenses, contact lenses, mobile phone screens and aircraft windows, many researchers have highlighted the weak properties of such materials such as poor resistance, corrosion and weather resistance [77].

2 . 5 . 1 Friction and wear behavior of PCs with solid lubricant

Polymers are still limited in their distinctive shape due to their thermal stability and properties of durability, stiffness and strength. The degradation of most thermoplastics occurs at relatively low temperatures. This behavior limits the use of most thermoplastic non-reinforced polymers in tribological applications at elevated temperatures. Given the weak corrosion rate of most basic polymers, various methods are presented to improve the tribological behavior of the polymers. One method is hardening with suitable fillers, blending with other polymers and adding lubricants [78]. In flexible plastics such as composites, wear particles are created by the following mechanisms: [79, 80] (a) adhesion and deformation during sliding, Fig(2.15 a), (b) plowing by superimposed solid protrusions or solid particles on the sliding surface, Fig (2.15 b) ,and ,(c) discharge resulting from indentation cracks below the surface Fig (2.15 c).

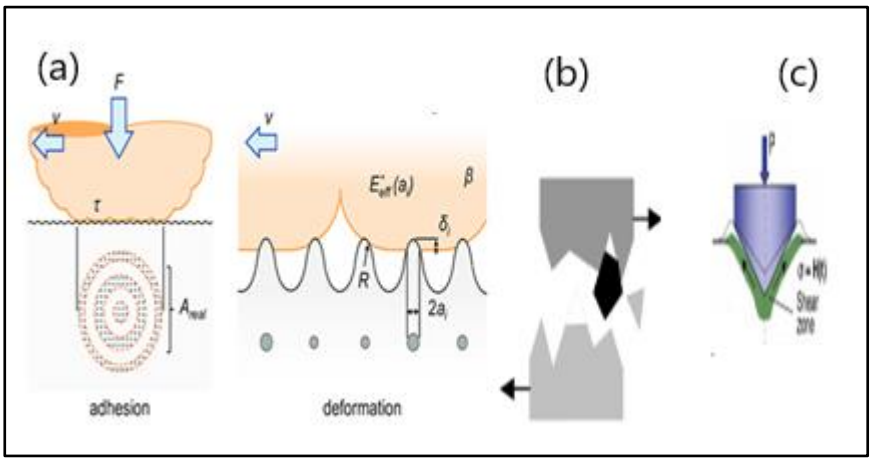

Figure 2.15 : Wear mechanisms (a) Adhesion and deformation [81]**, (b) Plowing** [82] **, and (c) Cracking** [83] **.**

Wear debris resulting from these mechanisms is dispersed particles, or these particles are transported to the surface by mechanical entanglement or by the adhesion property of the opposite surface. As for dynamic and stable wear, the removal of wounds is constantly progressed by deformation and fracture resulting from the effects of wear. Plowing also plays a distinct role in the process of surface wear and the formation of abrasive particles. The wear of a sample depends on a certain roughness, the extent of wear depends on the particle size [84]. Polymer and its compounds are facing an increasing demand in many industrial applications such as loading materials, pulleys, seals, gears, cameras, wheels, piston rings and clutches where the self-lubricating properties are utilized and operated to move away from the old methods and methods of liquid lubrication or grease and by using it, pollution and its associated problems are produced [85]. However, when contact is present between the sliding facade, friction and wear are prominent [86].A study has been conducted on the mechanism of PTFE transmission and wear. Movable PTFE films can reduce or increase the friction force depending on the differences in adhesion mechanisms in the contact area during layer formation. Low values of activation energy indicate that the corrosion of PTFE is mainly related to the breakage of weak molecular bonds and shear between surfaces and the slip of the accumulated crystal structure formed in the band structure of the materials [87]. While it was proven in similar studies conducted on PEEK compounds filled with CuS and PTFE powders during friction with a steel tool under ambient sliding conditions and adding PTFE resulted in reducing both the rate of wear and friction while the friction coefficient increased with the addition of CuS. Which indicates that the rate of corrosion of the composite depends on the ability to create transfer films on steel surfaces, which is a mechanical process that the particles of the removed material are confined to the cracks of the opposite surface [87–89] . The roughness of the corresponding surface is sometimes required to achieve an efficient transfer appropriate to a specific medium. Friction processes are often accompanied by residues

as a result of erosion and rubbing of the two surfaces, which leads to the formation of a friction layer through which a qualitative determination can be given and a description of the slip performance of that surface. These tribological processes can be understood separately for both polymers and compounds. It is possible to define the coefficient of friction (COF) as the ratio between the frictional force (F_f) and the normal load (F_N), as shown in the equation below, Fig.(2.16):

$$\mu = \frac{F_f}{F_N} \quad \ldots\ldots\ldots\ldots\ldots\ldots\ldots\ldots\ldots (2.1)$$

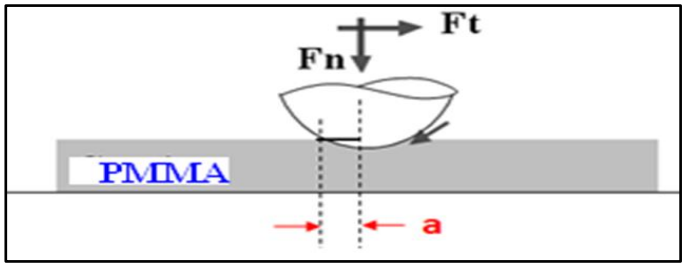

Figure 2.16 : Schematic illustrate COF of tribological processes[90].

The friction between two surfaces resulting in plowing with debris and crusts of the solid isotope and adhesion can be expressed as mechanical interactions at an atomic level as in the deformation of fillings. The shear method and the rupture of the material around the contact area between the two surfaces and around it during sliding has a real effect on friction [90].Bowden and Tabor demonstrated in 2005 that the true contact zone has a significant effect and is indirectly proportional to friction[91] .There are two phenomena involving under friction and causing energy loss: adhesion F_a, and F_d deformation, Fig.(2.17),[92]:

$$F_f = F_a + F_d \quad \ldots\ldots\ldots\ldots\ldots\ldots\ldots (2.2)$$

Figure 2.17 : Schematic illustrate friction phenomena [92].

Often the high pressure and the shear of the bonds between the surfaces that are in a relative movement is friction called adhesion friction and heat is generated as a result of the shear to the site melting of some types of materials and junctions arise at the local contact points [93].The self-lubricating compound should be providing effective support for the dynamic stresses caused by the applied load as well as the occasional friction stresses. If the polymer/ polymer compound cannot support these stresses, it leads to conditions: rapid wear (plastic deformation, brittle fracture, etc.). Catastrophic failure, increased wear down to the point where the polymer will support the contact area at low dynamic pressures, producing less deformation than wear. Stress is a factor that must be taken care of with self-lubricating compounds. A part shall be designed so that the self-lubricating compound is able to support the dynamic stresses of slip and roll. In the event that the self-lubricating polymeric compound possesses sufficient capacity to carry the impacted load, then there are different types of wear depending on the polymer, the additives used and the sliding conditions. In order to provide optimum lubrication, a kind of "shear layer" must be activated between the sliding surfaces. The shear layer has the ability to inhibit the adhesive and "plowing" reactions that occur in the contact area of moving surfaces and reduce friction, as well as reduce stresses in a larger area of the polymer compound. In most results, and in general, the thinner the cutting layer, the greater the effectiveness [10].Wear is a process that takes place at the interfaces between the interacting bodies under dry slip conditions , Fig.(2.18). The technological revolution has generated many advanced engineering products, most of which include high-speed sliding or rolling or small-dimensional geometric shapes for hostile environments, which can only be developed and included in the use fields by successfully overcoming the challenges of corrosion processes through an understanding and awareness of previous experiences and past and contemporary studies. Mechanical examples include: gas turbine engines, car engines, transmissions, tires and brakes, in the field of medicine: artificial human joints,

artificial teeth, artificial Knee, and in the technological field: hard drives for storing data and an increasing number of electromechanical devices for home and industrial use [94].The simplest way to reveal how much material has been lost due to wear. It gives the total amount of mass removed, but the distribution of wear depth in the contact surface remains unknown. Moreover, worn surfaces can be examined with the help of optical microscopes and scanning and transmission electron microscopes [95]. wear rate was obtained by using the equation below [96]:-

$$\textbf{Wear rate (W.R)} = \Delta W / \pi D.N.t \quad \textbf{gm/cm} \ldots\ldots\ldots\ldots\ldots \textbf{(2.3)}$$

where:-

D – the sliding circle diameter (cm);

t – sliding time (min);

N – steel disc speed (rpm).

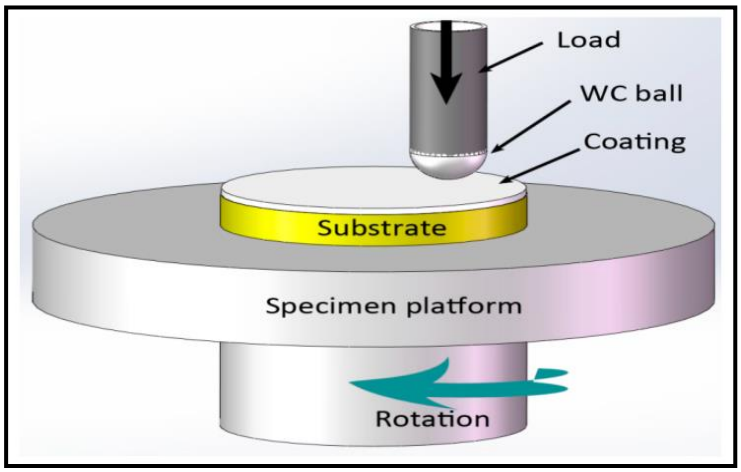

Figure 2.18 : Schematic of wear test [97] **.**

2 . 5 . 2 Scratch resistance of PCs with solid lubricant

Surfaces of polymeric materials are generally sensitive to scratches that define their applications for high performance optical devices. In contrast, the use of polymers in applications of moving mechanical parts, hence the source of friction and the properties of corrosion [98,99]. For this it was necessary to direct studies and research to find improved scratch resistance of polymers for applica-

tions that claim to be distinguished in the surface [100, 101]. Scratching is the effect of tangible grooves and/or facial damage; the striking position of this distinctive shape is characteristic of surfaces that bear deep moving loads in the form of rotors, ball bearings, etc.[102, 103].causing sensitivity to the surface of solid materials to scratch their surface easily. The infrequent presence of a third object (solid debris) can be considered a cause of scratches on polymer surfaces [104]. In technological applications, polymers are used for their attractiveness, and these scratches may significantly reduce this and thus reduce the service life of plastic products (especially optical) and coatings. Variously, these scratches may under some circumstances lead to an increase in pressure that gradually destroys their mechanical strength as well [101]. The Scratch method provides reliability data for studying the mechanical properties of organic polymers under a variety of slip conditions [98,105]. Polymers have some unique properties of flexible recovery and complex streamlined behavior. It is worth mentioning the conditions of analysis for such tests that are filled with much more complexity than mineral analysis [106] .The main variables that alter the damage response of polymers during scratching are defined as: opposing surface stress, scratch velocity, normal applied load, surrounding thermal effects due to friction and scratch, type of lubrication and the hardness characteristics of the scarifier [107,108].Some important characteristics were studied in our research through the scratch test represented by the total friction coefficient (which is the ratio between the tangential force to the normal applied force). Studies indicate the occurrence of two mechanisms: sticking and plowing. In addition to some factors that limit the overall friction coefficient in the scratch test, such as the type of material, the slip velocity between the two objects, the lubrication conditions, and the geometry of the indenter[109]. Presented by Gauthier et al. Local friction is highly dependent on the level of contact stress and the aging of the polymer [98,110], It is possible to provide a simple explanation and accurate description of the contact form at the contact area referred to as a moving end and a

polymer surface. In contrast, the contact angle has a front side and a back side in a variable manner with the contact stress [98,110].Elastomeric recovery of the polymer (back angle contact) and depends on the plastic deformation around the contact interface . Reduced friction leads to increased elastic and elasto-plastic bands. Due to the difference between the stress rate and the temperature, the differences in the contact area also arise greatly and may lead to a change in pressure in the vicinity of the contact from the visco-elastic state to the visco-plastic state [110,111]. In most cases the mechanical performance of the contact is evaluated in terms of a low coefficient of friction [111]. The description of medium contact stress dependent on friction of the stress hardening material indicated by Tabor can be applied to characterize the type of stress at the contact interface of the scratch [99]. It was found that the local friction coefficient is low. It is necessary to examine the level of scratch resistance mainly as an outcome of the reduction of the coefficient of friction [111]. The use of various plasticizers presents a field that has enormous potential for research and study. Plasticizers are commonly used in the areas of increasing elasticity, lowering costs, and developing the process-ability of polymers [112, 113]. Generally, optical device measurement (OM) was used to investigate the scratch surface characteristics ,Fig(2.19). The measured scratch width was used to calculate the scratch hardness (Hs) For elastic contact can be calculated from [112]:

$$\mathbf{H_s = \frac{4qW}{\pi d^2}} \qquad \ldots\ldots\ldots\ldots\ldots\ldots (\mathbf{2.4})$$

Where :

$\mathbf{\pi d^2}$ **–** Area of scratch tip

q – (unity for material have a completely elastic behavior and 2 for material have a completely polymer behavior).

While for material like polymers, the parameter q is between 1 and 2, due to viscoelastic behavior [108].

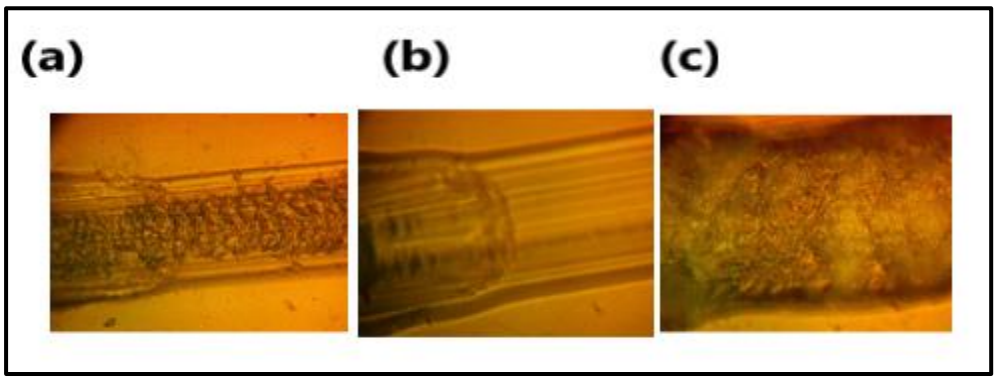

Figure 2.19 : Deformations types due to scratch test,(a)Plastic,(b)Elastic, and, (c) Viscoplastic.

2 . 5 . 3 Wettability

Wettability can be defined as the ability of the liquid to spread over the surface of the substrate. Hydrophilic surface can be determined when the contact angle is low while, for hydrophobic surfaces the contact angle is large, Fig(2.20). The contact angle is that angle formed by the intersection of the liquid-solid interface and the confrontation of the liquid vapor and is geometrically calculated by applying the tangent from the point of contact along the three-phase contact line . When the contact angle is less than 90 degrees, it leads to suitable surface wetting, and the liquid is spread over large areas on the surface; While contact angles greater than 90 degrees lead to unwanted surface wetting, so the liquid contracts to form a combined liquid droplet [114].

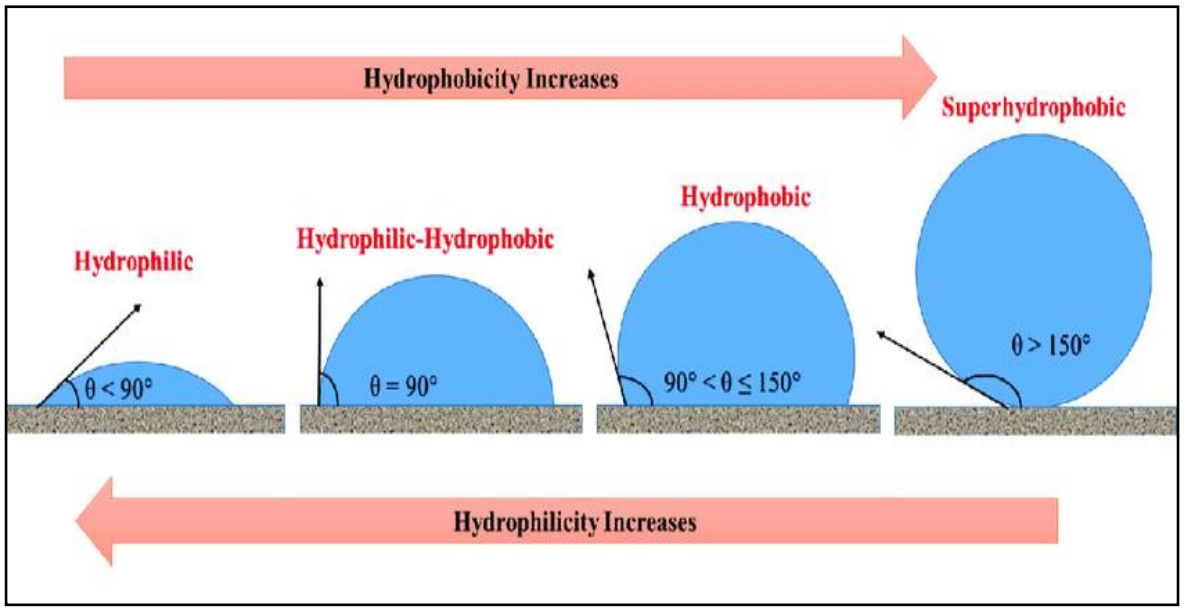

Figure 2.20 : Schematic of wettability of water on the flat surface of the sorbent [115].

2 . 6 Rheological behavior

Rheology is the properties of a substance (viscosity, molecular weight, particle size, etc.) that prevent it from being have under the influence of mechanical force or high temperature. Rheology differs from fluid dynamics by its concern for the three conventional states of matter rather than the liquid and gases alone. Important issues of rheological properties are evident in many different applications. Among the rheological measurements (shear, extended viscosity, pressure, storage modulus, and loss modulus) that work to understand the identity of materials and know their ability to operate [110]. Rheology of high molecular weight has a sensitive position in the characterization of materials, as well as the distribution of molecular weight, and subgroups. Flow measurements can be used to define boundary conditions through which to prevent problems before the material is fed into the extruder [111].

2 . 6 . 1 Rheological properties of capillary rheometer

In general, the rheological behavior of the molten polymer is evaluated using the capillary rheometer on a wide range in industrial and academic circles at high shear rates to verify its properties that control its ability during processing in industry, as shown in Fig. (2.21) [116,117]. Among the reasons that led to the study of polymer flow in the capillary flowmeter:

- Capillary flow provides information about the problems encountered in any molding flow (inlet flow, fully developed regions, and exit regions).

- Provides solutions to problems (low inlet pressure , extrusion swelling , molten fracture).

- Study of the effect of dimensions on shear rate and polymer melting [118].

- To accurately measure viscosity, due to (small diameter and long capillaries).

The regions of flow velocity are distributed due to the pressure on a liquid through a tube, where the maximum velocity is in the center (the maximum gradient in velocity or shear rate at the wall), zero (in the center of the tube), meaning that the flow is heterogeneous. Taking into consideration long heating cannot be used to sensitize easily thermally degraded polymers[119].

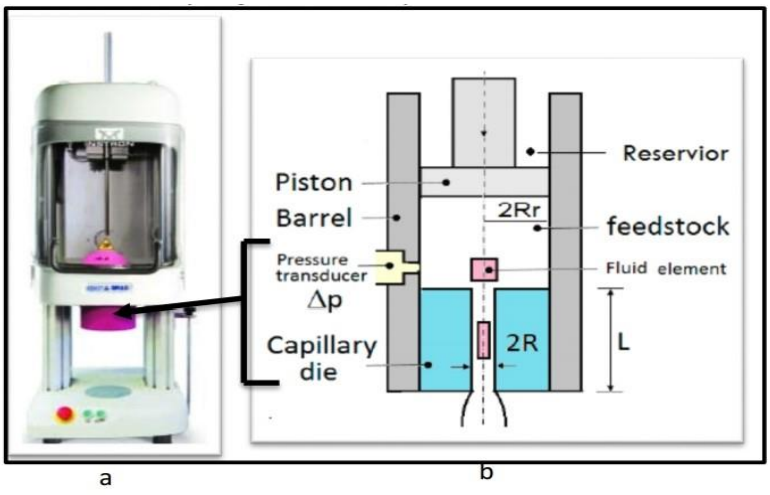

Figure 2.21: (a) Capillary rheometer SR20, (b) Schematic diagram of reservoir and die region[120] **.**

2 . 6 . 2 Rheological rheometer analysis

Shear stress profile inside the tube can be calculated from [121]:

$$\boldsymbol{\tau = \frac{r}{2}\ (\frac{\Delta P}{L})} \qquad \ldots\ldots\ldots\ldots\ldots\ldots\ldots (\mathbf{2.5})$$

at the wall (r=R): $$\boldsymbol{\tau_w = \frac{R}{2}(\frac{\Delta P}{L})} \qquad \ldots\ldots\ldots\ldots\ldots\ldots\ldots (\mathbf{2.6})$$

Velocity profile inside the tube [121]:

$$\boldsymbol{u(r) = \frac{\Delta P R^2}{4\mu L}[1\text{-}\ (\frac{r}{R})^2} \qquad \ldots\ldots\ldots\ldots\ldots\ldots\ldots (\mathbf{2.7})$$

Hagen-Poiseuille law for pressure driven flow of Newtonian fluids inside a tube [122]:

$$\boldsymbol{\Delta P = \mu L \frac{8Q}{\pi} R^{-4}} \qquad \ldots\ldots\ldots\ldots\ldots\ldots (\mathbf{2.8})$$

True shear rate for Newtonian fluids but Apparent shear rate ($\dot{\gamma}_{app}$) for non-Newtonian fluids

$$\boldsymbol{\grave{\gamma} = \frac{du}{dr} = \frac{\Delta P}{2\mu L} R = \frac{4Q}{\pi R^3} = \grave{\gamma}_{app}} \qquad \ldots\ldots\ldots (\mathbf{2.9})$$

For non-Newtonian :

$$\boldsymbol{\eta_{app.} = \frac{\tau_{app.}}{\grave{\gamma}_{app.}}} \qquad \ldots\ldots\ldots\ldots (\mathbf{2.10})$$

The true shear stress is [123]:

$$\boldsymbol{\tau_w = \frac{\Delta P}{2(\frac{L}{R}+e)}} \qquad \ldots\ldots\ldots\ldots\ldots\ldots (\mathbf{2.11})$$

Summary of Correction is :

$$\boldsymbol{\grave{\gamma}_{app} = \frac{4Q}{\pi R^3}} \qquad \ldots\ldots\ldots\ldots\ldots\ldots (\mathbf{2.12})$$

Using the Rabinowitch correction [124]:

$$\dot{\gamma}_w = \dot{\gamma}_{app}\left(\frac{3}{4} + \frac{1}{4}\frac{d\,ln\,Q}{dln\,\tau_w}\right) \quad \ldots\ldots\ldots(2.13)$$

Using Bagley correction [125]:

$$\tau_w = \frac{\Delta P}{2(\frac{L}{R}+e)} \quad \ldots\ldots\ldots\ldots\ldots(2.14)$$

True viscosity [126]:

$$\eta = \frac{\tau_w}{\dot{\gamma}_w} \quad \ldots\ldots\ldots\ldots\ldots\ldots\ldots(2.15)$$

Where:

P – the pressure drop (N/m^2);

Q – the volume flow rate (m^3 /s);

R– the capillary radius (m); and

L – the capillary length (m).

e – Bagley correction

A linear correlation between the wall shear stress and the apparent shear rate, indicating a power–law constitutive behavior (Mooney–Rabinowitsch correction)

$$\sigma_w = K\dot{\gamma}_a^n \quad \ldots\ldots\ldots\ldots\ldots\ldots\ldots(2.16)$$

Where :

k – consistency index ($Pa.s^n$)

n – power index .

The rheological behavior of the polymer is determined by a number of quantities, the most important of which are:

Melting is shear viscosity, extended viscosity, and normal stress coefficients.

2 . 6 . 3 . 1 Shear viscosity

The fluid resistance to flow (the ratio between the applied shear stress and the shear rate) is measured by the shear viscosity [127]. Viscosity can be considered as a ratio of the applied shear stress (transversely applied force (F), divided by the area of area A), and the shear rate (velocity V divided by the gap h) Fig. (2.7) [128]. This resistance appears as a reaction against the movement of any solid object through a liquid and the movement of the liquid itself. The shear viscosity of polymers depends on several parameters: shear rate, temperature, applied pressure, mold shape, average molecular weight and molecular weight distribution, shear viscosity can be calculated from the following formulation [129].

$$\eta = \tau/\dot{\gamma} \qquad \ldots\ldots\ldots\ldots (2.17)$$

The rheological properties of the fluid can be measured according to the behavior of the fluid when shearing, where the relationship between viscosity and shear rate in four cases , Fig(2.22) [130]:

- Viscosity is stable with the shear rate (Newtonian behavior).
- Viscosity decreases with increasing shear rate (shear thinning behavior).
- Viscosity increases with increasing shear rate (shear thicking behavior).
- Unlimited viscosity until a certain shear stress is reached (Bingham plastics).

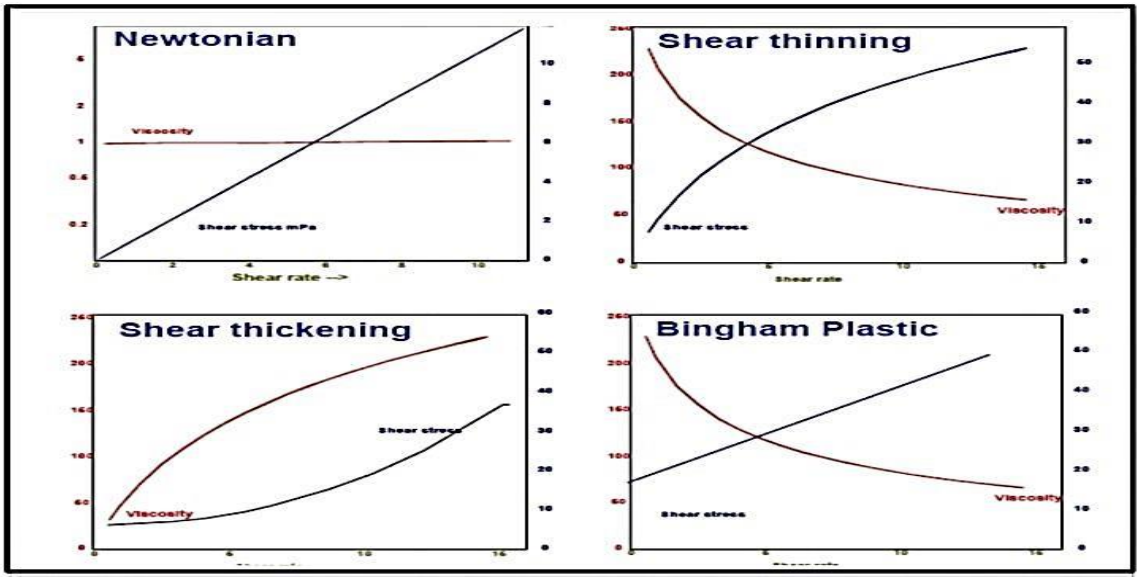

Figure 2.22 : The flow curves and viscosity curves of the four basic flow patterns [130].

2 . 6 . 3 . 2 Extensional viscosity

Three main types of oblong flow can be distinguished: uniaxial, biaxial and flat as shown in Fig.(2.23) at an area between the end of the barrel and the inlet of the mold, the melt exhibits a sudden contraction associated with the pressure drop. The pressure drop is important in the inlet zone. When plotting the inlet pressure drop against shear stress in a fully developed flow, we obtain results that are independent of molecular weight and sensitive to molecular weight distribution, chain branching, and fillings. The inlet pressure drop is used for a qualitative assessment of flow rheology [128].

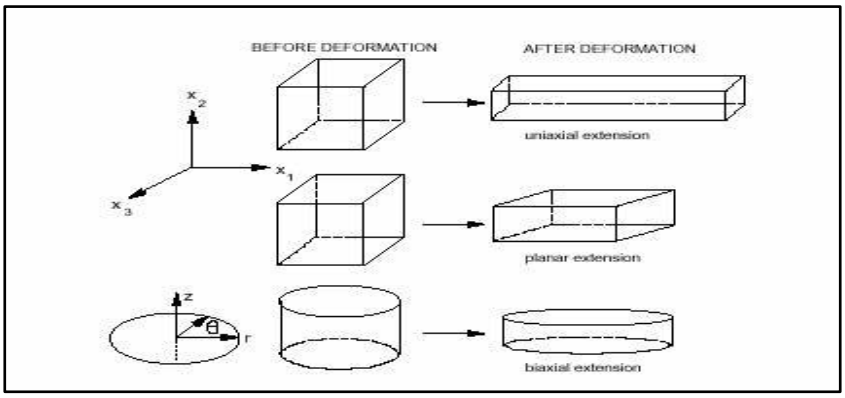

Figure 2.23 : Schematic representation flow types of extension[131] **.**

2 . 6 . 4 Defects Filament Of Polymer During Extrudate

It can be seen whether the flow is stable or unstable through the extrusion profile of the molten polymer through a die: at a low flow rate the flow is smooth, the extrusion is smooth and its cross section is constant, in this case the flow is quite stable. However, after the critical flow rate, the flow becomes unstable and extrusion defects abound, affecting its surface or volume [132]. These instabilities are generally defined under the term (dissolving fracture) [133]. There is more than one way to verify the instability of the polymer melt flow, namely, firstly, the experimental method, and secondly, the theoretical method. The experimental method includes an indirect approach that represents the classical rheology and the resulting experimental data are recorded as: shear stress, pressure, shear drag and flow rate during the individual instability test, and based on these data results for the treatment condition, the materials are studied. However, this approach includes inadequate basics for investigating entry flows due to their persistent disappearance within the extrusion matrix. The second method - includes the direct direction of optical measurements, which gives the perception of kinetic motion (velocity, deposited pressure) by the interaction of light with the flowing liquid, but the integration of the appropriate optical visualization system with the flow field without affecting it. PTV), laser Doppler velocity (LDV) and flow refraction [134] .

2 . 6 . 4 . 1 Sharkskin Defect

The sharkskin defect appears in the form of a surface defect, It develops continuously with the increasing of flow rate. Its onset is revealed initially by a loss of transparency of the extrudate, smooth less surface. Afterwards, small irregularities can be seen merly with the naked eye, then form very regular waves of short period, perpendicular to the flow direction, which gives the surface a very typical aspect ,Fig. (2.24) [128,135].

2 . 6 . 4 . 2 Volume Defect

Generally anther flow instabilities of molten polymers called (Volume defects) can be categorized into two types : (1) Can be observed as a regular helical shape; appear above a critical flow rate, (2) Can be observed a chaotic aspect (gross melt fracture) for all polymers which show a advanced and crooked deterioration of the cylindrical shape of the extrudate ,fig.(2.24) [136].

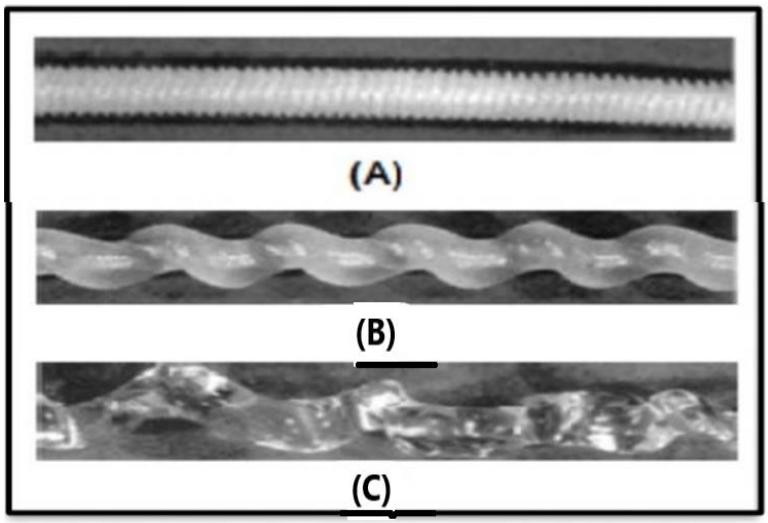

Figure 2.24 : Example of Extrusion Defects: A) Sharkskin, B, and C) Volume Defects[132] **.**

2 . 7 Material used in this work

2 . 7 . 1 Methacrylate monomer (MMA)

Methacrylate (MMA) is foundational for many acrylate polymers and is an essential co-monomer in paint, coatings, and adhesives resin formulations, Fig.(2.25). In free radical initiated copolymers, MMA elevates the Tg (glass transition) and contributes durability, strength, transparency, and UV and abrasion resistance [137].

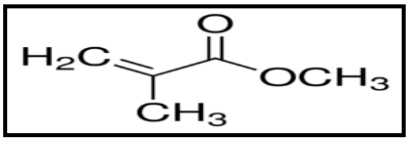

Figure 2.25 : Methacrylate (MMA) structure [137]**.**

2 . 7 . 2 Benzoyl Peroxide (Initiator)

Benzoyl peroxide is a chemical compound (organic peroxide) with the structural formula ($C_{14}H_{10}O_4$)and is often abbreviated as (BPO),Fig.(2.26). The molecule is described as consisting of two groups of benzoyl (C6H5−C) = O) -, Bz) are linked by peroxide (−O − O−). It appears in the form of a white granular solid with a slight odor of benzaldehyde. It has the ability to dissolve in water, but at a poor dissolving speed. It is noted that it is soluble in acetone and ethanol as well as in other organic solvents. Benzoyl peroxide is an oxidizing agent that is used primarily in the production of polymers[138] .

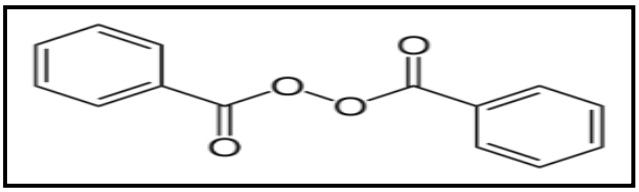

Figure 2.26 : Benzoyl peroxide structure [139]**.**

2 . 7 . 3 Polyethylene- wax

Polyethylene wax ($C_{20\text{-}40}H_{42\text{-}82}$, Tm= 145 °C), Fig(2.27) is white super fine powder its main advantages are high melting point and very small particle size, with the particle size at 1-2μm so can caot the powder coating effectively , it will not affect the flatting of powder coating compared with inorganic materials [140] .

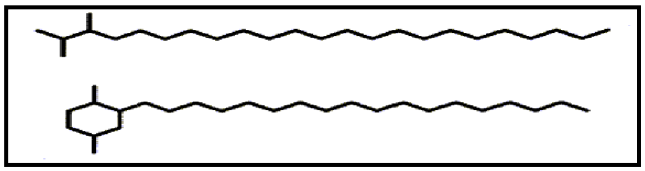

Figure 2.27 : Parrafin wax structure [140]**.**

2 . 7 . 4 Bees wax

Beeswax ($C_{15}H_{31}COOC_{30}H_{61}$, Tm= 75 °C),Fig.(2.28), it is consists of carbohydrates as raw materials mainly i.e. honey sugar, fructose, glucose and sucrose,

fresh from it is white in color, then turns yellow after a while. The typical yellow color arises from the relative quantities of different pollen and propolis pigments. It is an inert material with high plasticity (about 32 °C). From (30-35 °C), it becomes plastic, and from (46-47 °C) the general structure of the solid body is broken down and begins to melt between (60 to 70 °C). From (95-105 °C) a surface foam is formed, and the volatile parts are evaporated at (140 °C). When the temperature is lowered, the beeswax shrinks by about 10%, the remaining water is removed at (120 °C for 30 minutes) and the hardness increases as a result [141].

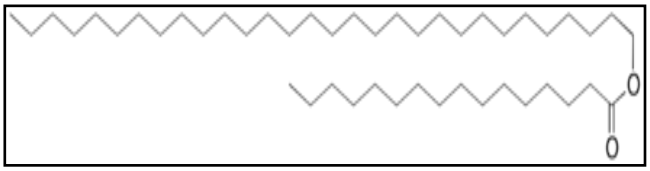

Figure 2.28 : Bees wax structure[141].

2 . 7 . 5 Calcium Streate

Calcium Streate [$Ca(C_{18}H_{35}O_2)$,Tm=170 °C],Fig.(2.29) is a compound made of calcium with a group of solid organic acids extracted from edible materials. Calcium stearate is a solid lubricant that reduces the friction between the particles of the additive, It is a solid-phase lubricant that diminishes friction among particles of the sample to which it is added. Citric acid is a saturated fatty acid that is naturally present in the glycerides of animal fats and most vegetable oils, and is derived from palm oil, soybean oil, or fats suitable for human use. The final compound is composed of calcium with different proportions of fatty acids and palmitic [142] .

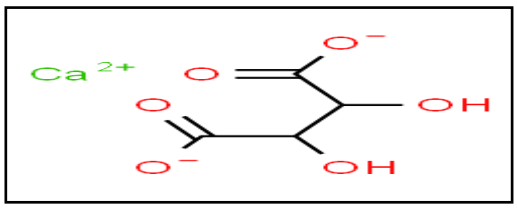

Figure 2.29 : Calcium Streate structure[142].

2 . 8 Applications of self-lubricating polymeric composites

Coating : By using Nano-diamonds as a coating for polymers, mainly it consisted of polymer Nano-fibers and microfibers loaded with high diamond particles of 5nm weight (up to 80% by weight in poly acrylonitrile and 40% in polyamide , which are Nano-fibers electrically spun as a delivery medium and have self-lubricating properties. This Nano coating exhibits high mechanical properties as it protects against UV rays and is scratch resistant with the help of self-lubrication for a variety of surfaces [143].

Aerospace : The formulations were optimized for self-lubricants in a second development stage (eg Duroid5813 and PGM-HT). To achieve low friction and suitable wear in vacuum (+80 °C to -80 °C), secondary goal is low friction in air as well. Reported Artes activity equipped a fully European self-lubricant for ball bearing cage applications and a related design to predict the life of the ball bearing in terms of wear characteristic, ball contacts, and the amount of lubricant transportation per ball cage. That would be a breakthrough in mechanism and tribology[144] .

Reinforcement : The meniscus simulation technology has been developed to modulate the nanoscale surface of long-term prosthetic hip implants, as a high-molecular-weight polyethylene (UHMWPE) lubrication pad to reduce acetabular lining wear and eliminate osteolysis. By inoculating poly (2-methacryloyloxyethyl phosphorylcholine) (MPC) on high-affinity UHMWPE (X-UHMWPE) using photopolymerization. The thickness of the poly layer (MPC) is 100-200 nm. This treatment increases the surface's susceptibility to water. This grafting reduces the production of wear particles and bone resorption responses. This simulation produces highly lubricated surfaces, suitable for preparing artificial hip joint substrates [145].

Biomaterials: Using poly (vinyl alcohol) hydrogels (PVA) with a high percentage of water in reciprocating tests to study the lubrication mechanism in artifi-

cial joints and to increase the service life of the artificial joint. Use a synthetic hydrogel cartilage that mimics biomimetics where hydrogels with properties similar to those of meniscus worked To increase the superior bearing capacity of heavy loads such as those found in human joints and the lubrication capacity of normal synovial joints, the hybrid gel showed very low friction using von Mises stress and interstitial fluid pressure comparison, and fluid flow were compared in biphasic finite element analysis, the friction was improved in terms of two-phase lubrication and surface lubrication [146].

Denture: In the artificial saliva lubrication environment representing dry friction, the wear rate decreased as the artificial lubrication content increased (0 wt%, 2 wt%, 5 wt%) by adding anion powder to PMMA, and a decrease in the volumetric wear rate, SEM showed that under the grinding condition On dry, the grooves and cracks on the surface of the sample are clear, and under the condition of artificial saliva lubrication, the surface of the sample is smoother. So it can enhance PMMA's tribological properties [147].

2.9 Literature Survey

In(2020) Antimo Graziano et el.: **[148]**

The working group highlighted the effect of the new carbon Nano-agent on the compatibility between polyethylene (PE) and polypropylene (PP), and took an easy and efficient way to implement multiple polymers to activate functional properties that might be difficult to achieve in practice without physical need. Overproduction of monomer in a two-phase macropolyolefin system. With PE as the total phase, however, most polymer compounds are thermodynamically poorly miscible, causing devaluation of the material in behavior and performance. They modified an alternative and lower material value of graphene oxide (GO) to synthesize new functional graphene. They achieved a substantial improvement of the structural features of PE, increasing its industrial value, through the co-activity of the PP micro-phase with the new modified interface of functional graphene.

In (2019) K.Palanikumar et al.: **[149]**

Their studies reported a comparison between pure PP and $CaCO_3$ \ PP (self-lubricating) by mixing calcium carbonate ($CaCO_3$) with PP in different proportions. Samples were prepared using a twin screw extruder and then tested for tribological properties using a Pin-on-Disc machine for variable load and speed. Sliding distance is constant. They showed that adding 10% calcium carbonate improves the wear resistance by 70% better than pure polypropylene and increasing calcium carbonate ($CaCO_3$) to a higher ratio improves the corrosion properties more than polypropylene assuming the loss of material and microstructure of the worn surfaces.

In(2018)Wang et al. : **[150]**

Promoting the idea of super lubrication achieved by researchers using black phosphorous (BP) as an excellent lubricant additive that significantly reduces friction and achieves superior lubrication (μ = 0.0006) using onboard ball gauge test and evoke the appropriate conditions to achieve superior lubrication, including wide-range concentrations of substances additive, inter-surface contact stresses at surface shear interactions and dry-slide velocities. They confirmed that the excellent tribological properties and the extremely low shear strength are due to the water layer retained by the BP Nano-sheets modified by the addition of NaOH .

In(2018) Narasingh Deep et al.: **[151]**

Their research included the effect of introducing Nano-fillers into pure PMMA matrix and under functional conditions of high effective dispersion rates of Nano-materials in the base matrix. of MWCNT up to 0.5% by weight and then reduced. With the addition of MWCNT, there is a 16% increase in tensile stress, fluctuations in their results are observed and the reason is due to the short preparation time of the injection molding process and its time dependence and solubility. Efficiently block the f-MWCNT differentiation process. Hence the lack of elasticity, which leads to a decrease in tensile strength. The tensile strength decreases sharply up to 0.3 wt.% of MWCNT and then decreases very slowly.

In (2018)Haiyan Li et al.: **[152]**

Anew challenges faced them by embedded the microcapsules in epoxy for make "self-lubricating composites" and made the new multi-layer composites micro-capsules loaded with oil and fitted them with "poly (urea-formaldehyde) (PUF) " shells and combined them with "carbon-oxidized" multi-dopamine nanotubes ("CNTs-o-PDA") on the face surface of the "PUF" micro-capsules Containing lubricant oil (LPMs), the capsules have an average diameter of 110 μm and a coating capacity of(83.5%). Compared to the composites containing LPMs, the

coefficient of friction and the wear rate are lower for the self-lubricating composites that comprise (20) wt% of the "CNTs-o-PDA" grouped "LPMs" (33.79% and 74.28%) which are (64.07%) and (99.54%) lower than those in Clean epoxy resin. The tribological properties of the composites of polymer were significantly enhanced by inserting "CNTs-o-PDA" onto the surface of the "PUF microcapsules" with the aid of the bonding forces between the epoxy and the microcapsules effectively .

In(2017)Haiyan Li et al. :**[153]**

Activation of self-lubricating properties using double-walled organic (PSF)/inorganic (SiO2) small hybrid capsules in which lubricating oil is incorporated for incorporation into a polymer (pp) matrix.The liquid lubricant is flowed and released from the embedded microcapsules during repeated rubbing processes, which significantly enhances the anti-friction properties. Synthetic microcapsules have shown excellent performance in high temperature resistance and can be applied in higher temperature surroundings, and microcapsules loaded with 10% wt% lubricant can improve the tribological properties of PP compounds.

In (2017)Haiyan Li et al.: **[154]**

Production of double functional coatings by incorporating microcapsules loaded with tung oil into epoxy. Using in-situ polymerization, small capsules were obtained loaded with tung-oil with polyurethane shell protection (urea-formaldehyde) (PUF) with an average diameter of about 105 microns with a basic content of more than (80.0% wt). The coating is self-lubricating by releasing a thin layer of capsules under the shell or wear condition. In comparison with pure epoxy, the coefficient of friction and the wear rate were the lowest fat capsules content of (10% wt) and decreased by(17.3% & 78.6%), respectively.

In (2017) Martha Margarita Rueda et al.: **[155]**

They reviewed real-time knowledge about the rheology and applications of high concentration molten polymers, focusing on solid particles ranging in size from several microns (100 nanometers) to a few microns. They discussed the rheology of compounds in terms of size distribution, particle nature and shape, and interactions, and they summarized mathematical models related to viscosity as a function of the filler content of highly concentrated mono- and bi-modal suspensions. The results of flow instability showed the emergence of non-linear behavior (wall slip, particle separation, bulge phenomenon and surface instability), and also provided the latest applications for highly concentrated systems (solid fuels, magnetic materials, etc.). They explained the importance of mixing as a special feature to reach a high-quality dispersion and distribution of particles in the matrix. They emphasized the use of organic dispersants to improve the degree of dispersion in the matrix and the flow properties of the material and how to control it.

In (2017) Recep Gunes et.el.: **[156]**

The mechanisms of damage and positive deformation of honeycomb sandwich structures reinforced with graded face plates were functionally under ballistic action. The honeycomb structure consists of two identical functionally graded sheets having different thicknesses of material combinations, an aluminum honeycomb core and functionally graded face sheets consisting of ceramic (SiC) and aluminum (Al 6061) phases. The mechanical properties of the total thickness of the face plates are assumed to vary according to the force law. The properties of the active materials are evaluated locally using Mori-Tankao diagram finite element method and they determine the values of the penetration and perforation threshold energy on the ballistic performance and the ballistic limit of the sandwich structures. The effective contribution of the honeycomb core to the ballistic performance of the sandwich structure was by comparison with spaced plates

(without honeycomb core) in terms of residual velocity, kinetic energy and damage area.

In (2016)Bin Shen et al. : **[157]**

Researchers produced a compact and continuous layer of graphene coating by activating the surface coating and electrostatic precipitation properties at an applied voltage (15 V) or higher. At the (15 V Gr) layer the tribology of microcrystalline diamond (MCD) obtained by horizontally stacked single micron sheets of graphene was raised with random Nano-sheets (MLG) combined together, showed that the graphene (EPD) coating significantly reduced friction. Ultra-high coefficient of friction (COF) of the MCD film ranged from ~0.08 to ~0.04-0.05 under 1 N normal load and decreased by more than 40%. The friction toughness under normal load is 4N higher and more than 36000 slip cycles, and the friction reduction arises from the three-body wear system.

In (2015)Noelia Saurín et al. : **[158]**

A new type and technical method were introduced in the field of self-lubricating, the new ionic nanofluids with graphene were used as basic lubricants, lubricant additives, anti-friction and wear-reducing additives in the new nanocomposites. Ionic nano-lubricants were produced from dispersion of nanoparticles with ionic liquids upon activation of Nano-phases. These phases may consist of various metallic nanoparticles, inorganic ceramic particles or carbon nanoparticles. Phases containing ionic liquids at room temperature can take forms such as mixtures, dispersions, surface-modified Nano-phases, or chemically functional.

In(2014) G. Styles et al. :**[159]**

By determined the topographical properties of contacting solid surfaces using Talysurf by combining topography and coating properties to develop the necessary properties for a corresponding boundary friction model. Based on the mixed hydrodynamic lubrication system, they developed a digital model consisting of the upper pressure ring and the cylinder liner. They recorded the results of friction and the effect of the coating on power loss and wear as follows: The rough

ends were proportional to the load they supported in terms of the friction factor, they tested the piston/cylinder liner coupling system from lubrication during piston strokes inside the engine cylinder. Equip the surfaces with hard coatings that resist wear by solid lubricants, as well as a mixed lubrication system at and near reversals coated at the piston rings and cylinder liner surfaces. They showed that these coatings improved the friction properties of the anti-surfaces due to the topography of their surface in addition to the mechanical properties of the materials.

In (2013)DONG-YA ZHANG et al. :**[160]**

Demonstration of the bonding properties of (SLC) using a ball-on-disk tribometer under different loads and frequencies of control sample to be prepared by spraying a polymer composite coating on(GCr15) disc. Solid polymer self-lubricating compounds (SLC) consists of matrix and filled regions synthesized by Lamination process – bonding. compared with the control sample, the coefficient of friction its (SLC) corrosion rate decreased by 57% and tripled at 4 N And 6 Hz respectively. So the coefficient of friction (SLC) was stable under low frequency and high with high frequency. The wear rate was proportional to the applied load and the frequency . The areas filled by sputtering with silicon on steel sheets and a polymer matrix filled with MoS2 and graphite, respectively. They detected the effectively of solid lubricant using ANSYS and with the aid of frictional heat .

In(2013) N. Espallargas et al: **[161]**

Utilizing both solid and liquid lubricants (MoS2, PTFE, graphite, etc.) the researchers produced coatings by thermal spraying and using liquid-filled capsules as reservoirs in thermally sprayed coatings. As the coating wears off, and after the lubricant contained in the capsules is released into the system, the thick-walled capsules show more heat resistance, and the sprayer injection system results in a more uniform distribution of the capsules which improves the capsules breakage. The most important properties that control friction and wear are the

mechanical properties, the coating matrix and the capsule wall. Thus, it affects the performance of friction and wear.

In(2011)M. Manshaa et al.:**[162]**

Bringing more resistant materials into innovative applications to find Scratch-resistant polymeric surfaces, especially after facing many obstacles in the application of some physical and chemical processes, such as annealing, as well as ionic culture techniques, to obtain better surface properties, especially transparent PMMA polymers. They used three amides of fatty acids, Erucamide, Behenamide and Stearamide, and studied the effect of each on the surface tribology at a wide range of temperatures. They achieved a decrease in the coefficient of friction by introducing these plasticizers in different proportions, whose effect became clear on the behavior of PMMA, and they found that Erucamide achieved more results than other plasticizers.

In(2010)R. A.Ibrahim et al.: **[163]**

The breadth of innovation methods, including the use of natural and industrial materials, prompted a group of researchers to use polyester compounds reinforced with graphite fibers of different diameters and saturated with vegetable oils (corn, olive and sunflower oil) and polyester compounds reinforced with graphite fibers consisting of 10% corn oil and 10% by volume of fibers. Graphite exhibits relatively low rate of friction coefficients and wear rates. Corn oil and sunflower oil show good tribological behavior of polyester compounds as a heavy-duty material due to their low coefficients of friction and high wear resistance.

In(2010) Oleg Kulikov et al. :**[164]**

A low-viscosity PPA made by reacting a mixture of polyethylene glycol with organic acids, phosphoric acid, and polyester of phosphorous oxides was prepared . Comparing the extrusion pressure and viscosity shown with the new PPA at lower temperatures is lower, than in the industry when fluorinated polymer

processing additives (PPA) were used to delay the emergence of shark skin to higher extrusion rates of polyethylene resins at higher temperatures during extrusion to reduce the viscosity Apparent melting. When PPA concentrations (0.1 to 0.5% wt) are applied, the extrusion pressure is reduced from (2 to 5) times.

In(2010)Marco Sangermanoet al. :**[165]**

One of the most important parameters of organic coatings is their resistance to scratching. Researchers in this field have developed a method by following two main strategies, the selection of polymer coating components and the other introducing fillers .They used the organic/inorganic nano-hybrid coating in a top-down or bottom-up approach. Following the first approach, the particles (metal oxide) were dispersed in the polymer matrix prior to nanoparticle surface modification, as an alternative approach, using inorganic free radical polymerization combined with the use of a colloidal solution gel precursor. It resulted in a good distribution of the inorganic phase within the polymeric matrix and reduced mechanical damage (scratching) .

In (2008) Li-Piin Sung.et al: **[166]**

They reported from this study about the quantitative effect of alumina nano additives on the mechanical properties of the surface and the performance of the scratching behavior of the two-part polymeric coating (polyurethane). They incorporated metal oxide nanoparticles such as nano-alumina and nano-silica into polymer coatings to enhance mechanical durability widely used in scratch-resistant technologies and under scratch test conditions on nano-coatings (nano-alumina/polyurethane) with different molecular concentrations and a wide range of applied forces and using a distance Indented with a conical diamond tip. , the scratch patterns for width/depth and deformation were observed using confocal laser microscopy. The results indicated that the durability of the coating and the scratching behavior strongly depend on the concentration of the nanomaterial and the surface treatment of the nano-alumina.

In (2008) Milen Stefanov et el.: **[167]**

By reviewed the usability of Born-Oppenheimer simulations of molecular dynamics. They obtained a local "nano coating" that yields friction coefficients similar to those of MoS_2 platelet-based lubricants. It decreased at high loads due to the explosion of the nanostructures under the applied high load and the formation of nano-platelets that are firmly attached to the surfaces of materials from the first contact, not to the effect of bearing the ball.

CHAPTER THREE

Experimental Part

3 . 1 Introduction

In this chapter, a brief description of the materials that used to produce polymethyl methacrylate composites reinforced with a variety types of solid lubricant materials and also the equipment that used to characterized the mechanical and tribological and rheological properties of the resultant composites , Fig.(3.1).

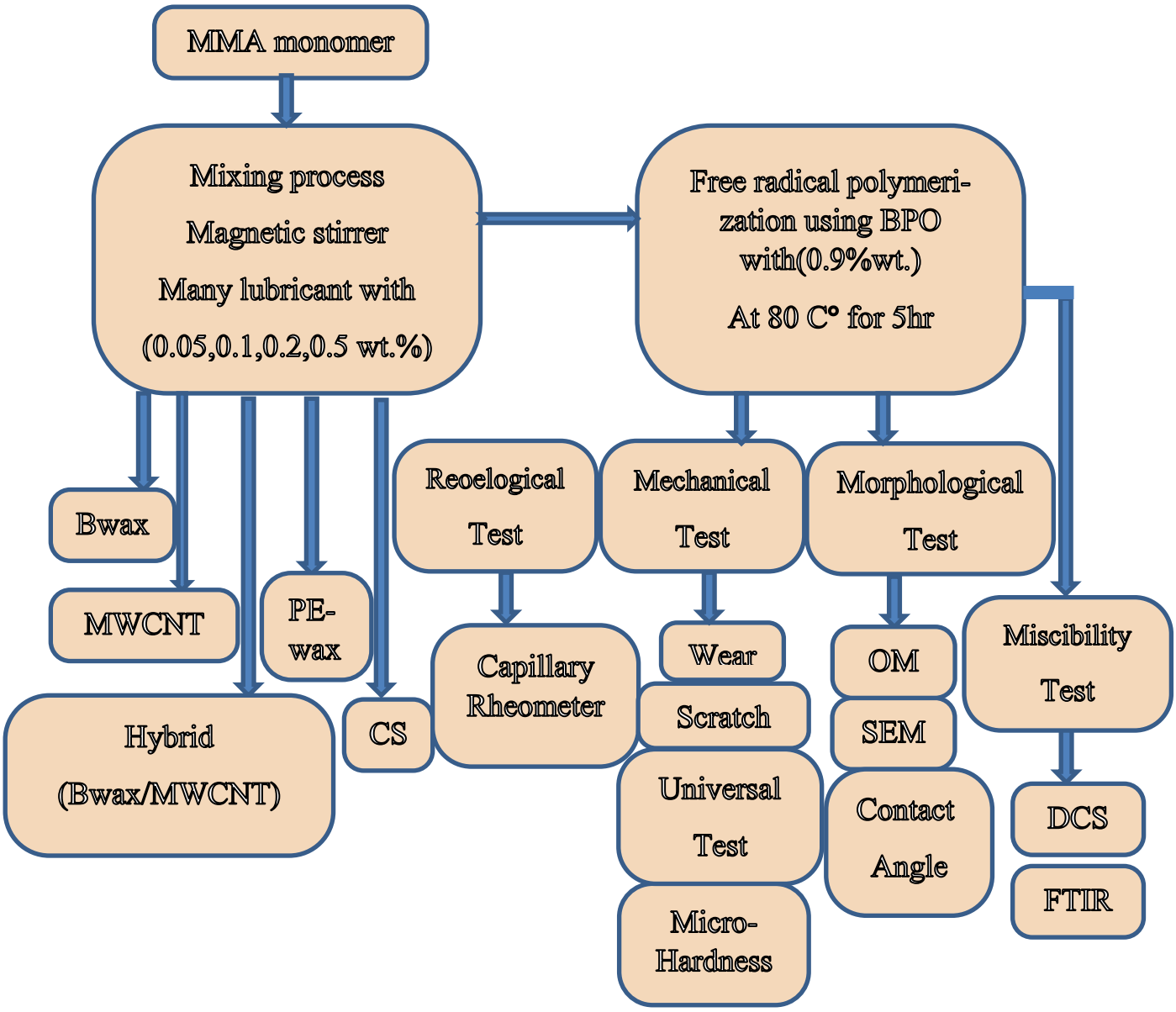

Figure (3.1) Work plan

3 . 2 Materials used in this work

In this work , the materials used : Methyl Methacrylate monomer (MMA),Benzoyl Peroxide (BPO) , Calcium Streate (CS),Polyethylene wax (PE-wax),Bees wax (Bwax), and , Multi wall carbon Nano tube (MWCNT), the specifications of Multi wall Nano tube (MWCNT) is indicated in the table (3.1) . All the above materials were all purchased from the local Iraqi market, the specifications of all material is indicated in the table (3 . 2).

Table (3.1) Specifications for MWCNT[168] **.**

Property	**Data**
Specific gravity (g cm^{-3})	**1.8**
Electrical conductivity (S cm^{-1})	**10^3-10^5**
Electron mobility($cm^2V^{-1}s^{-1}$)	**10^4-10^5**
Thermal conductivity (W mK^{-1})	**2000**
Coefficient of thermal expansion (K^{-1})	**Negligible**

Table (3 . 2) Specifications for used materials

Material	Chemical formula	Linear formula	Mw g/m	Density	Tm °C	Color	Referance
methacrylate (MMA)	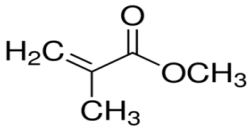	$C_5H_8O_2$	100	0.942	- 48	Colorless	[137]
Benzoyl Perox-ide(BPO)	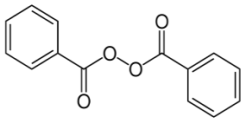	$C_{14}H_{10}O_4$	242.23	1.15	103	White	[139]
Calcium Streate(CS)	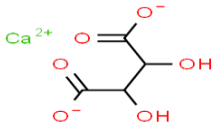	$Ca(C_{18}H_{35}O_2)_2$	(607.03)	1.08	179	white to yellowish	[142]
Polyethylene-wax (PE-wax)	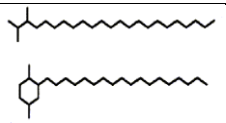	$C_{20\text{-}40}\ H_{42\text{-}82}$	436.84	930	145	Colorless	[140]
Beeswax (Bwax)		$C_{15}H_{31}COOC_{30}H_{61}$	676	0.950-0.965	61-65	white to yellowish	[141]

3 . 3 Surface treatment of MWCNT:

Given the difficulties facing the scientific researcher in the practical aspect when dealing with MWCNT in obtaining the optimum dispersibility in PMMA / matrix , therefore the Multi-wall Nano tube (MWCNT) were treated in an acid mixture solution, made with nitric and sulfuric acids in a ratio [1 : 3] by volume, the duration of the treatment were 6 hr at 80°C, MWCNT in the amount of (2g) were added to (40ml) of a mixture solution. The mixture was altrasonicated for (10 min) prior to acids treatment , the mixture was magnigatically stirred during the treatment to facilitate the reaction. When the reaction was completed , the mixture was cooled down slowly and washed with distillated water for several times using a vacuum filter to reaction the (PH=7) .The resultant filtered cake was dried in vacuum oven at 100°C for 8 hr.

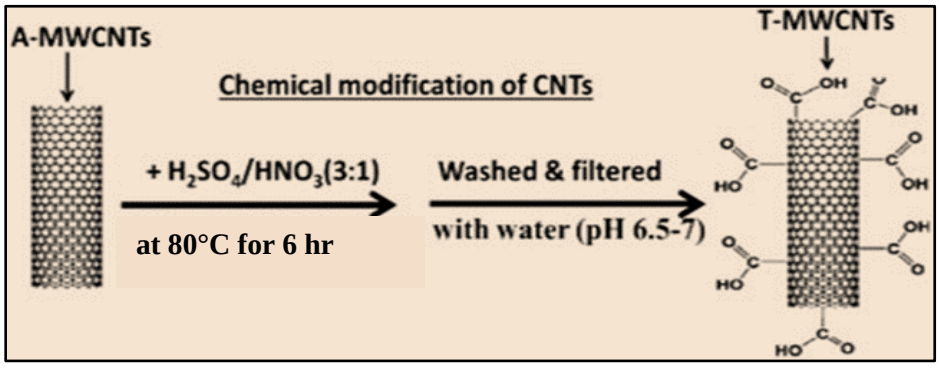

Figure 3.2 : Illustrate MWCNT Preparation Method.

3 . 4 Preparing Hybrid filler

The Hybrid compound of two materials carrying the properties of each substance included in its composition , in this paper a Hybrid compound was produced and the process summary is shown in Fig.(3.3) . Hybrid filler was prepared by mixing 50% wt. of acids treatment MWCNT with 50%wt. of Beeswax in acetone solvent using ultrasonication process for (20 min) at room temperature and then evaporated the acetone solvent using vacuum oven.

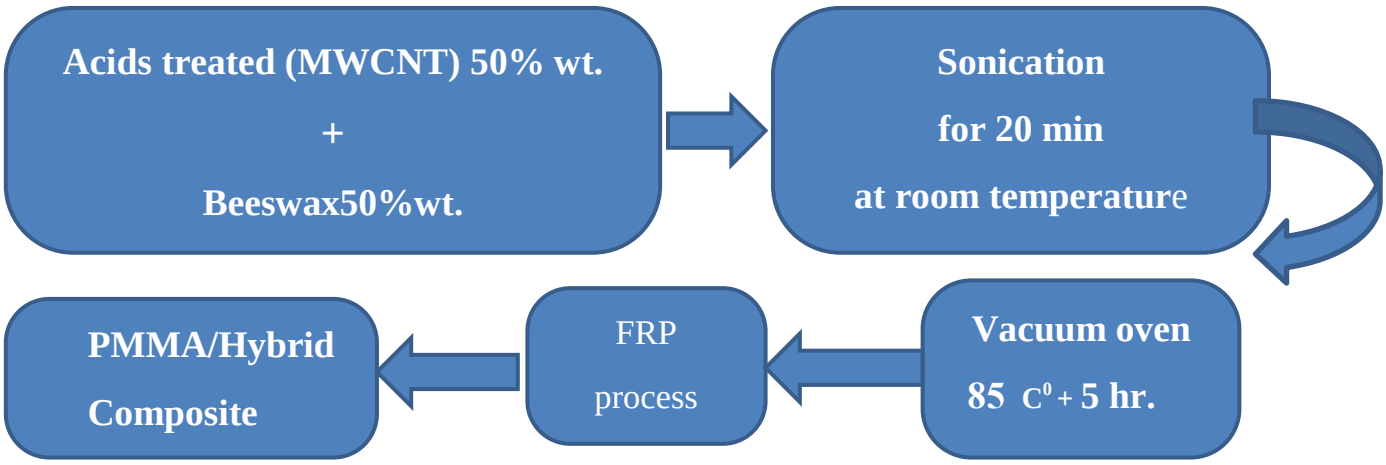

Figure 3.3 : Illustrate preparing Hybrid filler

3 . 5 In-situ Free Radical Polymerization (FRP)

The polymerization process(free radical method) was carried out in the laboratory using methyl meth-acrylate (MMA) and Benzoyl Peroxide (BPO) as initiator, The raction steps are summarized as follows:

- The polymerization molds were formed using glass sheets (20 cm × 20 cm) a (15 cm) long rubber tube, and four paper holders.
- The materials are injected into the mold using a syringe.
- The mold was brought into the oven for 6 hr at a temperature of 80 C^0.

3 . 5 . 1 PMMA/solid lubricant preparation process

The comparative effect of three types of lubricant solids used as fillers with proportions shown in table (3.3) carried out through FRP process except the solid lubricant fillers were added to the solution (MMA (100g) + BPO (0.9%wt.)) during mixing state with percentages illustrated in table (3.3) for (15 min). PMMA /Solid lubricants composites (PMMA/PE-wax, PMMA / Bwax, and , PMMA / CS) were prepared using magnatic stirrer ,while PMMA/MWCNT and PMMA/Hybrid filler

prepared using ultrasonication process, Fig.(3.3), for (20 min) at room temprature. Fig.(3.4) illustrates the preparation pross of PMMA /Solid lubricants composites(PMMA/PE-wax,PMMA/Bwax,PMMA/CS),PMMA/MWCNT,and,PMMA/Hybrid.

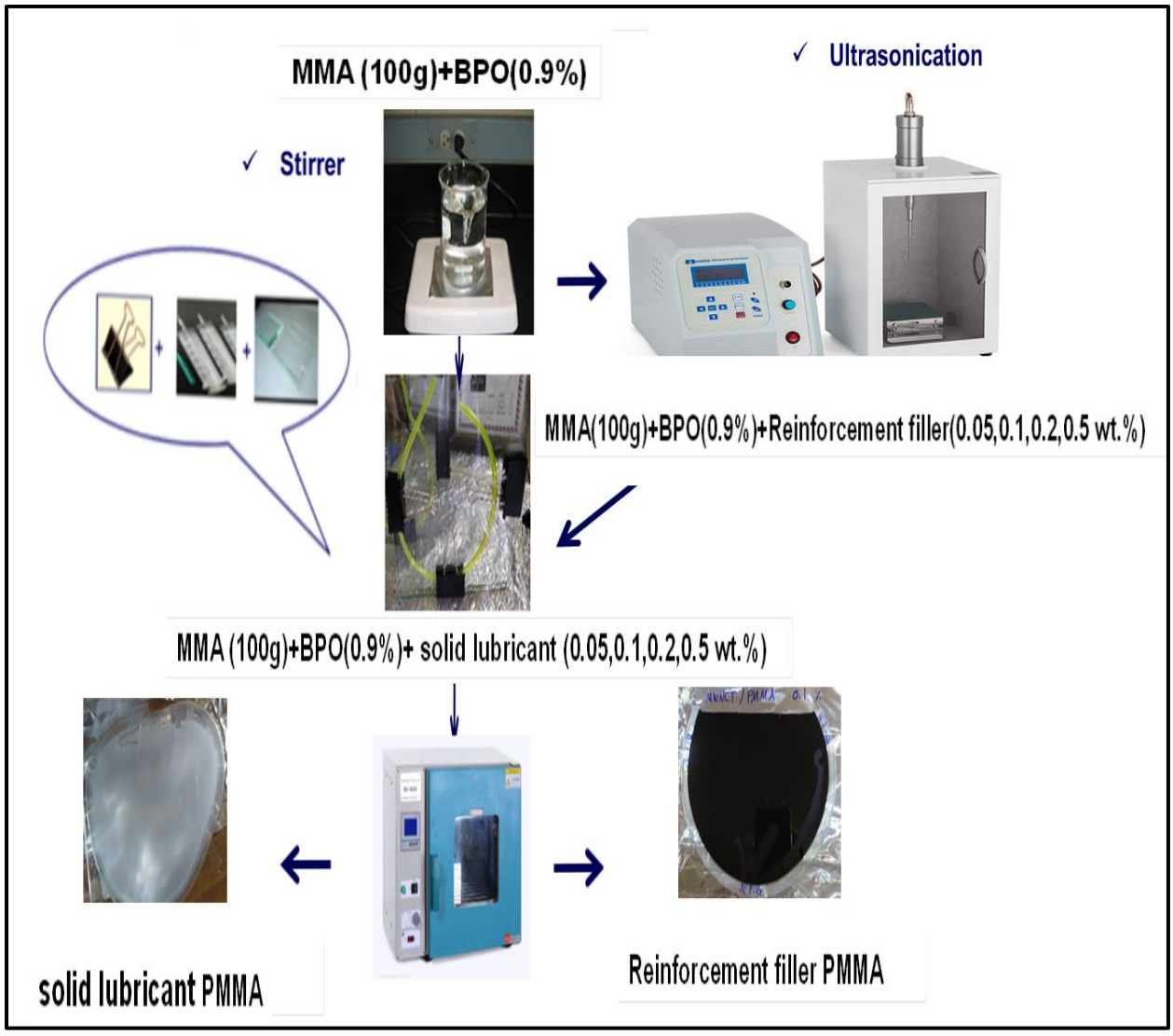

Figure 3.4 : Illustrate Polymeric Composites

Table (3.3) Polymeric Composites.

Sample Code		Sample Composition
1	Pure PMMA	PMMA without additives
2	PMMA/CS1	PMMA+0.05 %Calcium stearate
3	PMMA/CS2	PMMA+0.1%Calcium stearate
4	PMMA/CS3	PMMA+0.2 %Calcium stearate
5	PMMA/CS4	PMMA+0.5 %Calcium stearate
6	PMMA/Bwax1	PMMA+0.05 %Beeswax
7	PMMA/Bwax2	PMMA+0.1 %Beeswax
8	PMMA/Bwax3	PMMA+0.2 %Beeswax
9	PMMA/Bwax4	PMMA+0.5 %Beeswax
10	PMMA/PE-wax1	PMMA+0.05 % Polyethylene-wax
11	PMMA/PE-wax2	PMMA+0.1 % Polyethylene-wax
12	PMMA/PE-wax3	PMMA+0.2 % Polyethylene-wax
13	PMMA/PE-wax4	PMMA+0.5 % Polyethylene-wax
14	PMMA/MWCNT1	PMMA+ 0.05 % wt. MWCNT
15	PMMA/MWCNT2	PMMA+ 0.1% wt. MWCNT
16	PMMA/MWCNT3	PMMA+ 0.2 % wt. MWCNT
17	PMMA/MWCNT4	PMMA+ 0.5 % wt. MWCNT
18	Hybrid1	PMMA+0.05%wt.Hybrid(50%wt.MWCNT+50%wt. of Bees-wax
19	Hybrid2	PMMA+0.1%wt.Hybrid(50%wt.MWCNT+50%wt. of Beeswax
20	Hybrid3	PMMA+0.2%wt.Hybrid(50%wt.MWCNT+50%wt. of Beeswax
21	Hybrid4	PMMA+0.5%wt.Hybrid(50%wt.MWCNT+50%wt. of Beeswax

3 . 6 Characterization Techniques

3 . 6 . 1 Miscibility Tests

3 . 6 . 1 . 1 Fourier Transform Infrared Spectrometer (FTIR)

The Fourier transform infrared spectrometer is a technique used to distinguish between organic, inorganic and polymeric groups present in materials, and it has been used to characterize the molecular structure of PMMA, PMMA / Solid lubricant, reinforcement fillers and to interpret the links between solid lubricant and PMMA matrix. The tool that was used in this work is a type (IR Affinity-1) made in (Kyoto, Japan) and is located in the Department of Polymer Engineering and Petrochemical Industries / Faculty of Materials Engineering / University of Babylon. The sample test procedure involves calibrating the device with potassium bromide powder (KBr), and mixing the sample powder or a small drop of liquid with KBr (if the sample is in the form of particles, it must be ground into a fine powder first and then mixed) with the mixing ratio of 99%. The spectrum obtained is a two-axis shape, and the horizontal is a wavelength ranging (4000-400 cm^{-1}). The vertical axes are either absorbance or transmittance. The procedure is carried out in accordance with ASTM E1252 [170] .

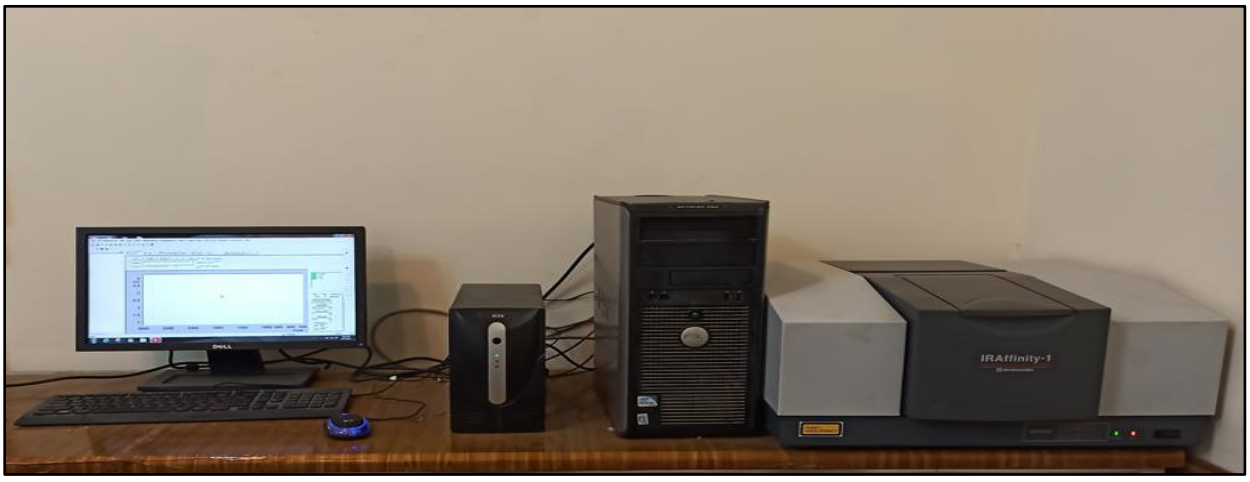

Figure 3.5 : FTIR spectroscope

3 . 6 . 1 . 2 Differential Scanning Calorimetric (DSC)

A differential calorimeter has been used to examine and quantify the temperature of the phase transitions of the samples powder was weighed, pressed, and placed in the machine. Samples were examined under nitrogen gas flow and the test parameters were determined with a heating rate of 10 ^{0}C /min and a temperature range from room temperature to 250 ^{0}C. Some characteristics such as the glass transition and melting temperatures can be determined by observing the peaks in the resulting DSC plot. The device used in this test is SH1MADZ-4 DSC-60 located in Polymer Engineering and Petrochemical Industries Department / College of Materials Engineering / University of Babylon and the test was performed under ASTM D3418-03 [171], Fig.(3.6).

Figure 3.6 : DSC Calorimetric SH1MADZ-4 DSC-60

3 . 6 . 2 Mechanical Tests

3 . 6 . 2 .1 Wear Test

The Pin-on-disk tool evaluated the dry friction and wear properties of unfilled PMMA and PMMA lubricant. An aluminum ball mounted in pin-shaped fixtures was used to slide against sample and. Ball diameter (10 mm), temperature during tests: RT, range of applied force: 1 to 12 N, distance: 500 m, speed: 110 rpm. The dimensions of the wear test samples were (1 mm wide, 2 mm long, 1.26 mm thick). All samples were processed to obtain a smooth surface. Each experiment was re-peated, at the end of each test the evolution of the friction coefficient along with the slip distance was measured directly by the CSM frictionometer. Unlike the ring on the disc, during the test of the pin on the disc, no reverse movement occurs and no breaks occur in the lubricating film between the wear components. So it can be assumed that there is pure sliding friction between the components.. The device used in this test is located in republic of Iran ASTM G99 – 05 [172] .

Figure 3.7 : Wear Device

3 . 6 . 2 . 2 Scratch Test

The scratcher was made of steel, and the testing speed was about 1 mm/s. Scratch tests were carried out on a Scratch Machine (Surface Machine Systems) according to the ASTM D7027-05 [173]. During the scratch test, linearly progressive normal loads from 5N to 20 N were applied on the surface of the specimen by the scratch tip, all samples were scratched using a spherical scratcher (570 μm tip diameter) with a variety of loads (10, 15, 20 N).Afterward, the scratch groove formed on the specimen was observed by optical light microscope, and the onset point of scratch damage was determined and its distance from origin was measured, thus the corresponding normal load at onset location of scratch damage can be identified. This normal load is termed as a critical normal load of scratch damage (Fcr), and can be used to quantify the scratch resistance of polymers. A constant scratch speed of 1 mm/s and a scratch length of 40 mm were specified for all scratch tests. A stainless-steel spherical scratch tip of 570μm diameter was used to conduct the tests Fig.(3.8). The device used in this test is located in Polymer Engineering and Petrochemical Industries Department / College of Materials Engineering / University of Babylon.

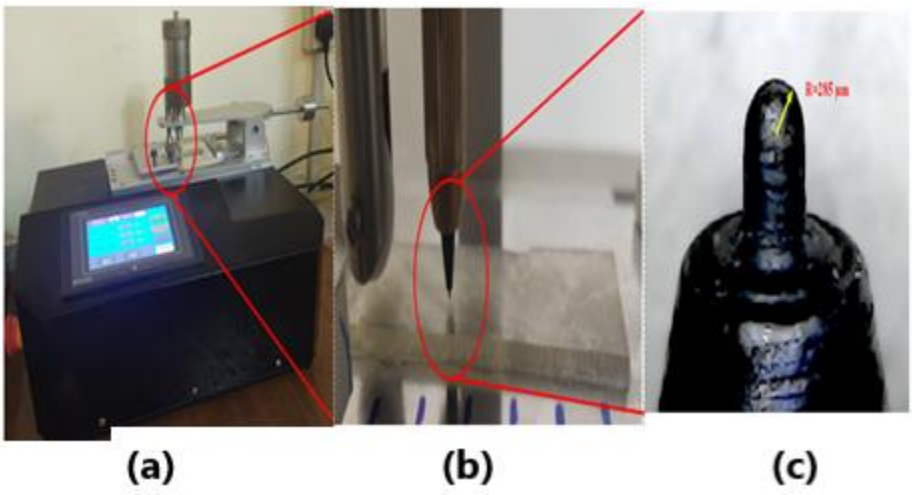

Figure 3.8 : (a) Scratch devise ,(b) PMMA under the tip of scratch device ,and (c) tip of scratch device

3 . 6 . 2 . 3 Universal Test

This test was performed by using (Bongshin model WDW-SE) instrument .The device applies load range (1-50KN) with speed range (0.1-50 mm/min). A characteristic of polymers in the bending diagrams depend on the shape and dimensions of the specimen. Fig. (3.9) show the instrument of Three point bending test that can be used for the examination according to ASTM D-790 [174] , The device used in this test is located in Polymer Engineering and Petrochemical Industries Department / College of Materials Engineering / University of Babylon.

Figure (3.9) Universal Test Device

The flexural strength is stress at failure in bending. It is equal or slightly larger than the failure stress in tension, for a rectangular sample, the resulting stress under an axial force is given by the following formula:

$$\sigma = \frac{F}{bd} \qquad \text{.....(3.1)}$$

This stress is not the true stress, since the cross section of the sample is considered to be invariable (engineering stress).

where :-

- **F** – the axial load (force) at the fracture point (N).
- **b** – width (mm).
- **d** – the depth or thickness of the material (mm).

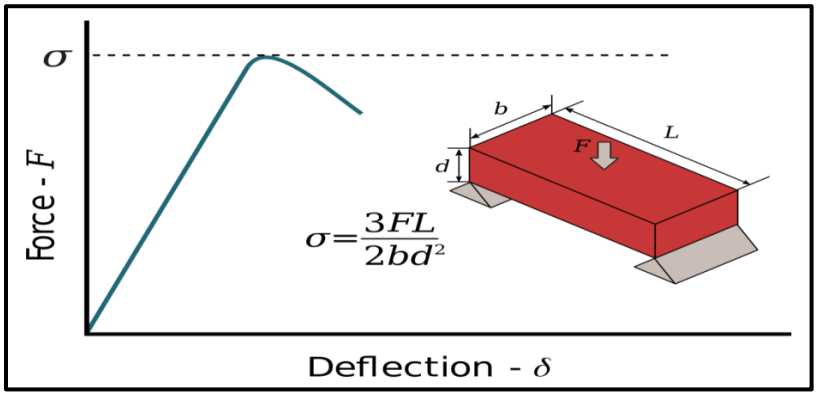

Figure 3.10 : Flexural strength schematic

The resulting stress for a rectangular sample under a load in a three-point bending setup (Fig. 3.10) .The equation of these two stresses (failure) yields:

$$\sigma = \frac{3FL}{2bd^2} \qquad \text{.....(3.2)}$$

Where:-

- **F** – the load (force) at the fracture point (N).
- **L** – the length of the support span (mm) .
- **b** – width (mm).
- **d** – thickness (mm).

3 . 6 . 2 . 4 Micro-Hardness Test

Vickers hardness test method is an accurate micro hardness test to measure the resistance offered by the polymer composite material when the load applied over the surface area of indentation. Vickers Pyramid number (HV) or Diamond Pyramid hardness (DPH) is the unit for measuring the Vickers hardness number. Readings

were taken on well-polished samples immediately after the indentation made as it highly depends on the elastic recovery of the material and surface homogeneity. The Vickers diamond hardness is found from:

$$VH = \frac{2P}{d^2}\sin\frac{136^\circ}{2} = 1.86\frac{P}{d^2} \qquad \text{.....(3.3)}$$

With d equal to the length of the diagonal measured from corner to corner. The device used in this test is located in Polymer Engineering and Petrochemical Industries Department / College of Materials Engineering / University of Babylon , ASTM E384 [175] , Fig. (3.11).

Figure 3.11 : Micro-Hardness device

3 . 6 . 3 Morphological Tests

3 . 6 . 3 . 1 SEM Microscopy

The major characteristic technique for analyzing surface morphology along (Pure PMMA,PMMA/Solid-lubricant ,PMMA/ Reinforcement ,PMMA/Hybrid).The samples were visualized in nitrogen atmosphere with SE (secondary electron) detecter using acceleration voltage 15 KV and the (35.0 Kx, 1.00 Kx ,90.0x) magnification were used for all samples. The surfaces of the samples are checked after wear testing, The collected results of SEM were analyzed using Image J software. The device used is (MIRA3 TESCAN) [176], is a high performance FEG-SEM

system that features a high brightness Schottky emitter, situated in Mashhad University of Medical Sciences / Islamic Republic of Iran, Fig. (3.12) .

Figure 3.12 : Scanning electron microscope

3 . 6 . 3 . 2 Digital Microscope

The polymer composites(pure PMMA,PMMA/Solid-lubricant ,PMMA/ Reinforcement , PMMA/Hybrid) samples was examined by using digital microscope (model AM4815T Dino-Lite Edge) made in (Kyoto Japan), with magnification rate (20x-220x), which is available in laboratory of college of materials engineering/University of Babylon. Fig.(3.13) shows an image for Digital microscope. Digital Microscope used to photograph surface of sample extrudate to observe melt fracture.

Figure 3.13 : The Digital Microscope Device

3 . 6 . 3 . 3 Contact Angle Test

The contact angle test was performed to evaluate the behavior of the surface tribology using solid lubricants and reinforcement fillers on wettability. The instrument used is the SL 200C - static photodynamic interfacial tension meter and contact angle meter manufactured by KINO Industry Co., Ltd. ASTM D7490-13 ,USA,[177] with range (0 to 180 degrees) which is available in laboratory of college of materials engineering/University of Babylon. Fig.(3.14). The contact angle device records the values of the contact angles and calculates their average value in two ways (Circle Fitting & Young Laplace Fitting methods)giving graphic values of the contact points in real time to monitor changes in the contact angle and images of the wetting drop and in both ways with video recording, Fig. (3.14).

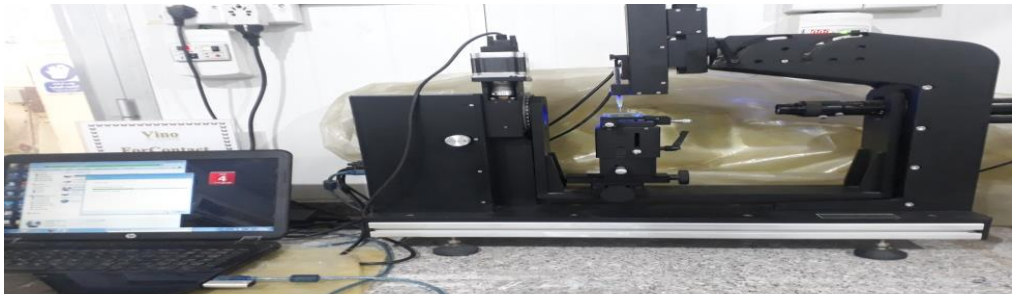

Figure 3.14 : Contact angle device

$$\gamma_S = \gamma_L \times cos\theta\, \gamma_{SL} \qquad \text{.....(3.3)}$$

Where :

γ_S – ***Solid surface Tension***

γ_L – ***Liquid surface Tension***

γ_{SL} – ***A solid and Liquid Boundary Tension***

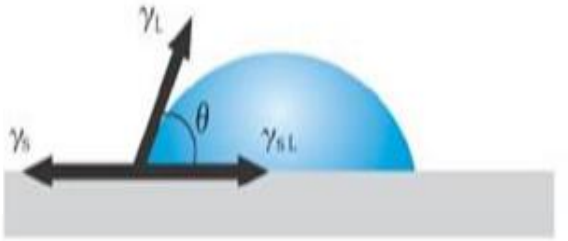

Figure (3.15) Contact Angle measurement

3 . 6 . 4 Rehological Test

3 . 6 . 4 . 1 Capillary Rheometer (SR20)

Capillary rheometer device (INSTRON CEAST, Country of Origin Italy), which is obtainable in laboratory of college of materials engineering/University of Babylon, as shown in Fig. (3.16 a). Capillary rheometer systems are manufactured in accordance with ASTM D3835 [178], international standards for rheology testing. This capillary rheometer simulates the method conditions, measuring the plastic materials flow conduct that symbolizes the rheology of materials through numerous capillary die. Control the device by a software program allows users to run the capillary rheometer. It offers the whole flow curve of tested materials and evaluation charts for material curves reference. Customized data export provides easy pstprocessing analysis and feeding for software simulation programs as in shown Figure (3.16 b).

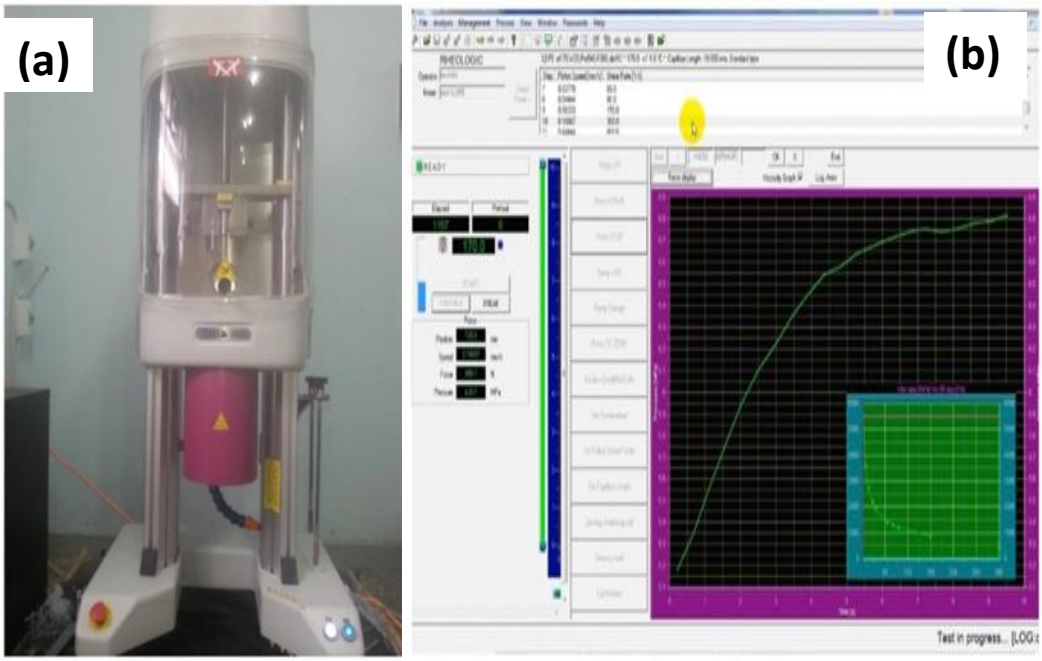

Figure 3.16 : (a) Capillary Rheometer (SR20) Device,(b) Software Program to Run the Capillary Rheometer.

CHAPTER FOUR

Results & Discussion

4 . 1 introduction

In this chapter, the results of the mechanical, tribological, and rheological tests of the prepared pure PMMA and PMMA with a variety of solid lubricant types will be discussed using, and also the physical and chemical properties will be discussed by using SEM, FTIR, and DSC techniques.

4 . 2 Mechanical Results

4 . 2 . 1 Hardness Results

Vickers hardness test method is an accurate micro hardness test to measure the resistance offered by the polymer composite material when the load applied over the surface area of indentation. Vickers Pyramid number (HV) or Diamond Pyramid hardness (DPH) is the unit for measuring the Vickers hardness number. Readings were taken on well-polished samples immediately after the indentation made as it highly depends on the elastic recovery of the material and surface homogeneity. The results showed that the presence of solid lubricants Paraffin wax and calcium Streate has a slight effect on decreasing the hardness of PMMA, while in the case of beeswax there is no real effect on the PMMA hardness which agreed with [179] . Adding fewer percentage of PMMA\MWCNT and PMMA\Hybrid increases hardness while high percentage decreases hardness which agreed with[180], Figure (4.1).

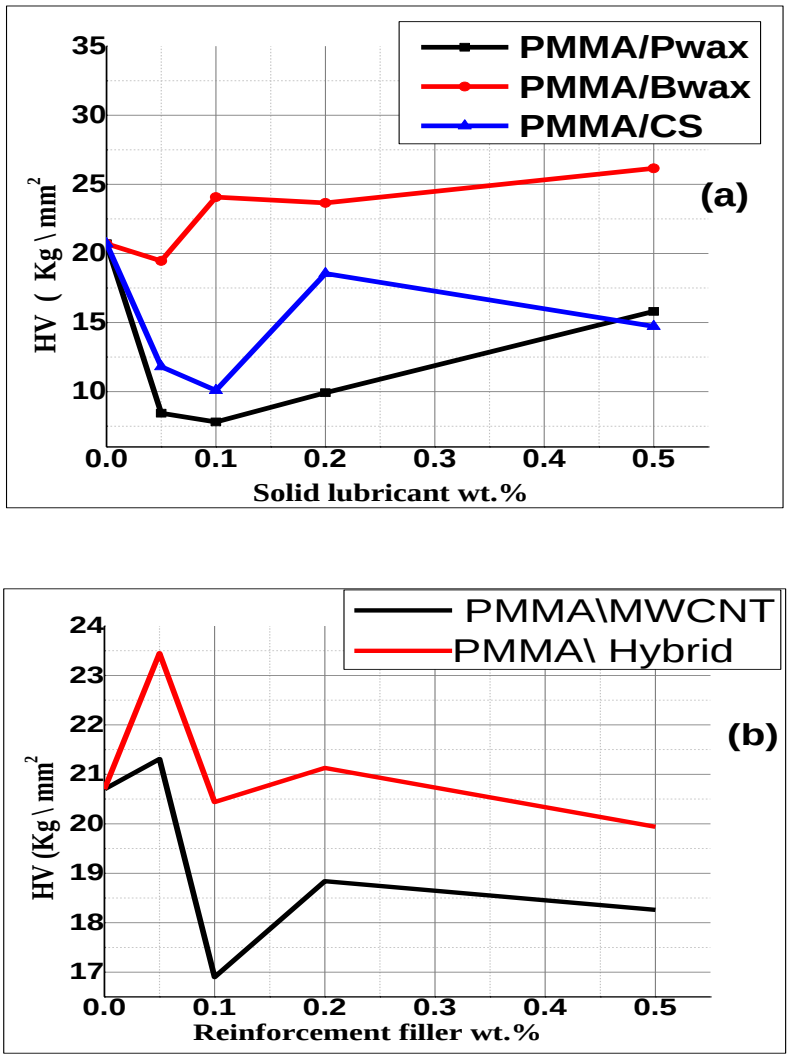

Figure 4.1 : Micro hardness measurement (a) As a function of solid lubricant wt.%,and (b) As a function of Reinforcement filler wt.%.

4 . 2 . 2 Flexural Results

The experimental results of flexural test for pure PMMA & PMMA with solid lubricant wt.% were detailed in table (4.1)

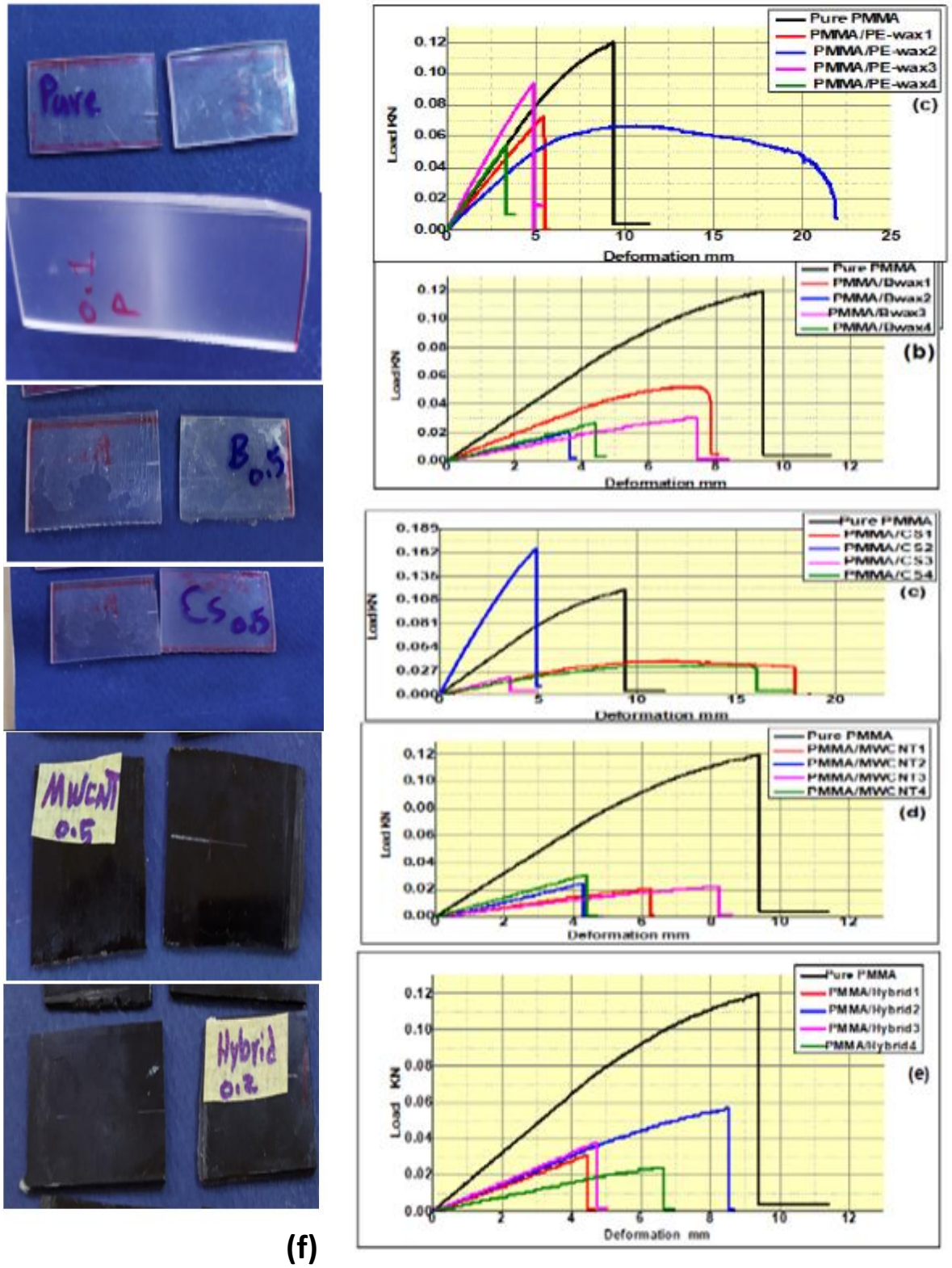

Figure 4.2 : Flexural results (a,b,c,d,e) Load-deformation of solid lubricant wt.%,and Re-inforcement filler wt.%, (f) Samples after test.

Different solid lubricants have a different effect on the flexural strength of PMMA based composites. The flexural strength of PMMA polymer filled with Beeswax decreased by 0.1 wt%, while the remaining percentages showed a less similar effect. Both of PMMA/PE-wax and PMMA/CS showed a less similar effect which agreed with [181]. The flexural strength of PMMA polymer filled with MWCNT decreased for all percentages This may be because the Nano-fillers acted as lubricants rather than as reinforcing fillings . PMMA polymer filled with Hybrid showed a less similar effect to PMMA polymer filled with Beeswax .

Table(4.1)Flexural test for pure PMMA , PMMA with solid lubricant wt.% & PMMA with reinforcement fillers wt.% .

Material	Flexural Strength *Mpa*	Max-deformation	Material	Flexural Strength *Mpa*	Max-deformation
Pure PMMA	72	11.4	PMMA/CS3	22	4.8
PMMA/PE-wax1	42	5.7	PMMA/CS4	37	4.5
PMMA/PE-wax2	——	21.9	PMMA/MWCNT1	36	4.6
PMMA/PE-wax3	40	5.3	PMMA/MWCNT2	24	8.6
PMMA/PE-wax4	23	6.8	PMMA/MWCNT3	28	4.8
PMMA/Bwax1	26	8	PMMA/MWCNT4	24	6.3
PMMA/Bwax2	12	3.8	PMMA/Hybrid1	35	8.6
PMMA/Bwax3	31	8.3	PMMA/Hybrid2	46	8.6
PMMA/Bwax4	32	4.7	PMMA/Hybrid3	35	6.9
PMMA/CS1	34	16.9	PMMA/Hybrid4	31	6.9
PMMA/CS2	180	5			

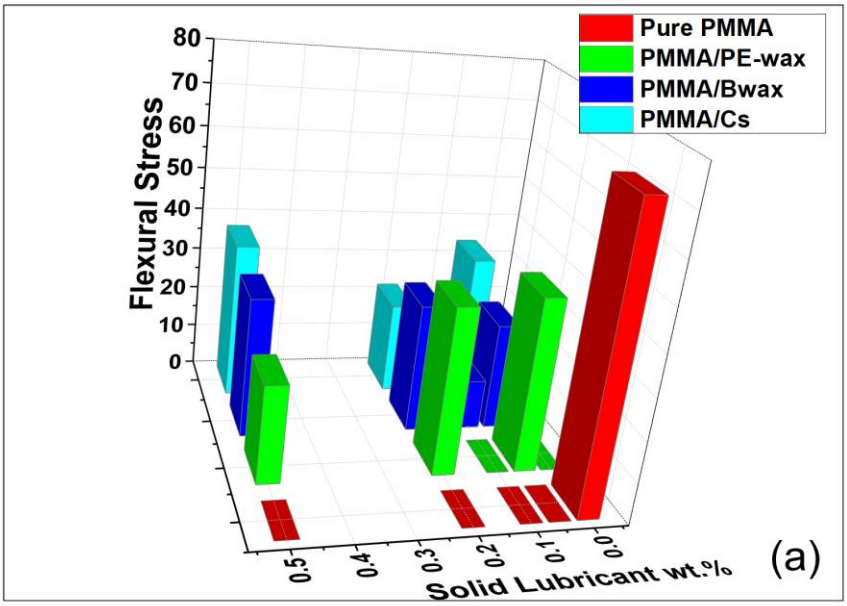

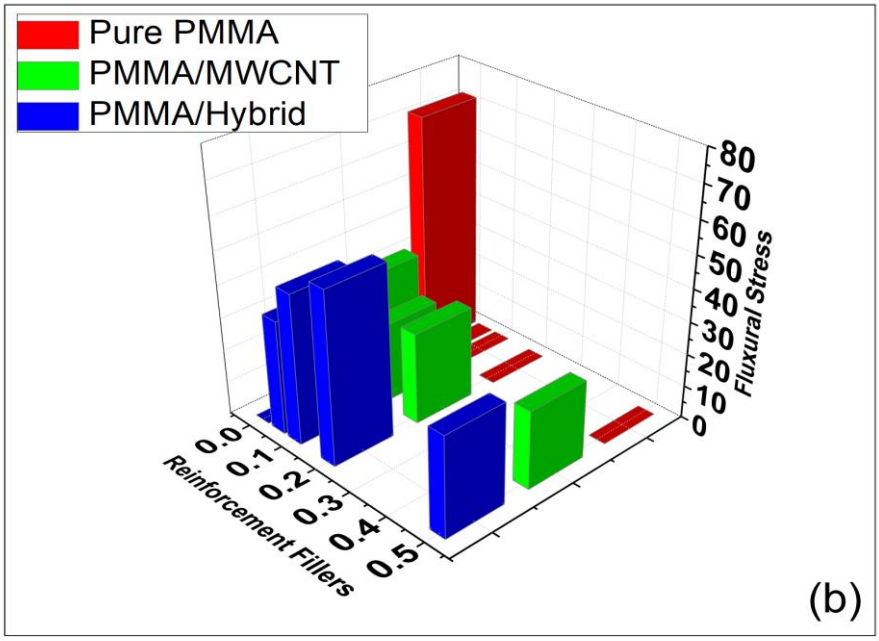

Figure 4.3 : (a) Flexural Stress as a function of solid lubricant wt.% ,and , (b) Flexural Stress as a function of Reinforcement filler wt.% .

4 . 2 . 3 Friction& Wear

4 . 2 . 3 . 1 Coefficient of friction

Fig. (4.4) shows the friction coefficient as a function of applied force of the Pure PMMA and PMMA based a variety solid lubricant materials. In general, the presence of the solid lubricants greatly reduces the coefficient of friction, as shown in Fig. (4.4 a) a decrease in the friction coefficient of PMMA/ PE-wax (0.5 wt. %) at (5 N) from (0.6 to 0.45) and this agreed with [182, 183]. While Fig. (4.4 b) shows that the friction coefficient of PMMA and PMMA based Bwax lubricant was decreased from (0.6) for pure PMMA to (0.1) for PMMA/Bwax2 , and this may be due to increasing the ability of the migration of the bwax to the surface of contact, which causing a significant decrease in the coefficient of friction. Figure (4.4 c) shows that the effect of the presence of Calcium Streate with different ratios on reducing the coefficient of friction of PMMA. It can be seen that the friction coefficient was decreased significantly from (0.55) for pure PMMA to 0.1 for PMMA/ CS (0.2 wt.%) at normal load 5N which agreed with [184].In terms of increased wear resistance and associated mechanical properties, calcium stearate was found to be the most effective for high molecular weight matrix, which reduces the surface temperature of the sample (the final product). It was observed that carbon nanotubes act as a solid lubricant, and under lubrication conditions, it could be classified as a type of lubricant additives. Under dry slip conditions, the addition of carbon nanotubes can lead to a significant reduction in friction and wear. Carbon nanotubes formed a carbon layer covering the contact surfaces as well as due to the low shear property of carbon nanotubes, the friction coefficient of (PMMA/MWCNT4)was decreased (at 6 N from 0.6 to 0.34 and at 12 N from 0.7 to 0.31) ,while the friction coefficient of(PMMA/Hybrid2) decreased (at 5 N from 0.56 to 0.1 and at 12 N from 0.7 to 0.37) Under dry friction as shown in fig. (4.4 d ,

e), the effective time of MWCNTs is limited, and the coefficient of friction decreases as the MWCNTs content increases. The wear mechanism under dry friction is mainly adhesive wear. Observations of worn surfaces by SEM provide knowledge about both, the role that lubricant solids play in the reduction of wear rate, and the acting wear mechanisms .Fig.(4.5) shows the worn surfaces of the PMMA and PMMA/PE-wax composite filled with additional solid lubricant tested under normal load 12N, the worn surfaces of the (0.1 and 0.2) composite were much smoother compare with the worn surface of pure PMMA composite.

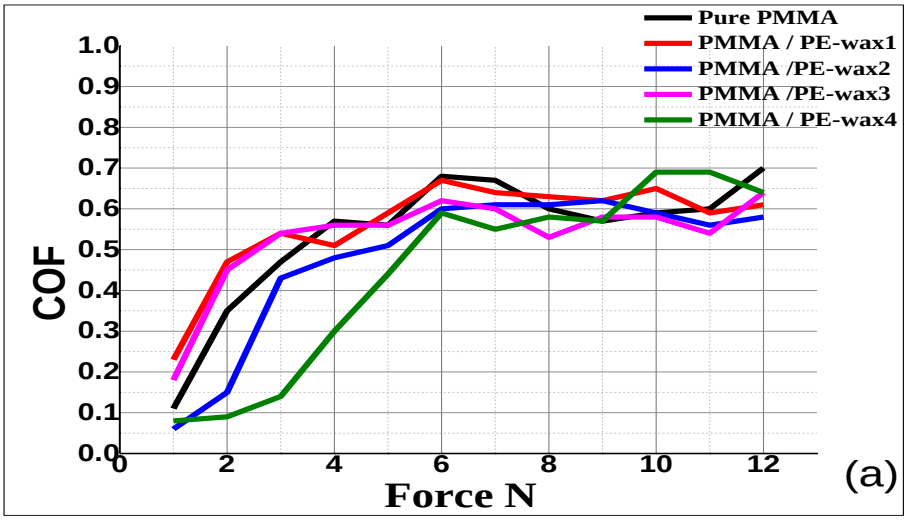

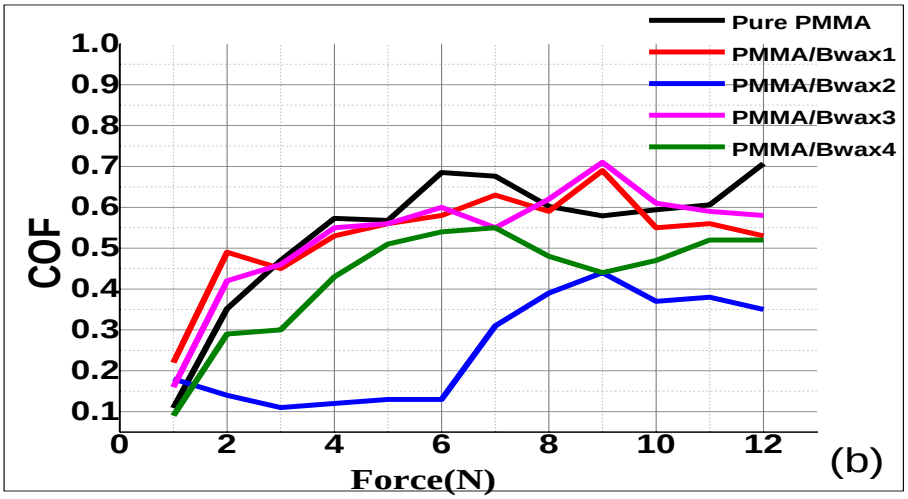

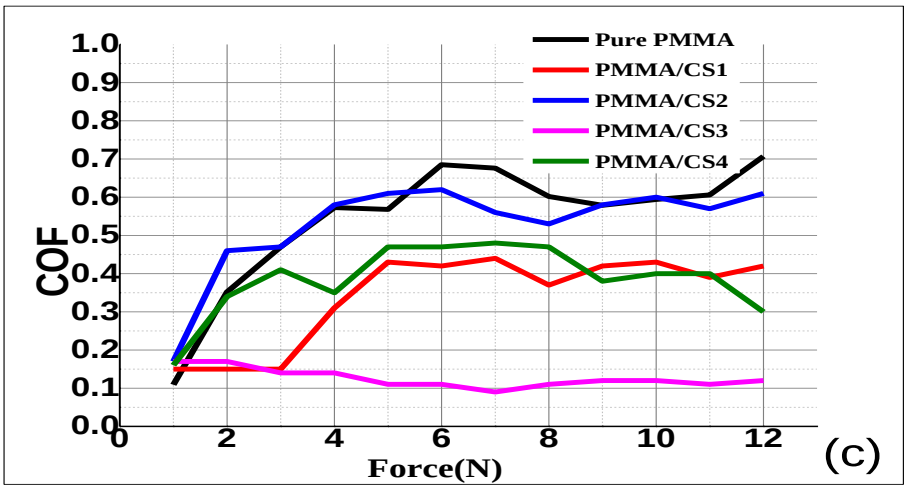

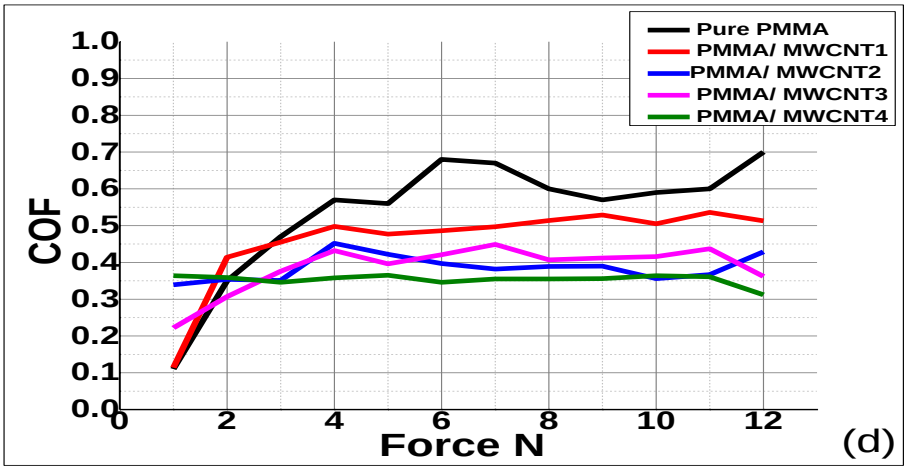

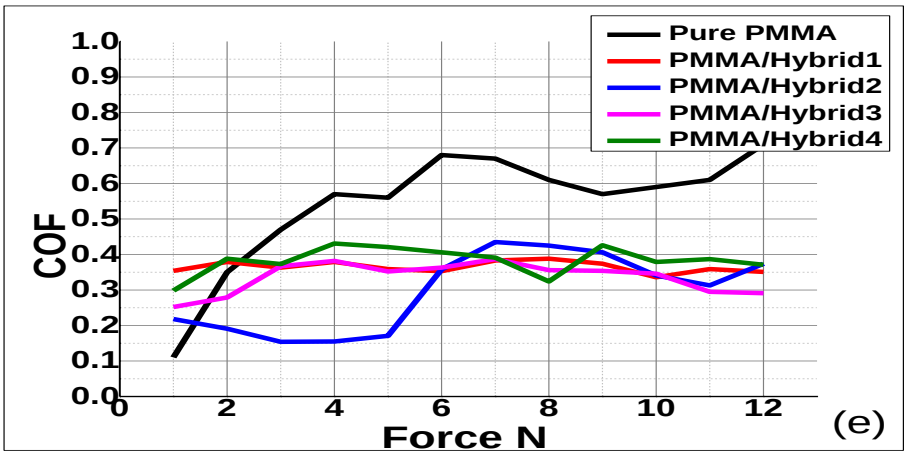

Figure 4.4 : Coefficient of friction vs. applied loads (a) PMMA/ PE-wax, (b) PMMA / Bwax , (c) PMMA / CS, (d) PMMA\MWCNT , and (e) PMMA\Hybrid.

4 . 2 . 3 . 2 Wear Rate Effect

After calculating the wear rate from the equation (2.3)in chapter (2),through the figure (4.3), it was found that the PMMA/CS2 at (0.1 wt.%) had a greater wear rate than pure PMMA. compared to the rest of solid lubricant, PMMA/Bwax recorded lowest wear rate. Generally , PMMA/Bwax3 and PMMA/Bwax4 have lower young's modulus as shown in Fig (4.3 a).With respect to reinforcement composites , PMMA/MWCNT3, PMMA/MWCNT4, PMMA/Hybrid1,and, PMMA/Hybrid2 recorded lowest wear rate as shown in Fig.(4.4 b).

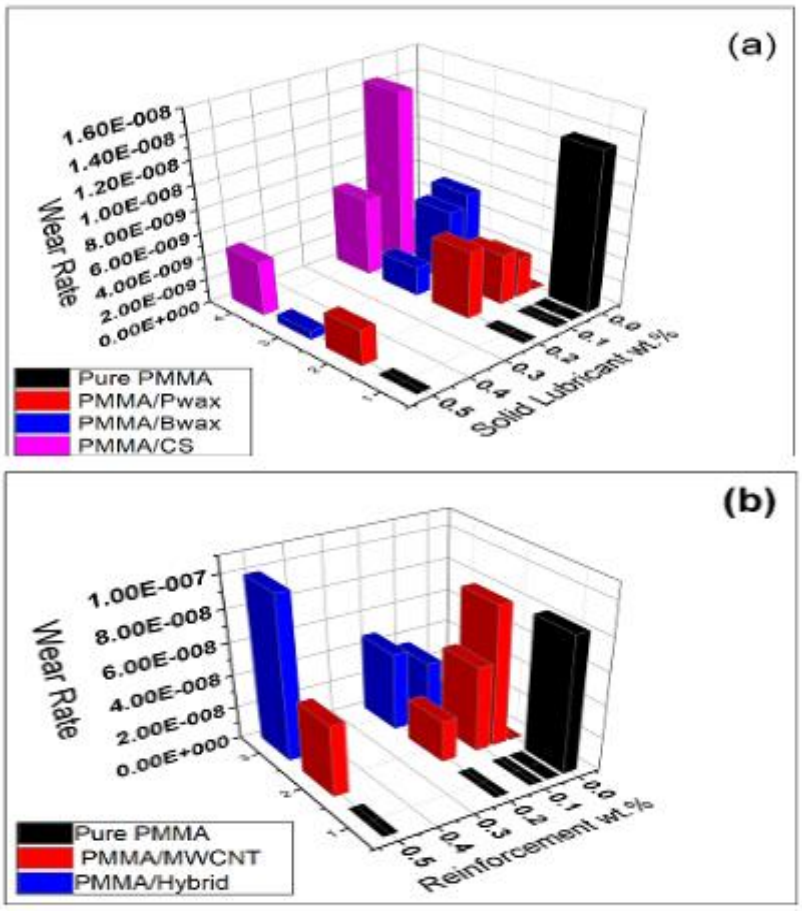

Figure 4.5 : Effect of applied loads on wear rate for:(a) As a function of Solid lubricated wt.%,and (b) As a function of Reinforcement wt.%, at constant sliding time of 180 min .

4.2.3.3 SEM Results

As shown in Fig. (4.6) where the worn surface of pure PMMA showed a clear plastic deformation due to adhesive mechanism of wear, breakage of the Pure PMMA matrix occurs at the interface.

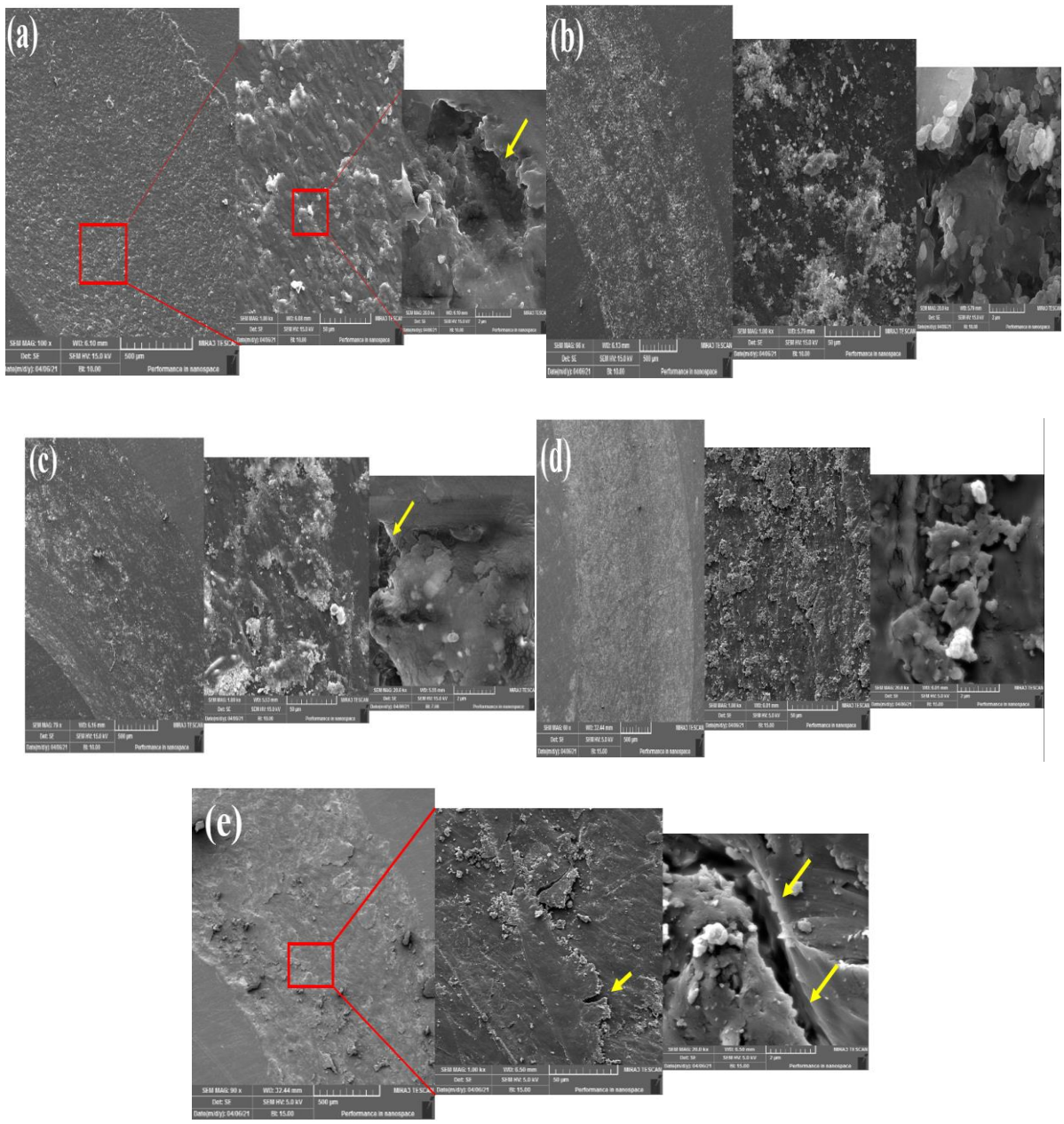

Figure 4.6 : Detailed morphology of wear surface of PMMA following micro abrasion under (12 N) load as a function of sliding distance(a) Pure PMMA , (b) PMMA/PE-wax1 ,(c) PMMA/PE-wax2,(d) PMMA/PE-wax3,and ,(e) PMMA/PE-wax PMMA/PE-wax4.

The presence of PE-wax caused enhancement in the worn surface due to the decreasing the adhesive nature of the contact zone Fig.(4.7), with increasing the weight percentage of PE-wax to 0.5% caused increase in wear rate due to a loss of mechanical properties because of solid lubricant materials assisted softening polymeric.

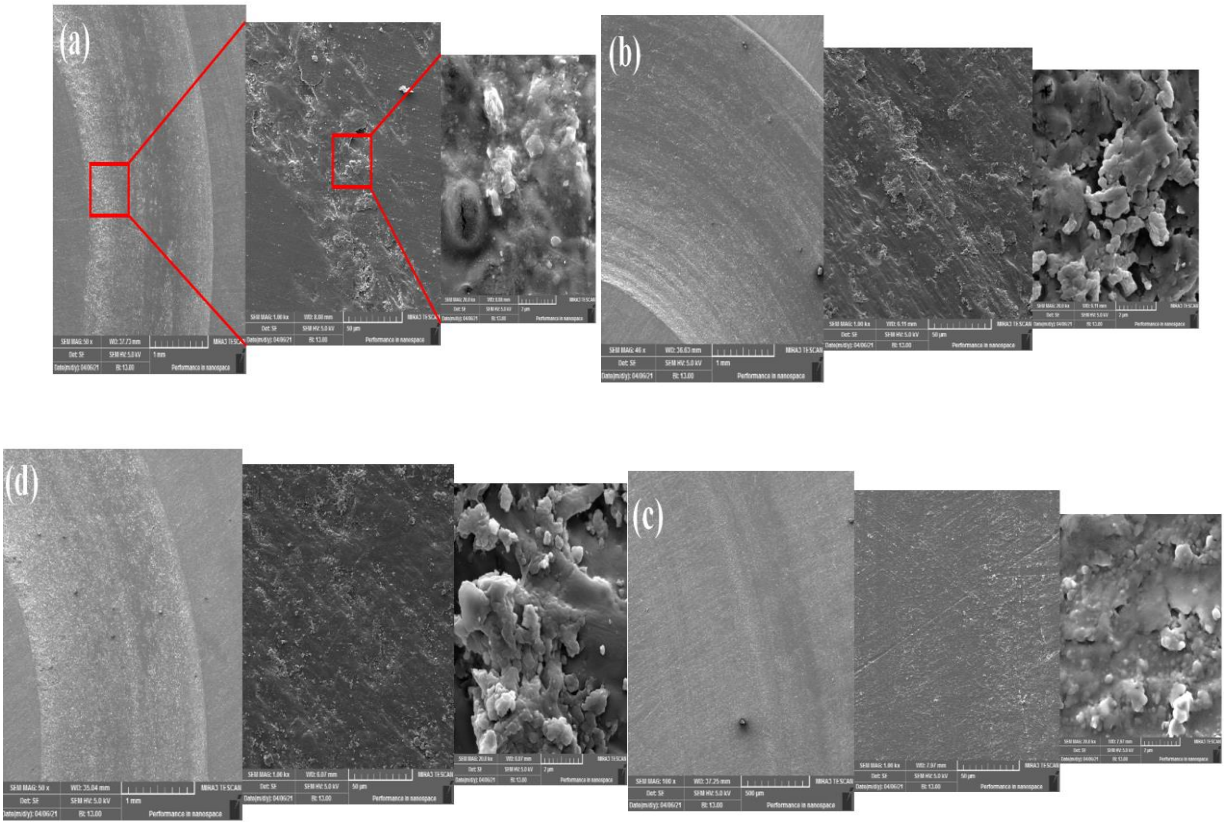

Figure 4.7: Detailed morphology of wear surface of PMMA following micro abrasion under (12 N) load as a function of sliding distance(a) Pure PMMA , (b) PMMA/Bwax1 ,(c) PMMA/Bwax2,(d) PMMA/Bwax3,and ,(e) PMMA/B-wax PMMA/Bwax4.

Fig.(4.8) where the worn surface of PMMA/Bwax showed a clear enhancement in wear resistance. The resulting surface is smooth and this indicates that the lubricating materials reduce the intermittent shear stress and thus reduce the adhesion friction compound . This confirms the ability of Beeswax to migrate through PMMA

structure to the interface and decreasing the coefficient of friction and therefore improve wear resistance. On the other hand, the surface of the worn of PMMA/CS Fig.(4.9) a clear enhancement in wear resistance. The resulting surface is smooth and this indicates that the lubricating materials reduces friction but does not protect against abrasive particles. Since calcium stearate is relatively soft in wear effect cannot save the matrix from the influence of fixed abrasive particles, as in [185].

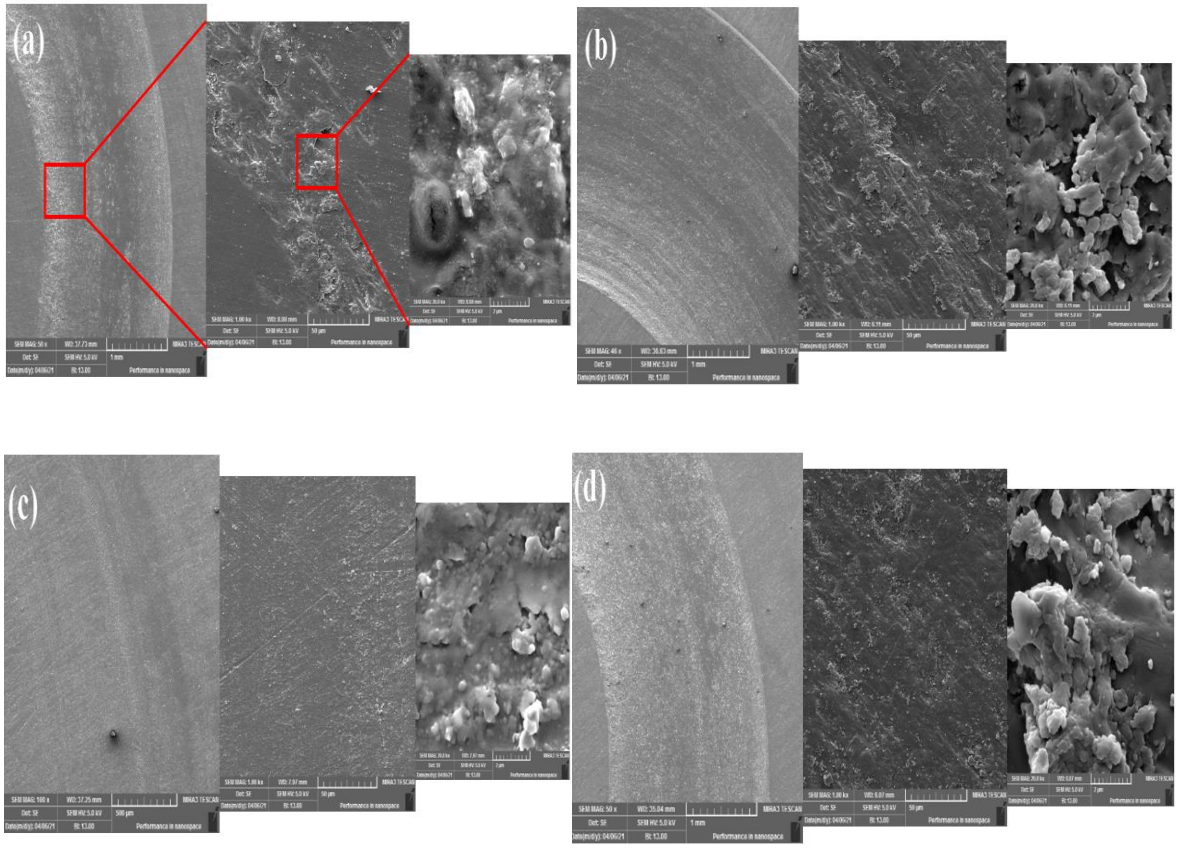

Figure 4.8 : Detailed morphology of wear surface of PMMA following micro abrasion under (12 N) load as a function of sliding distance(a) Pure PMMA , (b) PMMA/CS1 , (c) PMMA/SC2,(d) PMMA/CS3,and ,(e) PMMA/PE-wax PMMA/CS4.

Through Fig(4.9) the surface of the worn composites filled with MWCNT show areal changes in the pure PMMA behavior about wear resistance. The resulting

surface is achieved superior surface smoothness and this indicates that the reinforcement fillers reinforced tribological surface by reduces friction but it can be seen from the internal worn-out structure. The more friction, the less the internal structure's ability to withstand continuous rubbing.

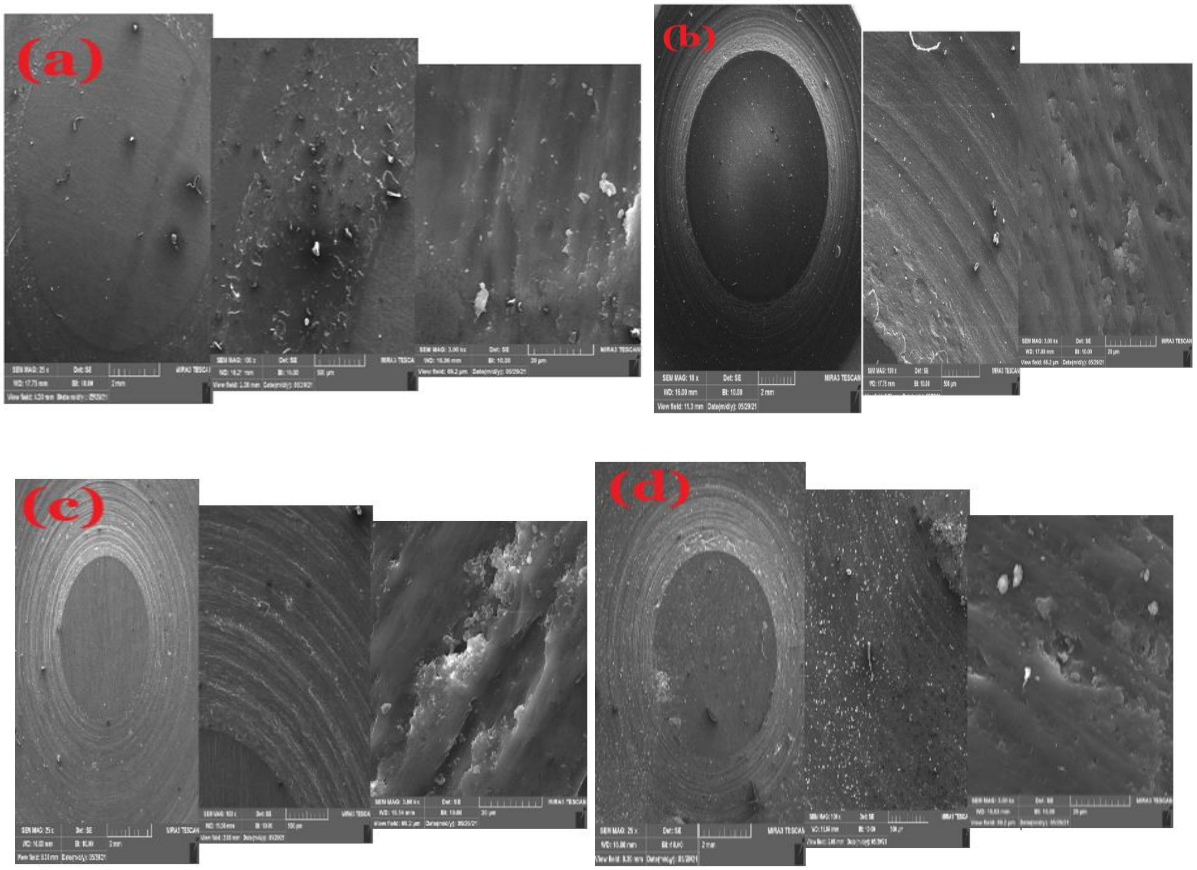

Figure 4.9 : Detailed morphology of wear surface of PMMA following micro abrasion under (12 N) load as a function of sliding distance(a) Pure PMMA , (b) PMMA/MWCNT1 ,(c) PMMA/MWCNT2,(d) PMMA/MWCNT3,and ,(e) PMMA/MWCNT4.

Through Fig (4.10) the surface of the worn Hybrid compound a clear enhancement in wear resistance. The resulting surface is smoother and this indicates that the Hybrid compound reinforced tribological surface by reduces friction but the abrasive effect still exists .

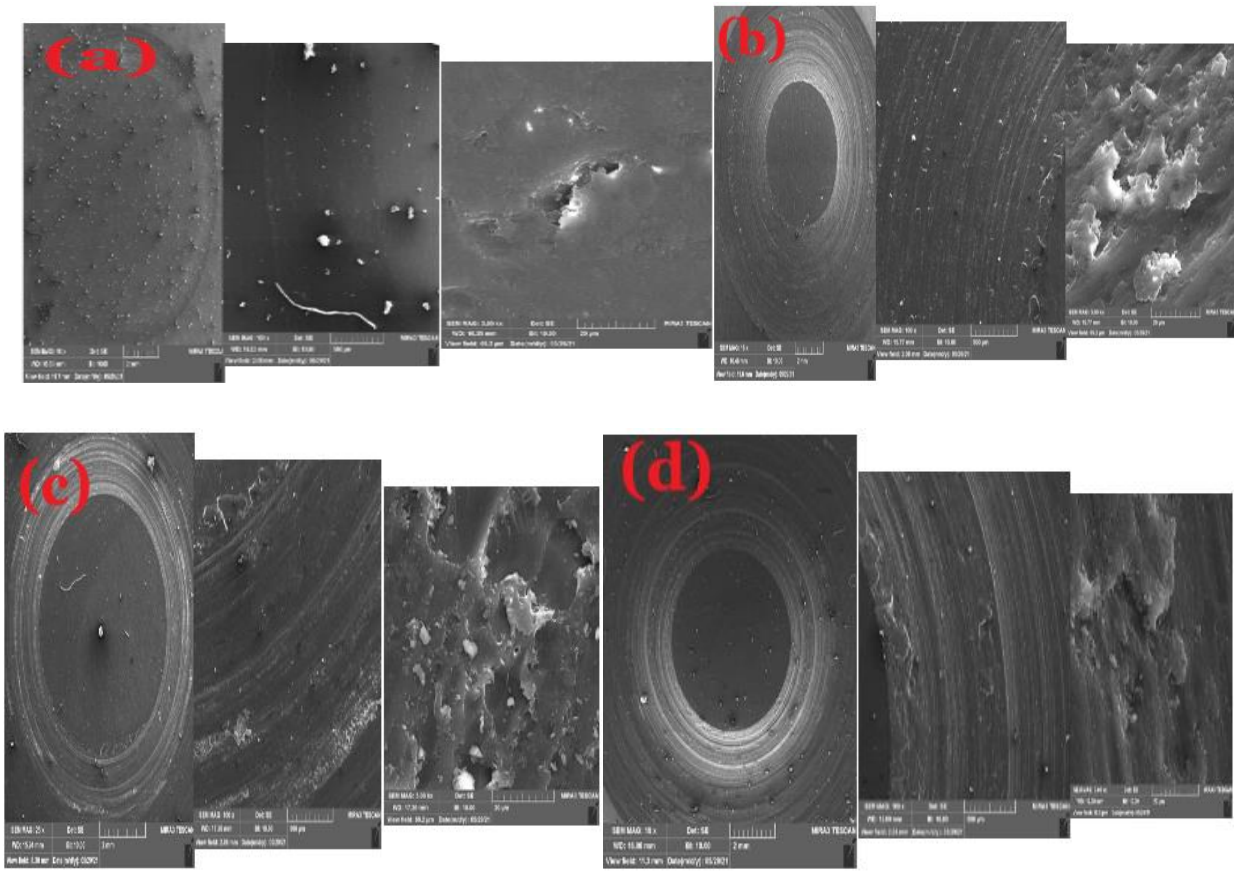

Figure 4.10 : Detailed morphology of wear surface of PMMA following micro abrasion under (12 N) load as a function of sliding distance(a) Pure PMMA , (b) PMMA/Hybrid1 ,(c) PMMA/Hybrid2,(d) PMMA/Hybrid3,and ,(e) PMMA/Hybrid4.

4 . 2 . 4 Scratch Test

The residual effect after performing the scratch test on the vertical force (15 N) and the diameter of the scratch ball (570 μm) and under test conditions (room temperature, constant distance, loads from 5-20 N) for all samples. Scratch damage is now being recognized as one of the key factors limiting the service life of polymer products in many engineering applications. The scratch track of the unfilled pure PMMA exhibited extensive cracking and tearing Fig. (4.11 a). Cracks generally occurred when the tensile stress behind the moving indenter exceeded the strength of the material. By adding 0.05 wt.% as-received PE-wax, the scratch damage changed to ductile plowing with no cracks inside the scratch track .Increasing the

wt. % of PE-wax to 0.1, further reductions in scratch width and depth were obtained. With 0.5wt% PE-wax large voids are formed caused by weak interfacial interaction between solid lubricant particle and matrix at identical test conditions. Fig.(4.11 b) shows the scratch damaged region for PMMA, PMMA/CS1,and, PMMA/CS3 revealing the parabolic and repetitive pattern of scratch tracks with enhanced plastic flow comparing with pure PMMA. With (CS 0.5wt.%) exhibited again extensive cracking and tearing like the behavior of pure PMMA, because the high percentage of the solid lubricants may weaken the structure of PMMA. Fig. (4.11 c) a change in the apparent plastic deformation behavior for pure PMMA was observed, and through the change in the width and shape for PMMA filled with Bwax (at 0.1, 0.2 and 0.5wt.%) the residual crack decreased and showed a clear change in the deformation behavior, and the elastic deformation component increased and the residual groove showed a very smooth area which indicated that the Bwax efficiency to immigrate to the contact zone and play major roles in decreasing the interfacial shear stress. In general, the presence of solid lubrication (Bwax) in PMMA had a positive effect in raising the value and resisting scratch hardness. Fig.(4.11 d)) shows the results of abrasion resistance due to scratching on the surface of the samples. (PMMA / Bwax) showed the highest values of hardness for scratch resistance and for all filling percentages.

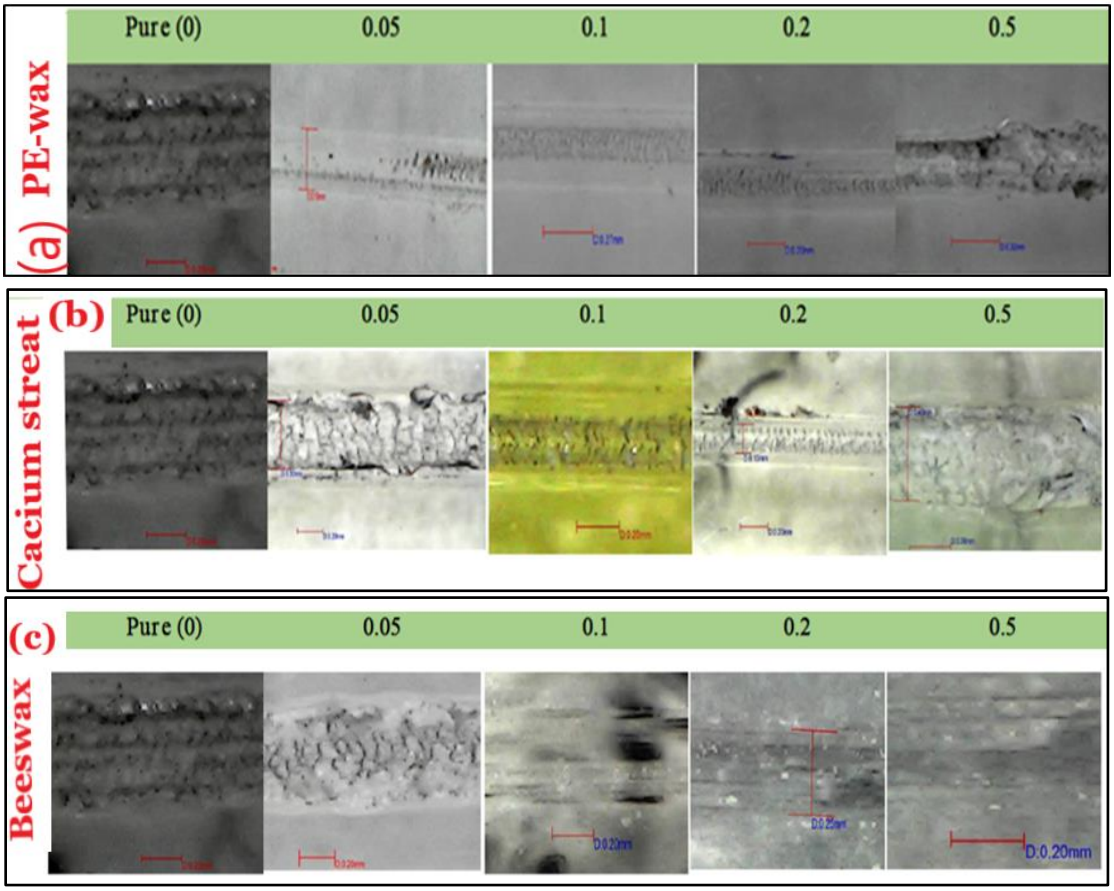

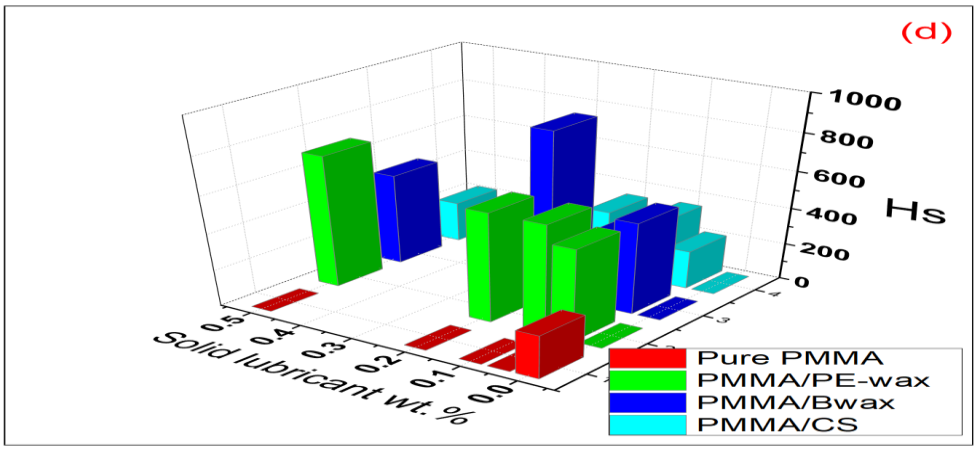

Figure 4.11 : (a,b,c) OM topography showing scratch morphology of pure PMMA, PMMA/ solid lubricant wt.%,(d) Scratch hardness of pure PMMA,PMMA/solid lubricant wt.%.

In Fig.(4.12 a) the transformational crack deformation were observed from the plastic behavior of the pure PMMA to the elastic behavior for Hybrid composites. It showed a significant decrease in interfacial shear stresses and crack width. furthermore , there is a noticeable change in the apparent plastic deformation behavior of Pure PMMA due to the presence of MWCNT in PMMA that had a positive effect in raising the value and resisting scratch hardness for all samples alike. The PMMA/(MWCNT at ratio (0.1, 0.2 and 0.5 wt%) showed the residual crack decreased and showed a clear change in deformation behavior, the elastic deformation component increased and the residual groove showed a very smooth area indicating that the efficiency of the (MWCNT) to migrate to the contact area and play a major role in reducing interfacial shear stress. This information provides insight into the mechanical faults that occur during scratching , enabling researchers to discover and diagnose mechanical defects and further investigate the scratching behavior of the material under test, and scratch hardness tests can be completed within 10 minutes with good accuracy and repeatability. Compared with the traditional indentation procedure, the scratch hardness test in this study provides an alternative solution for measuring hardness ,and is useful for quality determination and development of new polymeric materials. Fig.(4.11 d) shows the results of abrasion resistance due to scratching on the surface of the samples. (PMMA / Bwax) showed the highest values of hardness for scratch resistance and for all filling percentages, while PMMA \ MWCNT at (0.2) and PMMA / Hybrid at (0.1) recorded the highest values for hardness Scratching, Fig. (4.12 c).

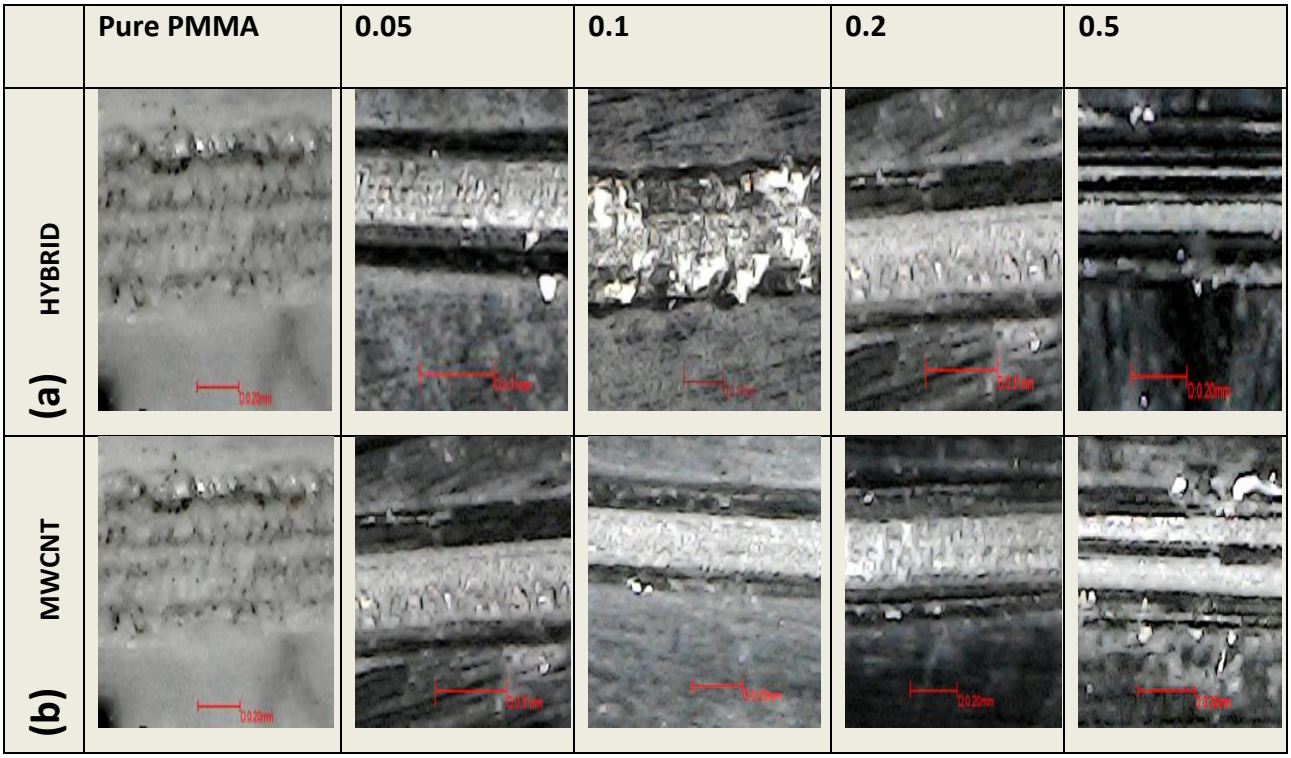

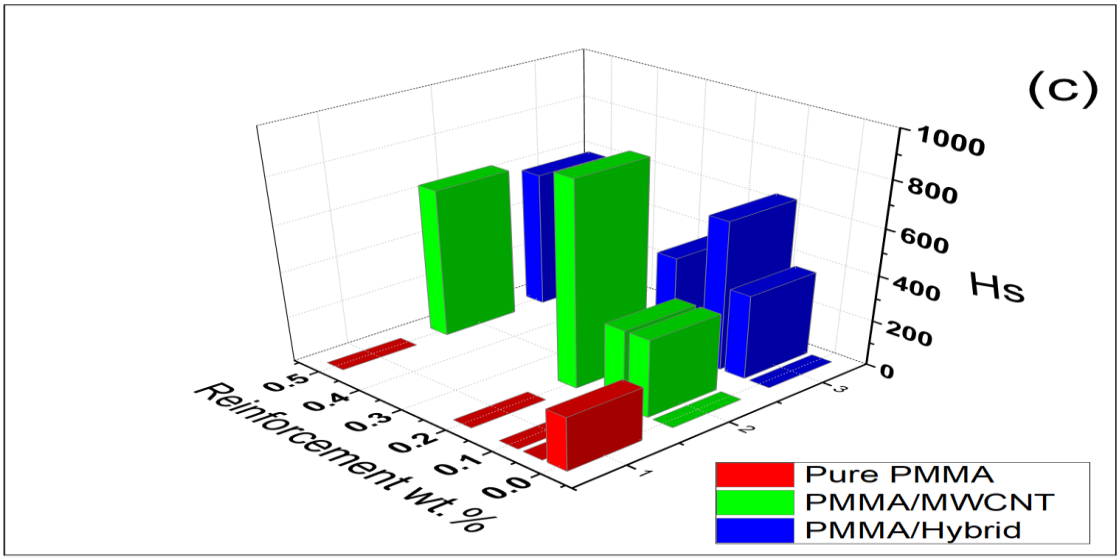

Figure 4.12 : (a,b) OM topography showing scratch morphology of pure PMMA, PMMA/ reinforcement filler wt.%,(c) Scratch hardness of pure PMMA,PMMA/reinforcement filler wt.%.

4 . 3 Rheological Results

4 . 3 . 1 Shear Viscosity Results

Pure PMMA was extruded as well as all lubricated PMMA prepared with different proportions of solid lubricants. As discussed above one of the main objectives of this work was to identify a processing solid lubricant suitable for PMMA processing. In other words identify a processing solid lubricant that would postpone the onset of helical flow and thus gross melt fracture to higher rates. From all the solid lubricant particles tested, the only ones which had an effect on the gross melt fracture of PMMA were the internal solid lubricants of Bees wax. Fig. (4.13 a) shows the flow curve of pure PMMA ,PMMA/PE-wax , It seems that the use of these lubricants cause a decrease in the extrusion process. The trend of the shear viscosity of PMMA with solid lubricant Bwax shown in Fig. (4.13 a) initially followed the typical pseudo-plastic shear-thinning behavior, and the shear viscosity decreased significantly, when the shear rate increased from approximately (50 to 400 s^{-1}) , then change in the shear viscosity tended to be flatter, in contrast PMMA/PE-wax and PMMA/CS showed gross melt fracture from (50 to 500 s^{-1},50 to 300 s^{-1}) respectively as shown in Fig.(4.13 b , c). Fig. (4.13 e) shows the flow curve of pure PMMA ,PMMA with MWCNT and Hybrid, it seems that the use of these fillers cause a decrease in the extrusion process .The trend of the shear viscosity of PMMA with MWCNT initially followed the typical pseudo-plastic shear-thinning behavior close to PMMA with solid lubricant (Bwax) results as shown in fig.(4.13 a), and the shear viscosity decreased significantly, when the shear rate increased from approximately (50 to 400 s^{-1}) , then change in the shear viscosity tended to be flatter too. Fig.(4.13 e) ,in contrast ,PMMA\Hybrid1, PMMA\Hybrid2 showed gross melt fracture from (50 to 400 s^{-1}),PMMA\Hybrid3,PMMA\ Hybrid4 showed flatter shear viscosity from (400 to

900 s^{-1}). During the sonication process, there is a break and fluctuation in the polymeric chains, so the viscosity decrease, the molecular weight and the shear stress increase accordingly. As the chains are broken up, the molecular weight distribution tends to be the broad molecular weight distribution.

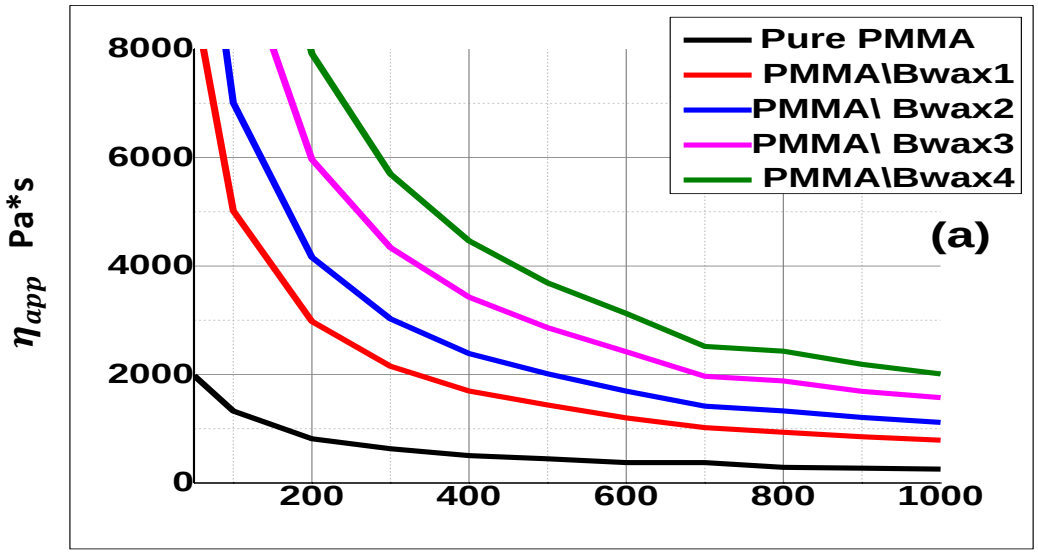

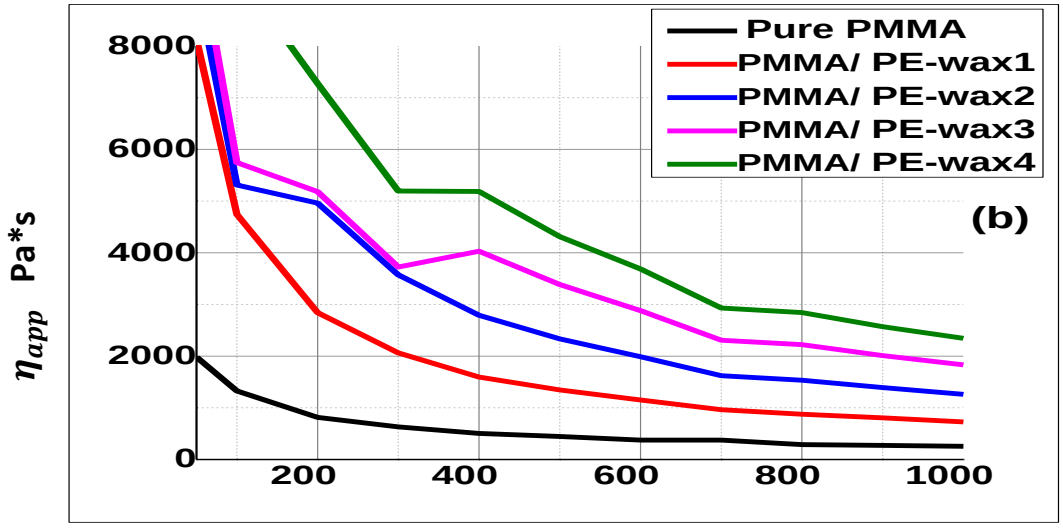

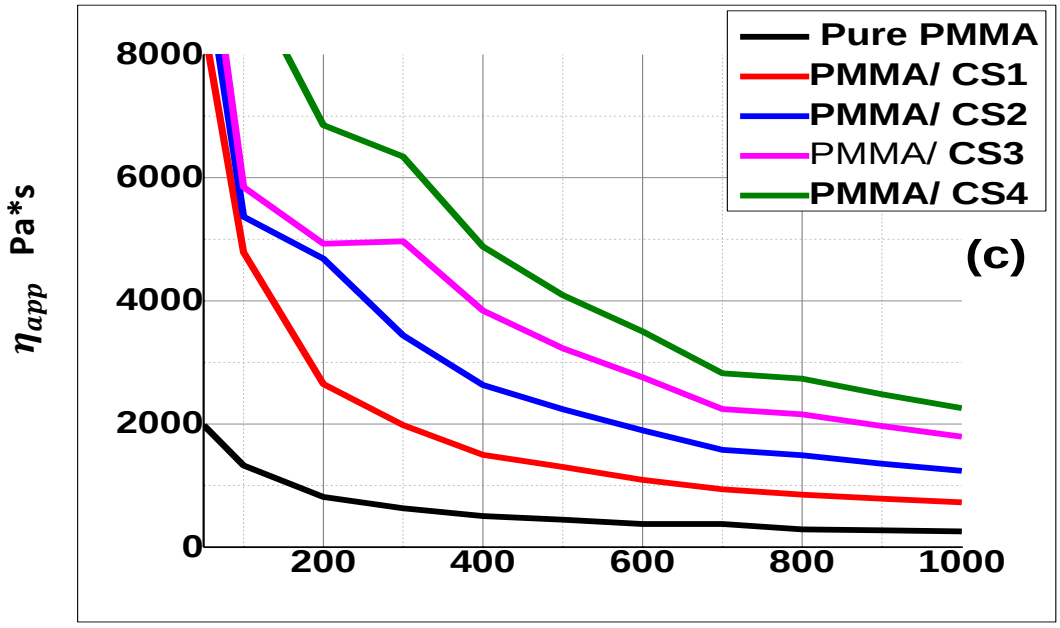
Pure PMMA
PMMA/ CS1
PMMA/ CS2
PMMA/ CS3
PMMA/ CS4
(c)
8000
6000
4000
2000
0
200
400
600
800
1000
η_{app} Pa*s
$\dot{\gamma}_{app}\ s^{-1}$

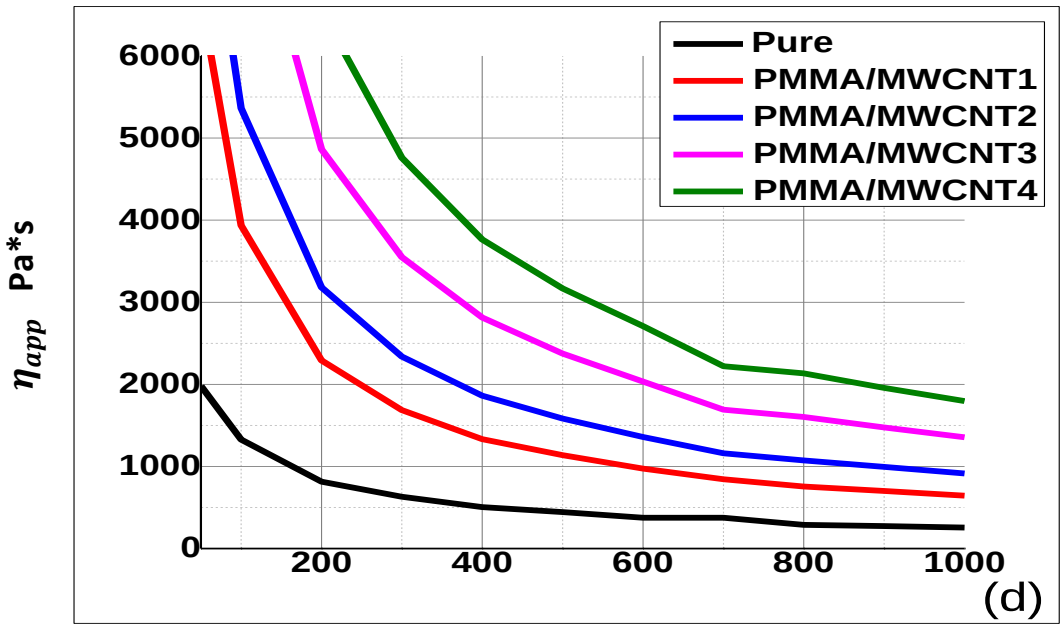
Pure
PMMA/MWCNT1
PMMA/MWCNT2
PMMA/MWCNT3
PMMA/MWCNT4
(d)
6000
5000
4000
3000
2000
1000
0
200
400
600
800
1000
η_{app} Pa*s
$\dot{\gamma}_{app}\ s^{-1}$

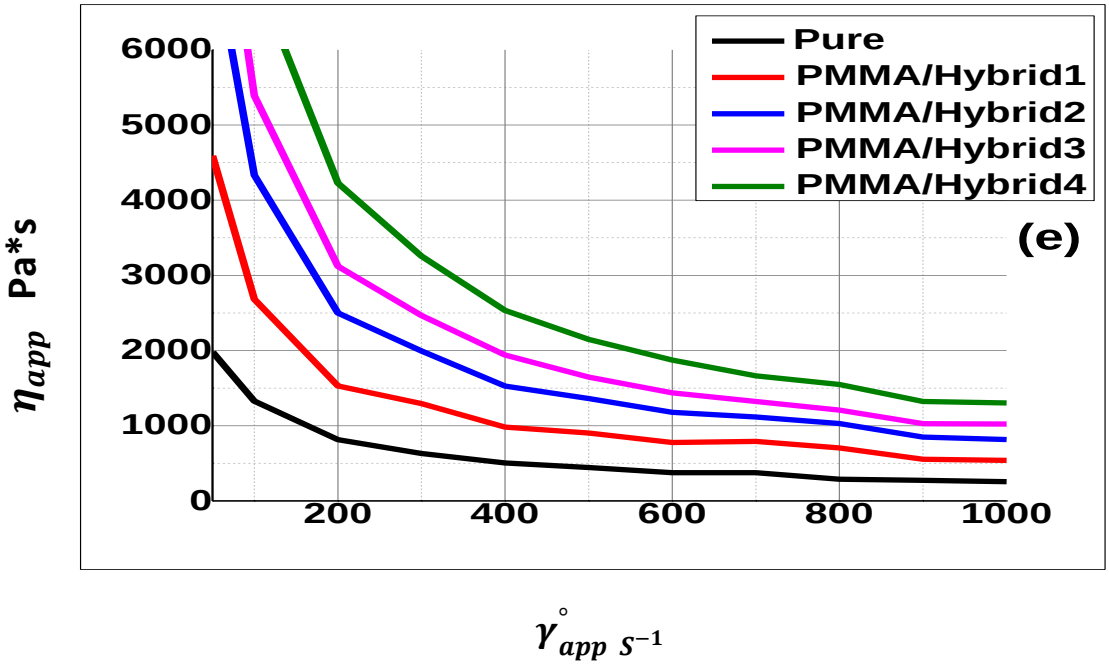

Figure 4.13 : Shear viscosity behavior of pure PMMA melt with: (a,b,c) PMMA/solid lubricant wt.% melts , (d,e) PMMA/reinforcement fillers & Hybrid compound melts ,with the shear rate increasing in a capillary at die 1 mm ,temperature 240 C°.

4 . 3 . 2 Shear Stress Results

Shear stress plays an important role to indicate the critical value of the surface quality. Figure (4.14), shows the flow curve of pure PMMA ,PMMA with solid lubricant for a tube with a diameter of 1 mm and 240 **C°**. These curves are perfectly continuous with change in the slope around PMMA/PE-wax1, PMMA/PE-wax2 at (0 s^{-1} and 600^{-1}) respectively as shown in fig.(4.14 a ,b) , shows the flow curves of pure PMMA ,PMMA /Bwax are perfectly continuous with change in the shear stress tend to be flatter, shear stress increased with shear rate increased from approximately (0 to 600 s^{-1}). PMMA/CS2 , PMMA/CS3, PMMA/CS4 at (100 s^{-1}, 300 s^{-1} and 200 s^{-1}) respectively ,the shear stress increases with the shear rate increasing for temperature 240 **C°** at Die = 1mm.The processability in capillary extrusion of pure PMMA ,PMMA with solid lubricant is determined in terms of the

onset of melt fracture phenomena. The critical shear rates and stresses at which extrudate distortions appear. The polymer processability was effected by increasing the solid lubricant on their processability. The increase in the ratio of solid lubricant and the type of solid lubricant are the main factors in reducing the friction between the mold wall and the material due to the ease of flow of the material.

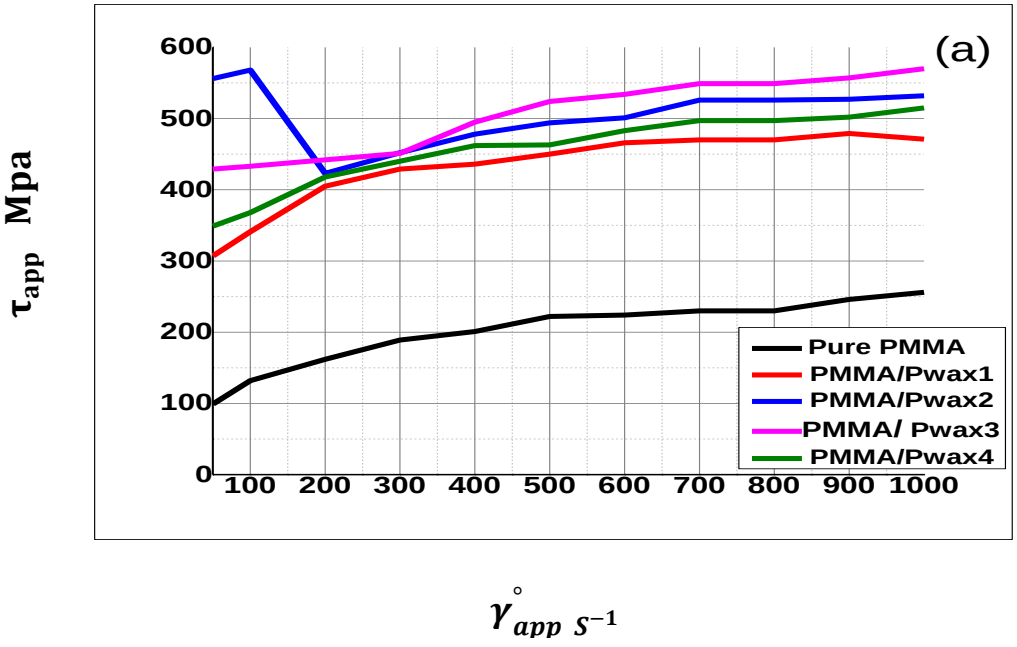

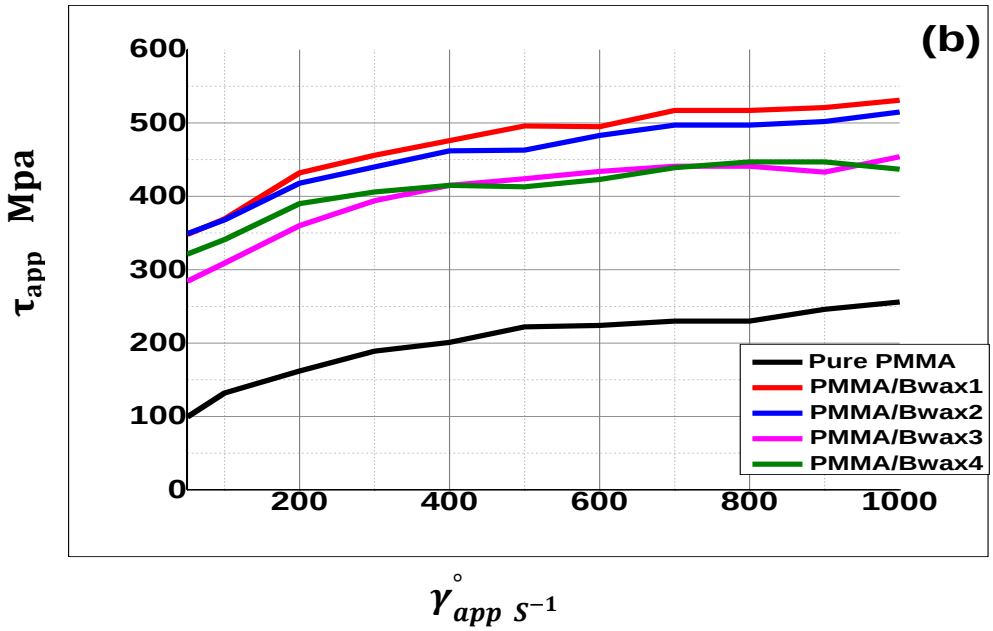

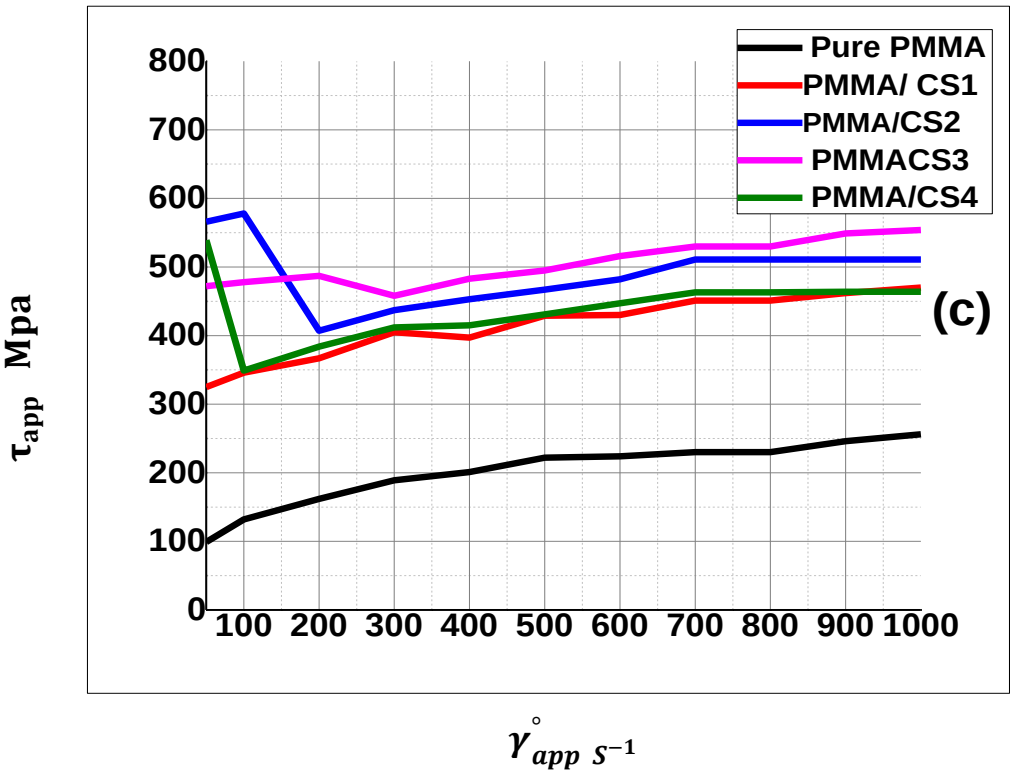
Pure PMMA
PMMA/ CS1
PMMA/CS2
PMMACS3
PMMA/CS4
(c)
800
700
600
500
400
300
200
100
0
100 200 300 400 500 600 700 800 900 1000
τ_{app} Mpa
$\dot{\gamma}_{app}\ s^{-1}$

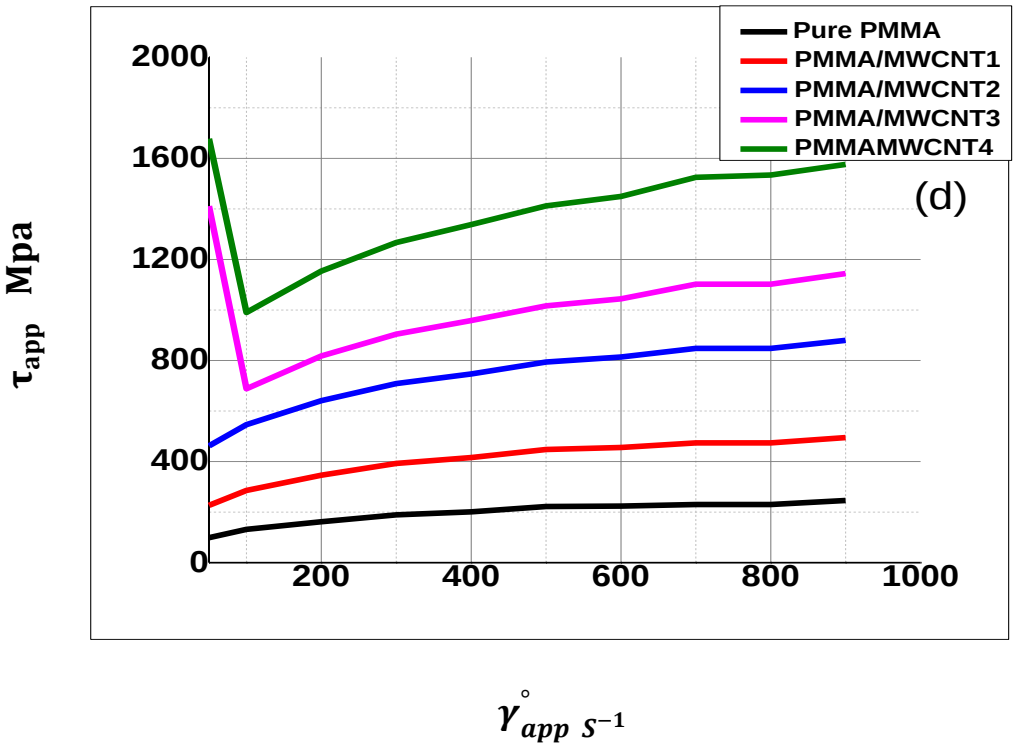
Pure PMMA
PMMA/MWCNT1
PMMA/MWCNT2
PMMA/MWCNT3
PMMAMWCNT4
(d)
2000
1600
1200
800
400
0
200 400 600 800 1000
τ_{app} Mpa
$\dot{\gamma}_{app}\ s^{-1}$

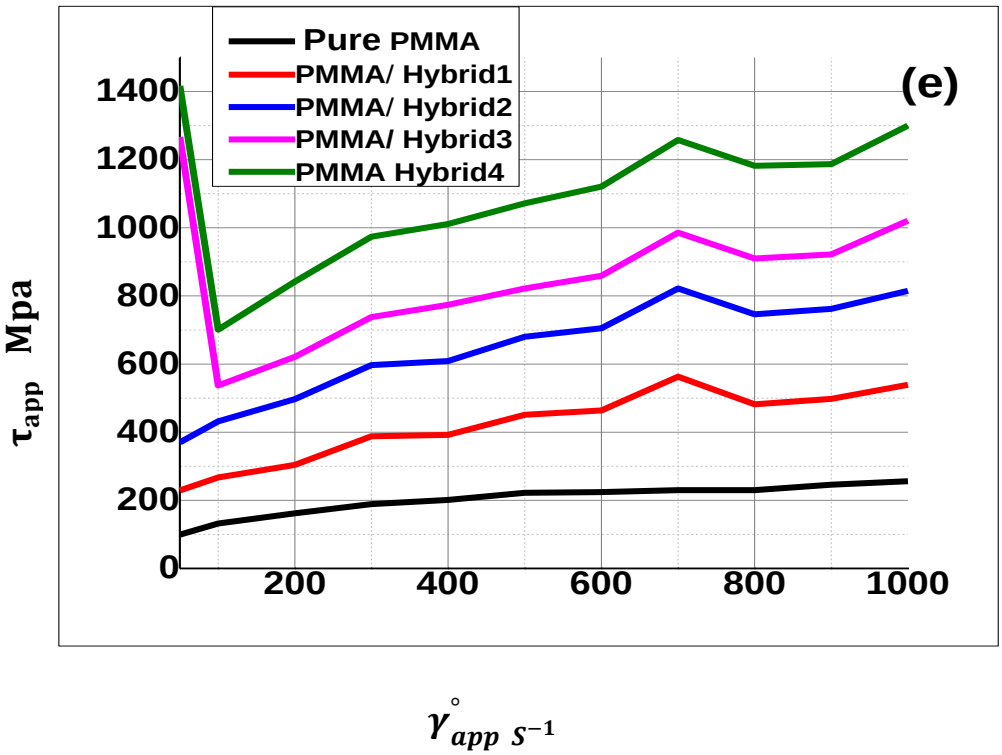

Figure (4.14) shear stress behavior of Pure PMMA melt with: (a,b,c) PMMA/solid lubricant wt.% melts , (d,e) PMMA/reinforcement fillers & Hybrid compound melts ,with the shear rate increasing in a capillary at die 1 mm ,temperature 240°C.

The shear stress behavior of PMMA/MWCNT is similar to PMMA/PE-wax2,PMMA /CS2, PMMA /CS4 as shown in fig.(4.14 d),when shear stress increased with shear rate increased , shear stress tend to be flatter .Shear stress behavior of hybrid causes turbulent extrusion lead to a variety of the elastomeric effects. PMMA\Hybrid shear stress curves are perfectly continuous with change in the slope around PMMA| Hybrid3, PMMA\ Hybrid4 from (50 to 800 s^{-1}) as shown in fig. (4.14 e).

4 . 3 . 3 Melt fracture

Extrusion deformation arises when the extrusion process occurs at high rates. Then the shear rate exceeds the critical shear rate to break a particular polymer melt that is initially in the die entry region when the material is directed into the capillaries from the die reservoir. Where the melt movement is in the part parallel to the die. Other effects occur on the die wall, as the melt fracture phenomenon occurs when extruded through the small diameter with high shear rate ,process occurs at high rates. Then the shear rate exceeds the critical shear rate to break a particular polymer melt that is initially in the mold entry region when the material is directed into the capillaries from the die reservoir. Where the melt movement is in the part parallel to the mold. In general, there is an instability that may occur in the capillaries pure PMMA,PMMA with solid lubricant, PMMA / MWCNT and Hybrid extrusion. First, there is a critical shear stress in which low-amplitude periodic deformations exist on the extrusion surface causing surface melting fracture. When high shear stress is present, the flow creates massive deformations that appear on the material surface upon extrusion known as the total melt fracture. The polymer shows diffuse defects on the surface, the real problem being the inability to have simple quantification of the turbulent nature of extrusion. These observations can only be recorded on the basis of the visual aspect and the accurate description indicating the increasing degradation with an increase in the flow rate (shear rate). In all cases, irregular pressure at an extremely high flow rate (shear rate) causes turbulent extrusion.

4 . 3 . 4 Flow instabilities of molten polymers

The main defect faced for Pure PMMA filament shape was volume defect. It generally occurs for all polymers under very severe flow conditions. A chaotic aspect and a gradual and irregular deterioration of the cylindrical shape of the extrudate is always observed (total melt fracture) [51], due to high shear stress, the flow creates massive deformations that appear on the material surface upon extrusion.as shown in Fig. (4.15).

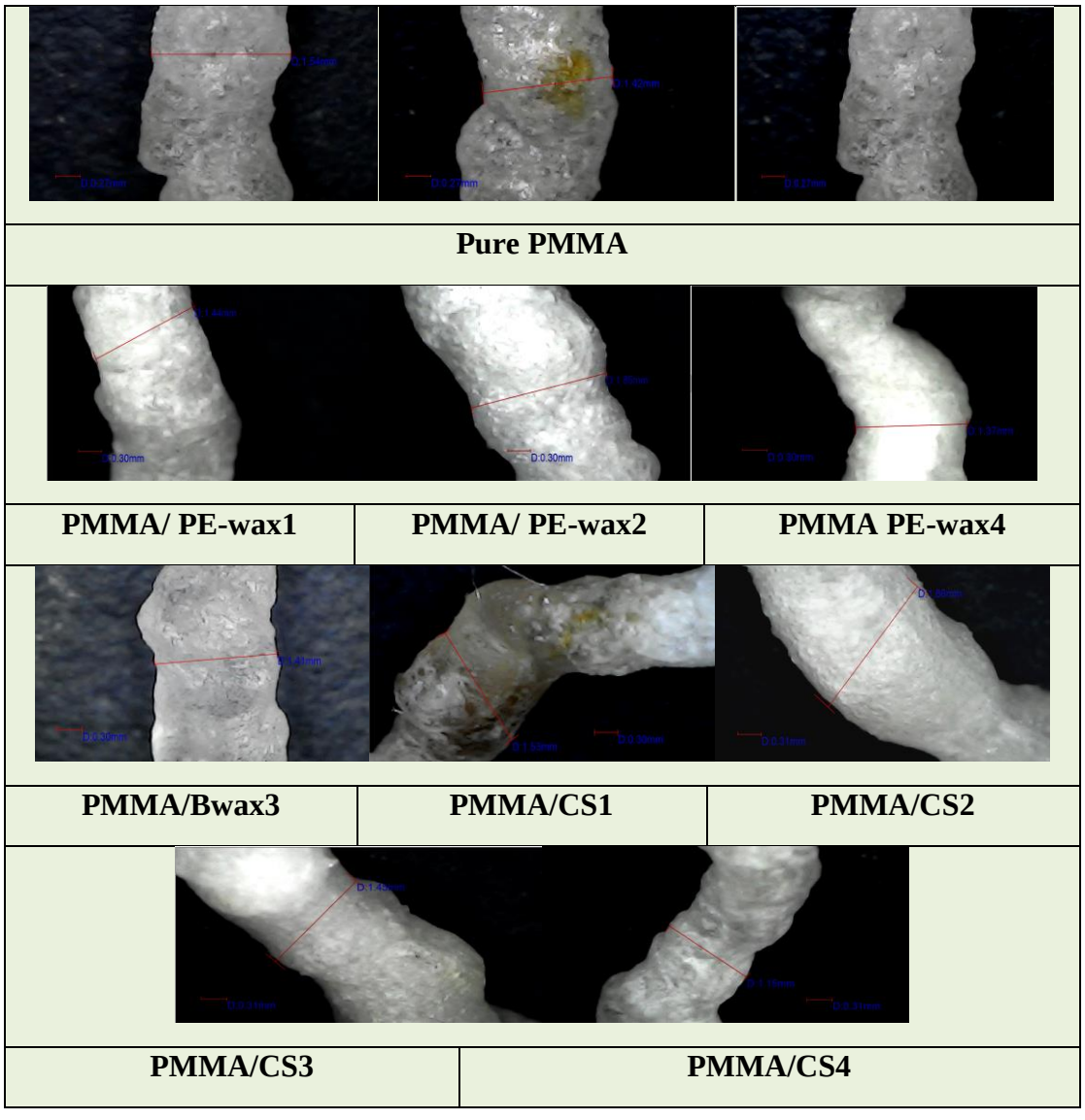

Figure 4.15 : Filament shapes and extrusion defects at 100 s^{-1} shear rate (Volume defect) for pure PMMA & with PMMA solid lubricant wt%.

Volume defect filament shape can be seen also for PMMA with reinforcement filler as in Fig.(4.17).

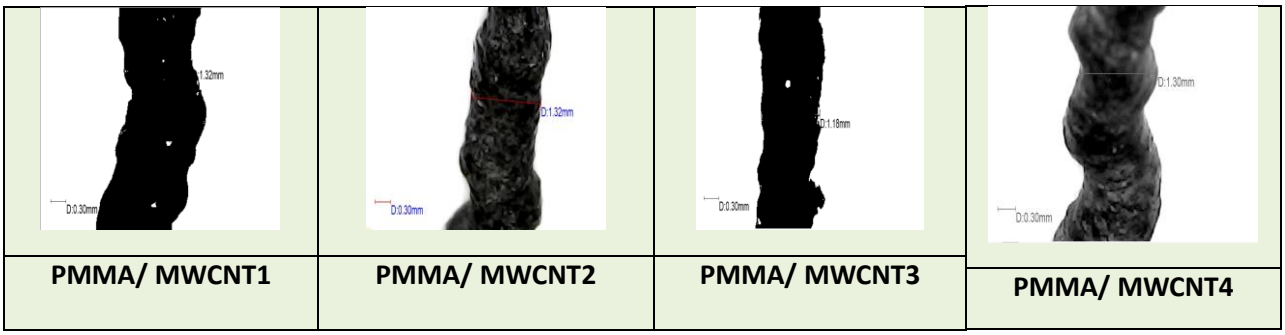

Figure 4.16 : Filament shapes and extrusion defects at 100 s^{-1} (Volume defect) for PMMA with reinforcement fillers wt.%.

A sharkskin defect occurs when a surface defect increases and extends to the flow rate. It can be distinguished initially by the loss of transparency of the extruded material and a dull surface [128,135].The sharkskin defect can be seen by the filament shapes of PMMA with solid lubricant, Fig. (4.18), as well as for PMMA with reinforcement filler as in Fig. (4.19).

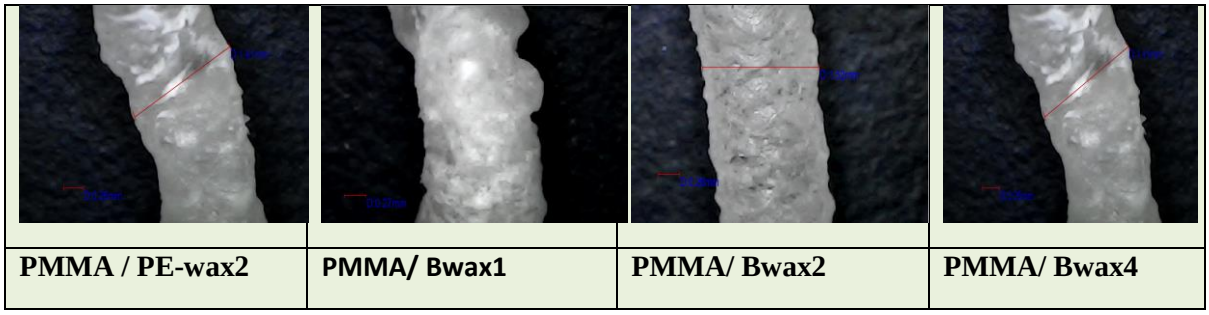

Figure 4.17 : Filament shapes and extrusion defects at 100 s^{-1} (Sharkskin) for PMMA with solid lubricant wt%.

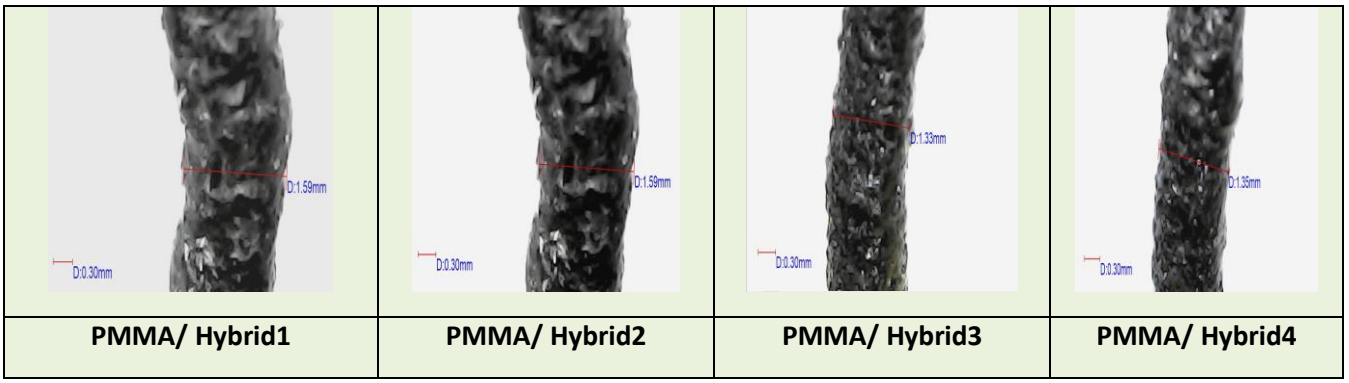

Figure 4.18 : Filament shapes and extrusion defects at 100 s^{-1} (Sharkskin) for PMMA /MWCNT.

4 . 4 Contact Angle Results

Through the Fig. (4.19)and Fig. (4.20) , an increase in the contact angle value was observed for all samples that used solid lubricant materials , MWCNT fillers ,and , Hybrid fillers, but with varying proportions, It was observed too, the samples filled with Beeswax that had a high contact angle with water surface compared to the rest of the solid lubricant materials types. Due to the difference in the ability and rate of migration of particles for Solid lubrication materials to the surface, where the results proved that a higher percentage of migration particles to the surface for Beeswax partials .This behavior was reflected in most of the surface properties of the composite material that were previously discussed.

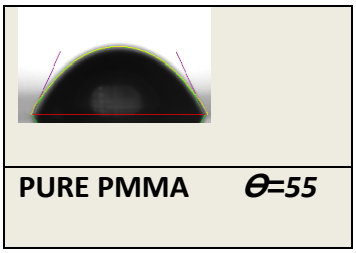

(a)

PMMA/ MWCNT1	PMMA/ MWCNT2	PMMA/ MWCNT3	PMMA/ MWCNT4
Θ=74	Θ=74	Θ=66	Θ=74
PMMA/ Hybrid1	PMMA/ Hybrid2	PMMA/ Hybrid3	PMMA/ Hybrid4
Θ=75	Θ=68	Θ=66	Θ=73

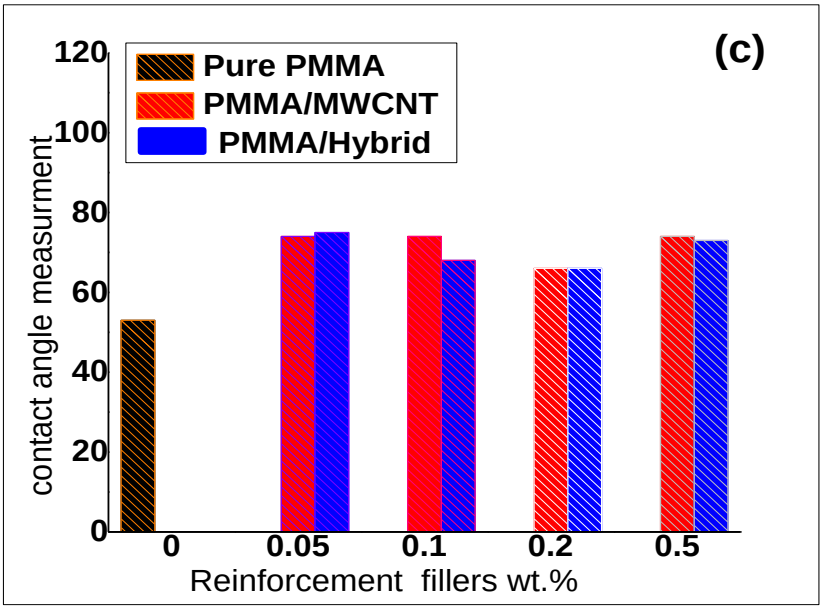

Figure 4.19 : (a) Illustrate the droplet of contact angle of experimental result of Pure PMMA, PMMA/reinforcement fillers wt.%, and , (b) Contact angle measurement as a function of reinforcement fillers wt.%.

(a)

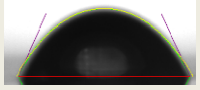

PURE PMMA $\Theta=55$

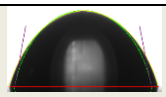	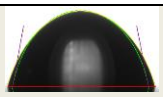		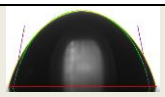
PMMA/ PE-wax1	PMMA/ PE-wax2	PMMA/ PE-wax3	PMMA/ PE-wax4
$\Theta=64$	$\Theta=69$	$\Theta=66$	$\Theta=70$
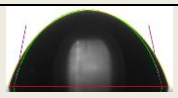		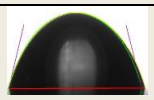	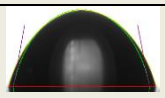
PMMA/ Bwax1	PMMA/ Bwax2	PMMA/ Bwax3	PMMA/ Bwax4
$\Theta=93$	$\Theta=74$	$\Theta=94$	$\Theta=94$
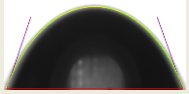	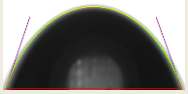	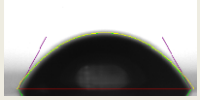	
PMMA/ CS1	PMMA/ CS2	PMMA/ CS3	PMMA/ CS4
$\Theta=60$	$\Theta=61$	$\Theta=60$	$\Theta=94$

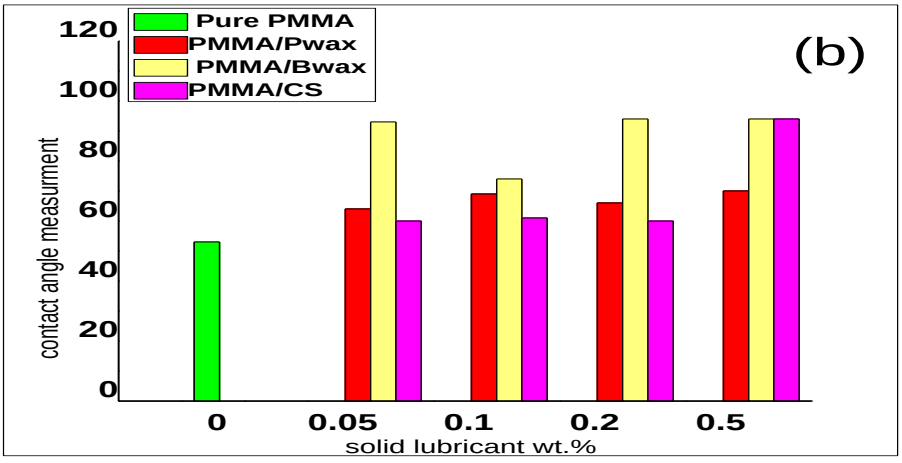

Figure 4.20 : (a) Illustrate the droplet of contact angle of experimental result of Pure PMMA, PMMA/ solid lubricant wt.% , and , (b) Contact angle measurement as a function of solid lubricant wt.%.

4 . 5 Miscibility Results

4 . 5 . 1 FTIR Results

Fig.(4.21 a) shows that the intensity of the bands observed in the spectrum (O-H Stretch) starts increasing with the emergence of a doublet at (3757–3456 cm^{-1}), indicating the structural transformation of the molecule, also , at (3903-3672 cm^{-1}) for Pure PE-wax, but show took a wrinkled shape for Pure PMMA . The spectrum (C-H Stretch) shows this doublet at (2947–2846 cm^{-1}) for Pure PE-wax and (2924 cm^{-1}) for Pure PMMA ,but less shifting for PMMA/PE-wax at (2846 cm^{-1}), the (C-O stretching bands) observed at (1550-1660 cm^{-1}) in Pure PMMA is less shifting in PMMA/PE-wax at 1635 cm^{-1} ,the (C-C stretching bands) observed at (1110 cm^{-1})in PMMA/PE-wax. Fig.(4.21 b),(C–O Stretch) at (1550-1600 cm^{-1}) respectively for PMMA is higher shifting in PMMA/Bwax peak appear at (1643 cm^{-1}). The (O-H Stretch) here less shifted with the emergence of a doublet at (3572 - 3433 cm^{-1}) for PMMA\Bwax. The(C-H Stretch) here less shifted at (2384cm^{-1})for PMMA \Bwax. Fig.(4.21 c),(O-H Stretch) for PMMA\CS show decrease of this peak in the same position for Pure PMMA. The(C-H Stretch) is less shifting for PMMA/CS spectrum at (2769 cm^{-1}) , the same band appear for pure CS at doublet (2962-2769 cm^{-1}), the (C-O Stretch) is higher shifting for PMMA/CS at (1635 cm^{-1}), the(C=O Amide) observed at (1658 cm^{-1}) in PMMA/CS. Fig.(4.21 d) ,pure PMMA, PMMA/MWCNT and Hybrid compound are shown. When comparing the FTIR specification set for pure PMMA and PMMA /MWCNT composites, only small peak shifts and one significant change can be seen. Specifically, the(C-O stretch) observed at (1627 cm^{-1} & 1573 cm^{-1}) in pure MWCNT and PMMA\MWCNT respectively, they took a wrinkled shape in both PMMA/MWCNT and the hybrid composite. The decrease of these peaks in the range (1597-1490 cm^{-1}) indicates the changes in the structure of the carbon nanotubes when carboxylate is used which

agreed with [186,187]. It is also correct to refer to such a decrease in these peaks to the presence of hexagonal asymmetric carbon which agreed with [188]. The (O–H stretch) appeared in PMMA/ MWCNT at (3500 cm^{-1}) and less shifted in Hybrid at (3332 cm^{-1}),New chemical group observed for Hybrid and Pure MWCNT , the (C=O stretch) at (1689 cm^{-1}) and at (C≡C Stretch) at (2384 cm^{-1}) respectively .

Table (4 . 3) Absorption areas of Fig.(4.21 a)

Type of bond	Pure PMMA	Pure Pwax	PMMA/Pwax
O - H Stretch	3448 cm^{-1}	3903-3672 cm^{-1}	3757 – 3565 cm^{-1}
C - H Stretch	2924 cm^{-1}	2947 – 2846 cm^{-1}	2846 cm^{-1}
C - O Stretch	1550-1600 cm^{-1}	1519 cm^{-1}	1635 cm^{-1}

Table (4 . 4) Absorption areas of Fig.(4.21 b)

Type of bond	Pure PMMA	Pure Bwax	PMMA/Bwax
O - H Stretch	3448 cm^{-1}	3417 cm^{-1}	3572 - 3433 cm^{-1}
C - O Stretch	1550-1600 cm^{-1}	1774 cm^{-1}	1643 cm^{-1}
C - H Stretch	2924 cm^{-1}	2916 cm^{-1}	2384 cm^{-1}

Table (4 . 5) Absorption areas of Fig.(4.21 c)

Type of bond	Pure PMMA	Pure CS	PMMA/CS
O - H Stretch	3448 cm^{-1}	3919 - 3672 cm^{-1}	3919 - 3672 cm^{-1}
C - H Stretch	2924 cm^{-1}	2962 - 2769 cm^{-1}	2769 cm^{-1}
C - O Stretch	1550-1600 cm^{-1}	1550 cm^{-1}	1635 cm^{-1}
C = O Amide			1658 cm^{-1}

Table (4 . 6) Absorption areas of Fig.(4.21 d)

Type of bond	Pure PMMA	Pure MWCNT	PMMA/MWCNT	Hybrid
O - H Stretch	3448 cm^{-1}	3433-3556 cm^{-1}	3500 cm^{-1}	3332 cm^{-1}
C - H Stretch	2924 cm^{-1}	2862-2947 cm^{-1}	2870 – 2985 cm^{-1}	2916 cm^{-1}
C - O Stretch	1550-1600 cm^{-1}	1627 cm^{-1}	1573 cm^{-1}	

C = O stretch				1689 cm^{-1}
C ≡ C Stretch		2384 cm^{-1}		

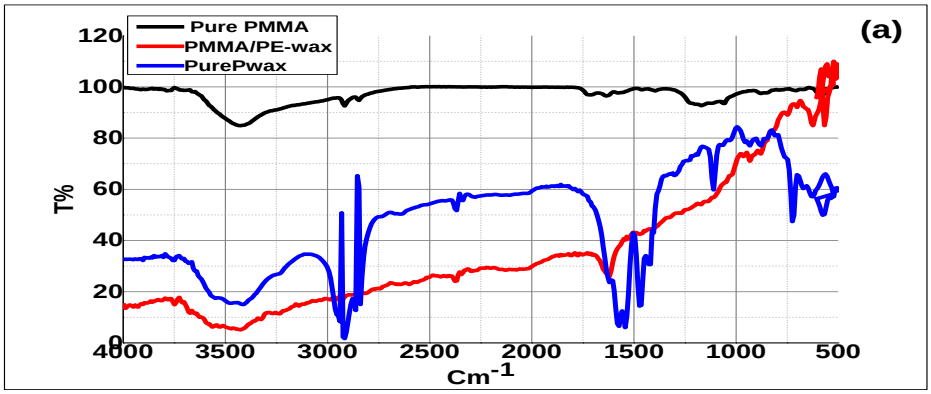

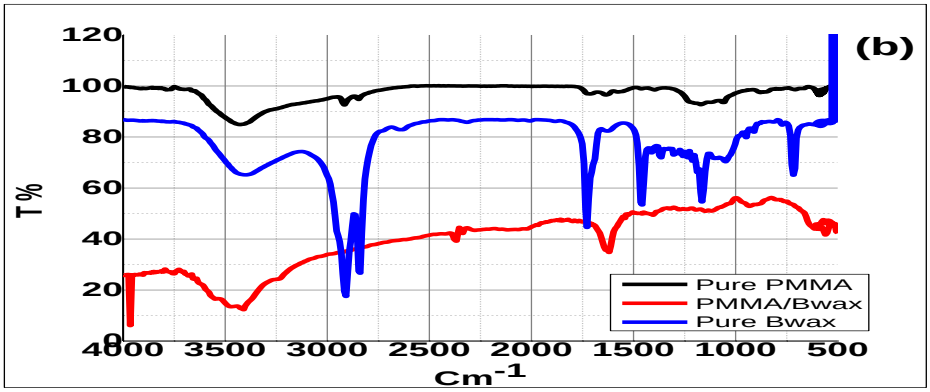

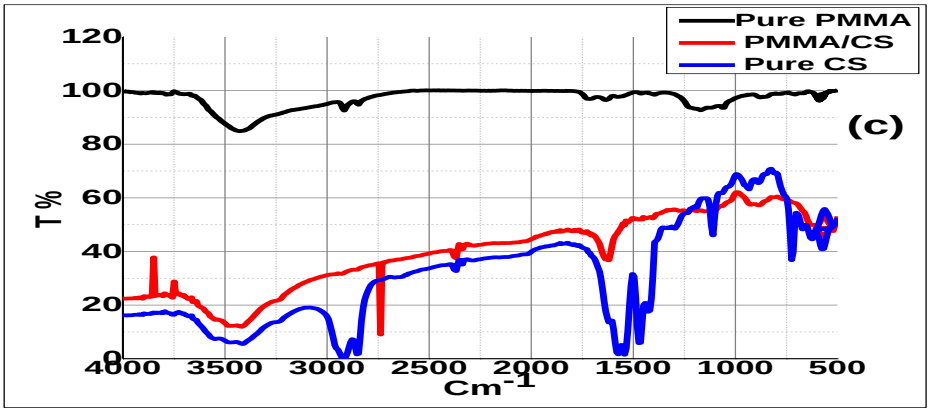

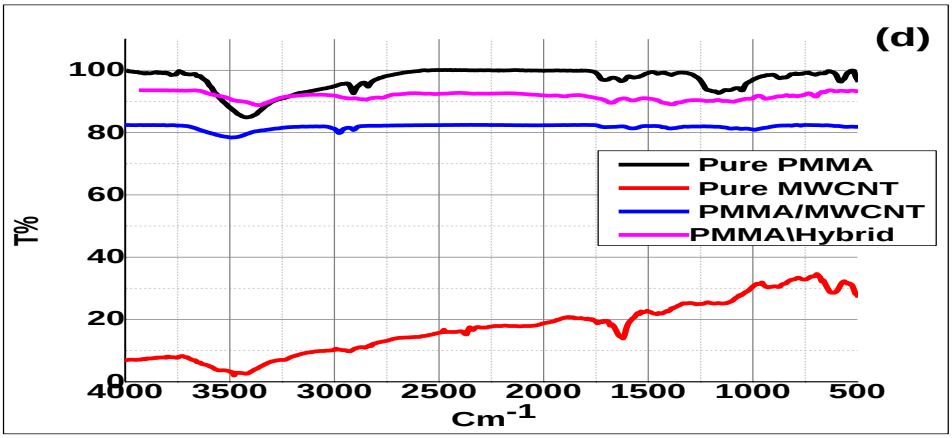

Figure 4.21 FTIR spectrum for Pure PMMA with (a),PMMA/PE-wax , Pure PE-wax ,(b)PMMA/Bwax , Pure Bwax , (c)PMMA/CS , Pure CS , and (d) Pure MWCNT,PMMA/MWCNT, PMMA\Hybrid .

4 . 5 . 2 DSC Results

From second thermodynamic low:

$$\Delta S = \frac{\Delta Q}{T} \quad \text{.....(4.1)}$$

$$\Delta H = Q = m\ cp\ \Delta T \quad \text{.....(4.2)}$$

$$\Delta H = T\Delta S \quad \text{.....(4.3)}$$

Fig.(4.22) shows radar graph representations of lubricants, orientations, and entropy values. Here it can be visualized more clearly that, regardless of the general trend, the polymeric materials filled with solid lubricants showed the amount of heat lost in the thermodynamic system through the movement of particles and their ability to move to the surface (migration). (PMMA/Bwax) showed the highest value of particles migrating to the surface .

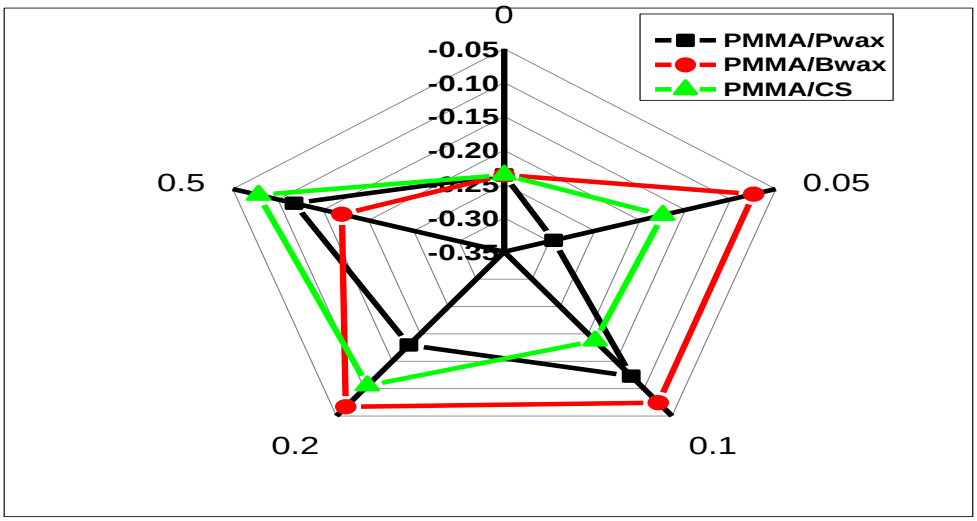

Figure 4.22 : Radar chart of entropy for PMMA with solid lubricant wt%.

DSC-based investigations confirmed the good miscibility and uniform structure of PMMA with solid lubricants. Moreover, the main differences in specific heat capacity, crystallographic temperature and melting point have an effect on the crystal structure of the polymeric matrix, as all samples (PMMA/PE-wax, PMMA/Bwax, PMMA/CS) showed an increase in specific heat capacity with increasing the filling percentage is attributed to the role played by solid lubricants in migrating to the surface and lubricating the appropriate surface to increase the hydrophobic susceptibility of the polymer, as well as an increase in heat flow upon heating and passing through the glass transition phase, with a decrease in the crystalline temperature and melting point with an increase in the filling percentage. The heat capacity is greater upon heating above the glass transition temperature and when it reaches a certain temperature it gains enough energy to enter into a more organized structure known as "crystals", which release latent heat upon crystallization because it is an exothermic reaction.Table (4.7) Represented the results of NETZSCH / Proteus 70 software programs as Delta Specific Heat Capacity (J/ g K),Crystalline temperature (Tc), Area (J / g) , and melting point (Tm) from Fig.(4.23) .

Table (4 . 7) DSC analysis (Solid lubricant)

Samples	(Cp) (J/ g K˚)	(Tc) (˚C)	Area (J / g)	(Tm) (˚C)
Pure PMMA	0.001	211.3	-6.622	208
PMMA / PE-wax				
0.05 wt.%	0.000	206.4	-10.93	202
0.1 wt.%	0.021	190.4	-4.91	191
0.2 wt.%	0.018	200.6	-4.737	193.25
0.5 wt.%	0.104	175.3	-3.713	179.25
PMMA / Bwax				
0.05 wt.%	0.018	190.7	-3.828	189
0.1 wt.%	0.041	198.1	-3.682	188.75
0.2 wt.%	0.062	176.8	-3.521	188.125
0.5 wt.%	0.072	199.4	-8.054	186.375
PMMA / CS				
0.05 wt.%	0.043	200.1	-7.344	190
0.1 wt.%	0.088	194.5	-6.187	187.5
0.2 wt.%	0.006	184.0	-5.720	190.875
0.5 wt.%	0.136	186.6	-3.531	187.5

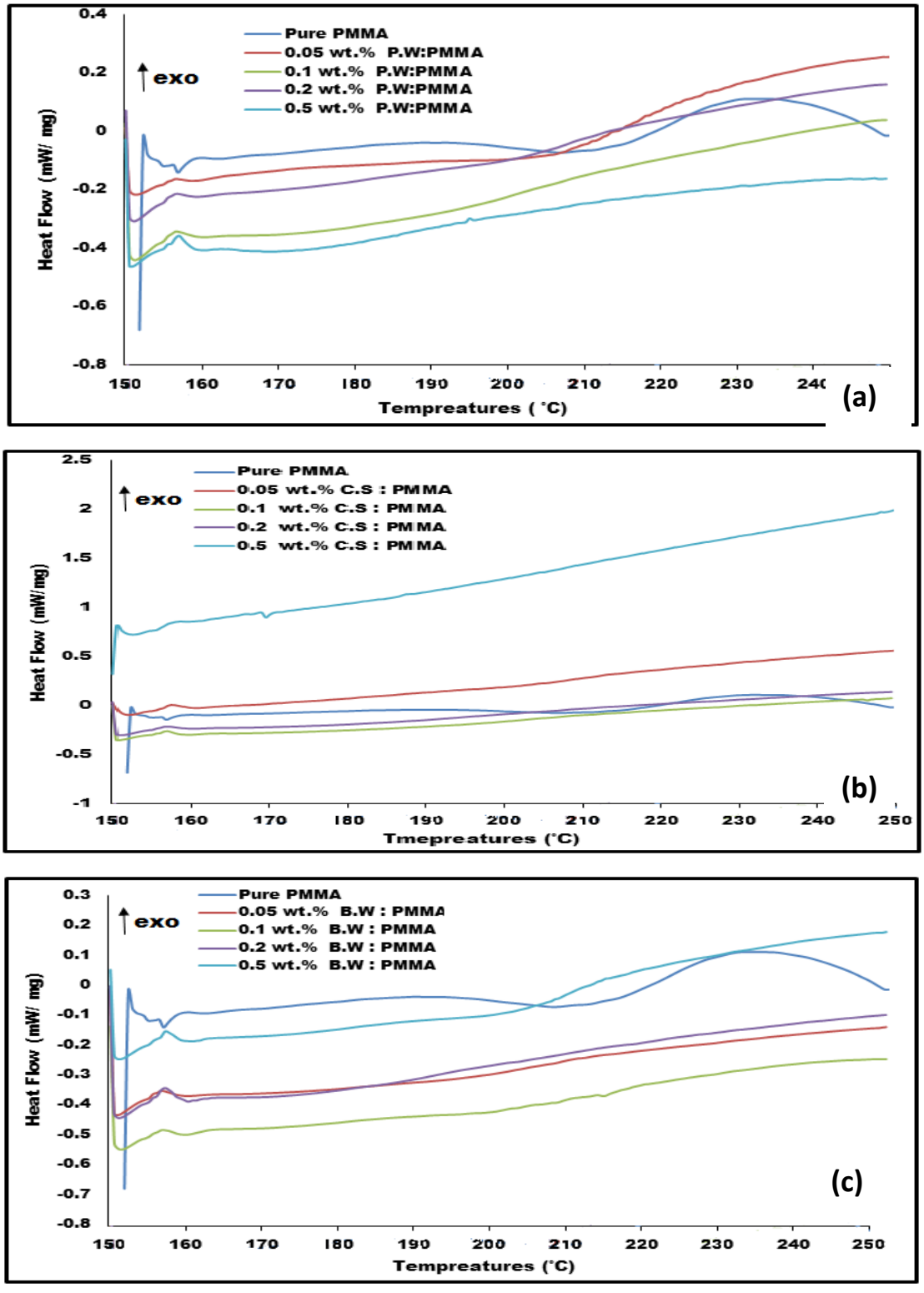

Figure 4.23: DSC result of Pure PMMA and PMMA/sold lubricant wt.% from (150 to 250)˚C .

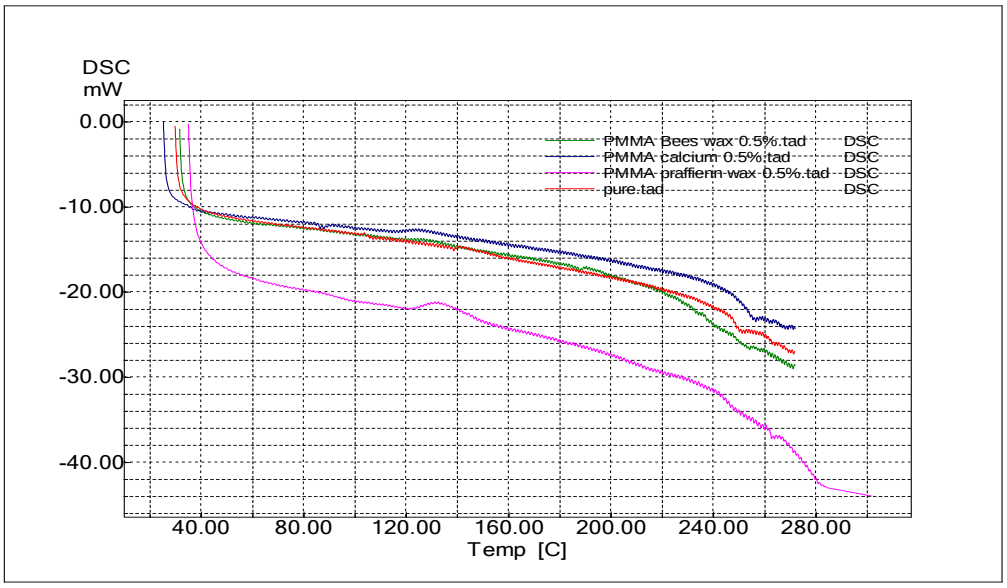

Figure 4.24 : DSC result of Pure PMMA & PMMA/sold lubricant (0.5wt.%) from (0 to 150 ˚C).

Fig.(4.24) showed DSC result for pure PMMA,PMMA filled with solid lubricant at (0.5 wt. %) . It reveals the glass transition temperature for all sample (pure PMMA, Tg=102), (PMMA/PE-wax. Tg=106), (PMMA/Bwax. Tg=85), and , (PMMA/CS , Tg=95).

CHAPTER FIVE

Conclusions & Recommendations

Conclusions:

From the acquired results we can conclude the following

1- In-situ free radical polymerization is quite acceptable technique for producing pure PMMA ,PMMA loaded with solid lubricant and nanoparticles.

2- The wear rate tests for the resulting composite materials PMMA/Bwax showed an improvement in the wear rates, which decreased to (9.4 %) , while PMMA/MWCNT & PMMA/Hybrid showed an improvement in the wear rates, It is increased with increasing the content of reinforcement.

3- The Wear coeffecint test results for PMMA/solid lubricant wt.% composites showed an improvement in the wear rates which decreased to (0.6%,0.7%,0.8%),respectively, while PMMA/Reinforcement fillers showed an improvement in the wear rates which decreased to (0.7% and 0.8%) respectively.

4- PMMA / Bwax showed improvement in contact angle tests for resulting composites and achieved higher contact angle values for hydrophobic surfaces.

5- Results of the scratch hardness tests for the resulting composite materials : PMMA/solid lubricant wt.% showed an improvement in the rates of friction coefficient , which decreased to (0.8 %, 0.7%, 0.8 %) respectively.

6- The flow results in capillary rheometer of PMMA/ solid lubricant wt.% & PMMA/ Reinforcement fillers wt.% showed that a shear thining behavior- which is the critical shear rate and shear stress can be easily predicated.

7- Determine the critical area to be able to change the surface quality and relate its results to pressure, shear stress and shear rate. This provides a de-

termination of the appropriate boundary conditions for a capillary rhemom-eter or polymer processing machine to produce the ideal surface quality, and the characteristics of the final product to save time, effort and energy.

Recommendations:

- Study of the tribological and mechanical behavior of self-lubricating layers using Nano-indentation technology.
- Use of lubricant-filled microcapsules for self-lubricating applications.
- Preparation and study of a multifunctional coating as a transparent anti-friction coating for optical applications.

Appidex I

Programming simulations using Ansys workbench were conducted for engineering tests (Flexural strength, wear, hardness, scratching) as shown below:

- Flexural Strength Test:

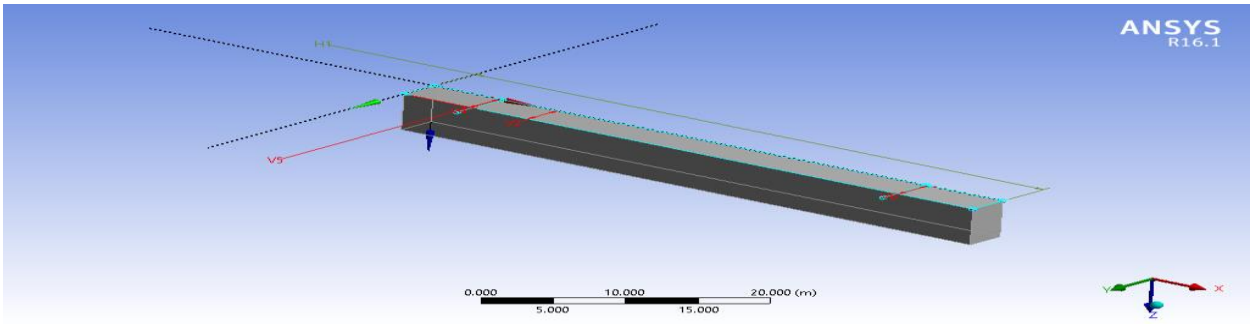

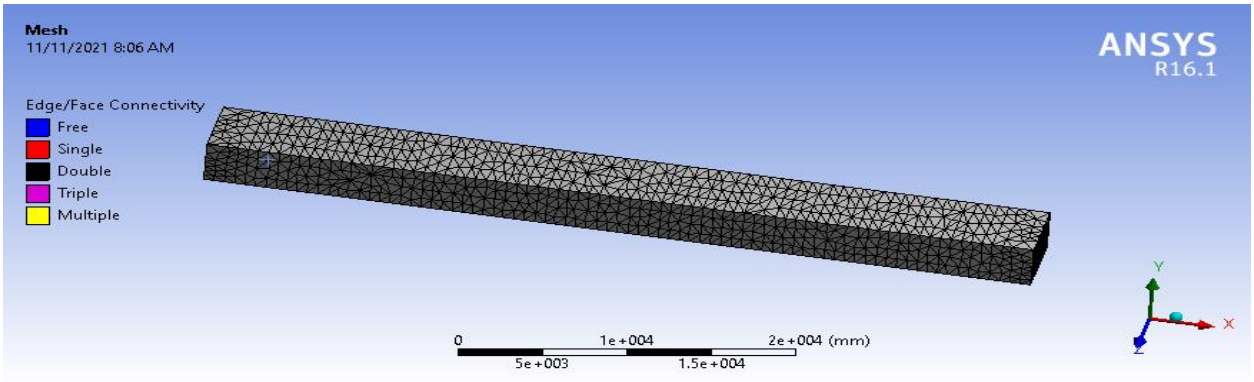

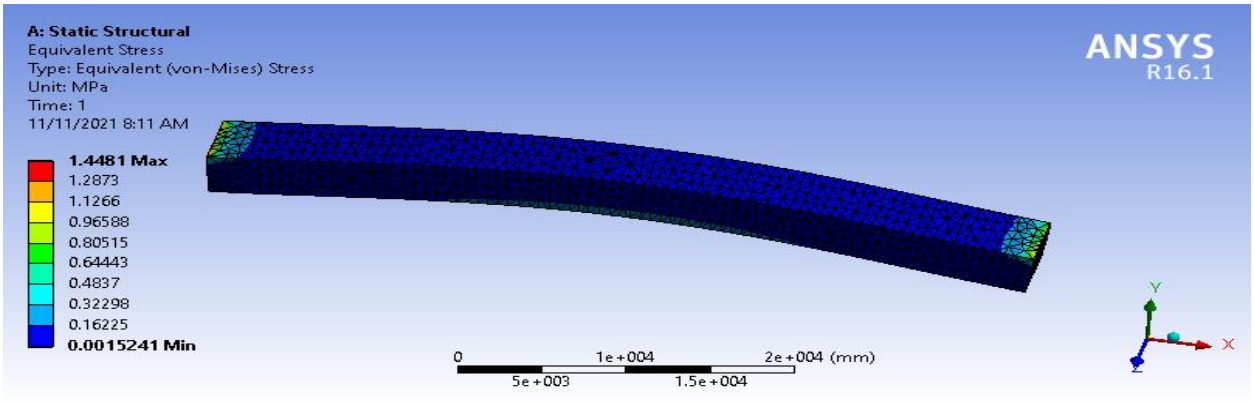

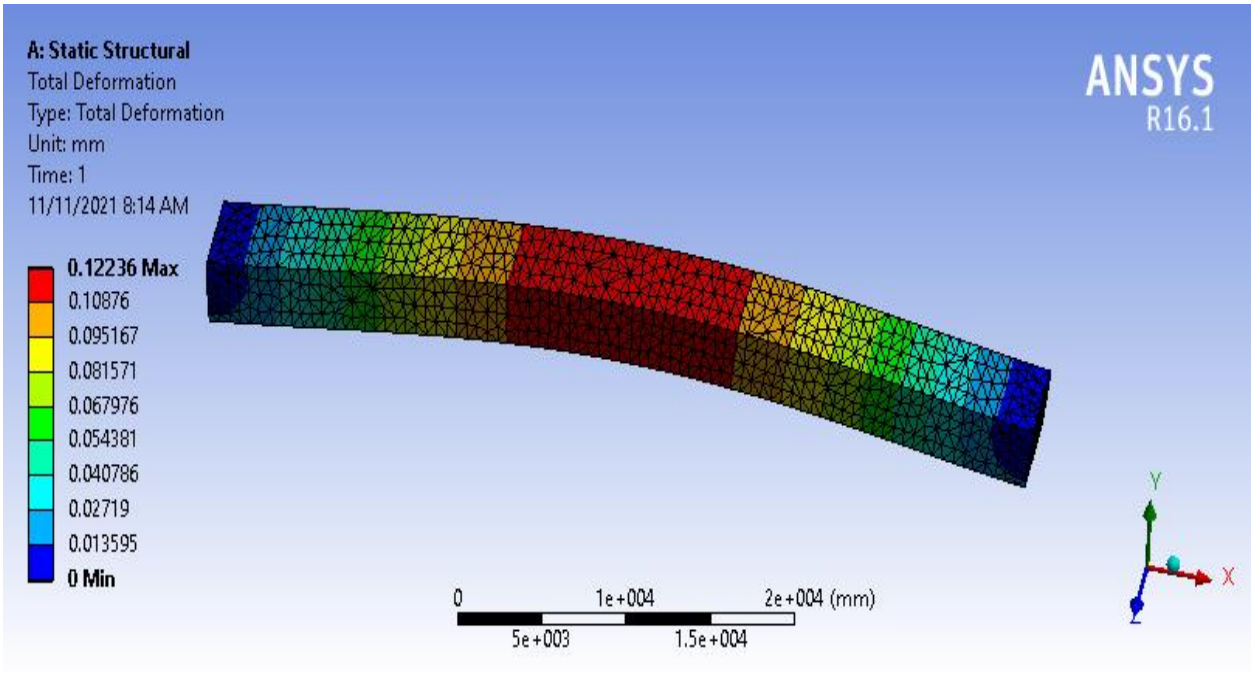
A: Static Structural
Total Deformation
Type: Total Deformation
Unit: mm
Time: 1
11/11/2021 8:14 AM
0.12236 Max
0.10876
0.095167
0.081571
0.067976
0.054381
0.040786
0.02719
0.013595
0 Min
ANSYS
R16.1
0
1e+004
2e+004 (mm)
5e+003
1.5e+004
Y
X

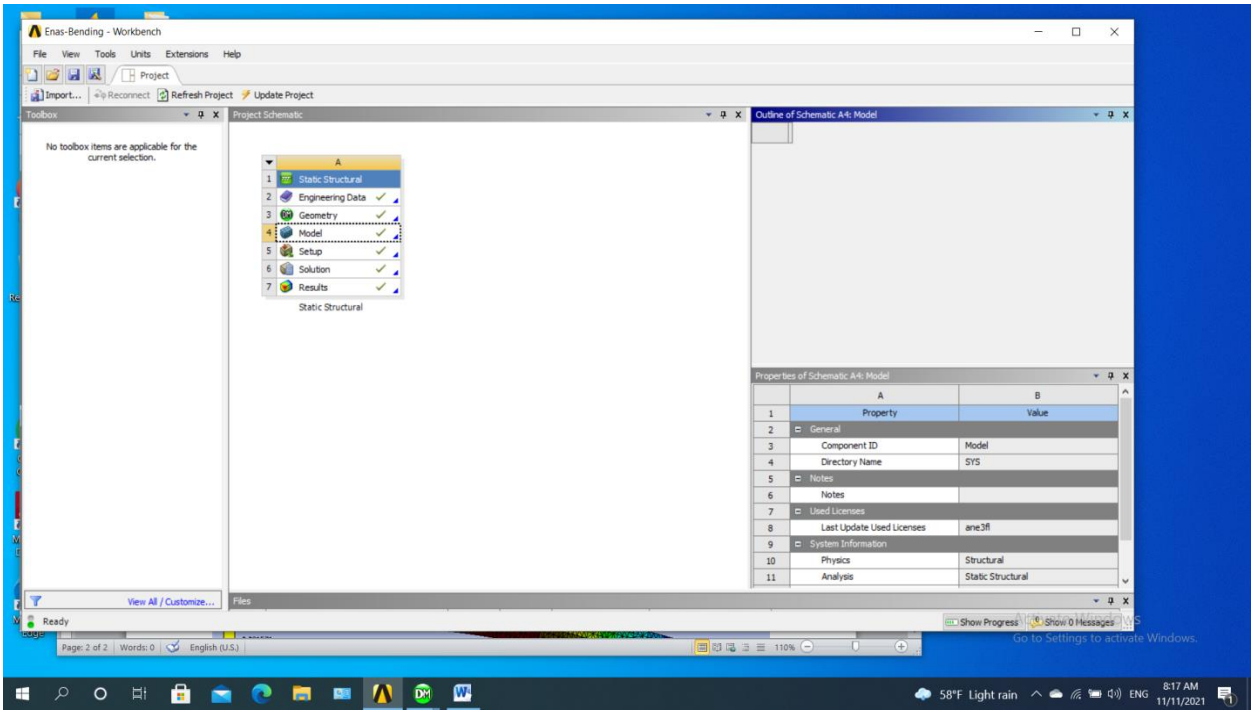
Enas-Bending - Workbench
File View Tools Units Extensions Help
Project
Import... Reconnect Refresh Project Update Project
Toolbox
No toolbox items are applicable for the current selection.
Project Schematic
A
1 Static Structural
2 Engineering Data
3 Geometry
4 Model
5 Setup
6 Solution
7 Results
Static Structural
Outline of Schematic A4: Model
Properties of Schematic A4: Model
Property
Value
General
Component ID
Model
Directory Name
SYS
Notes
Used Licenses
Last Update Used Licenses
ane3fl
System Information
Physics
Structural
Analysis
Static Structural
View All / Customize...
Files
Ready
Show Progress
Show 0 Messages
Page: 2 of 2
Words: 0
English (U.S.)
110%
58°F Light rain
ENG
8:17 AM
11/11/2021

- Wear Test

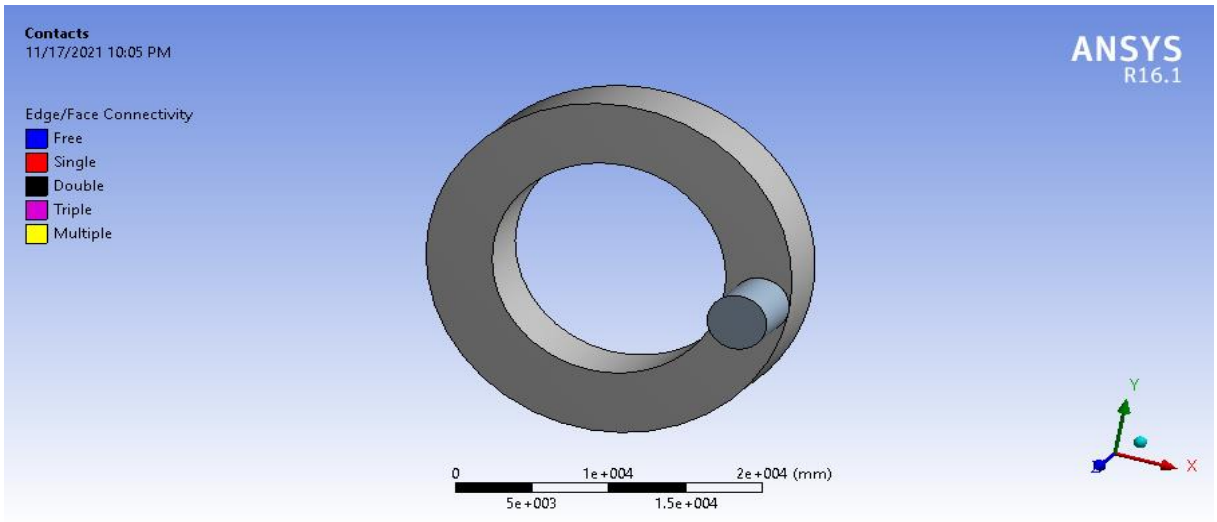
Contacts
11/17/2021 10:05 PM
Edge/Face Connectivity
Free
Single
Double
Triple
Multiple
ANSYS
R16.1
0
1e+004
2e+004 (mm)
5e+003
1.5e+004
Y
X

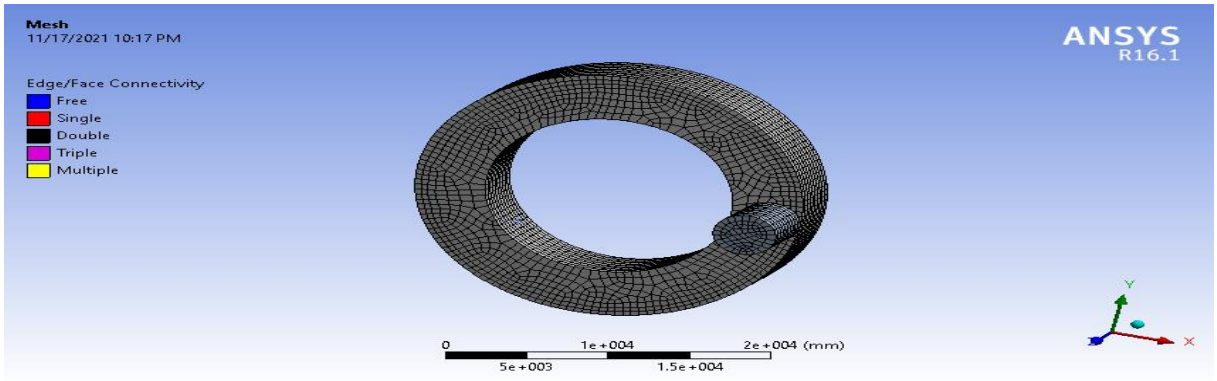
Mesh
11/17/2021 10:17 PM
Edge/Face Connectivity
Free
Single
Double
Triple
Multiple
ANSYS
R16.1
0
1e+004
2e+004 (mm)
5e+003
1.5e+004
Y
X

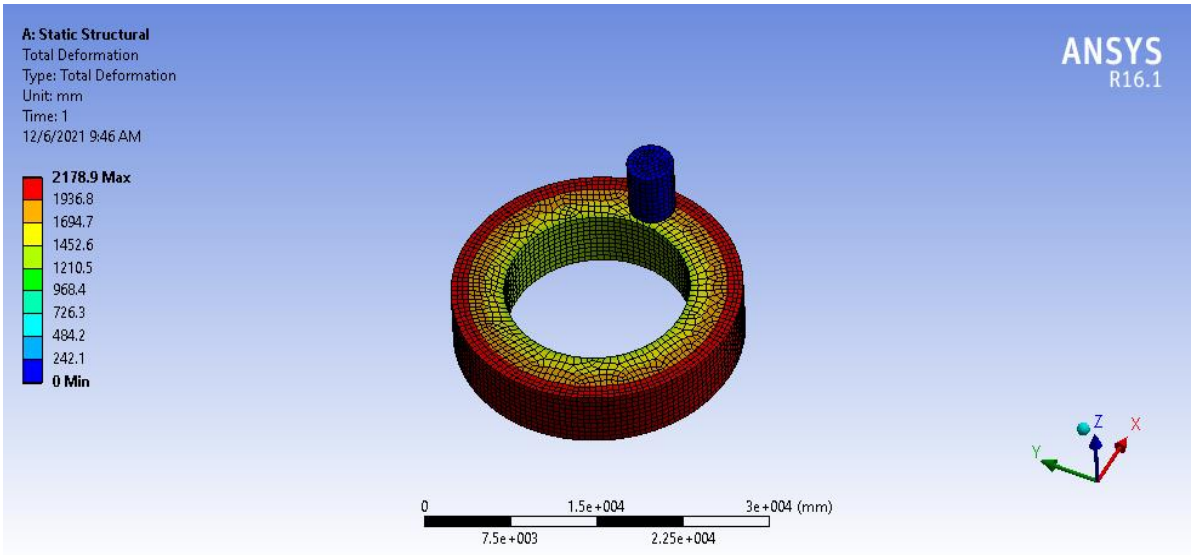
A: Static Structural
Total Deformation
Type: Total Deformation
Unit: mm
Time: 1
12/6/2021 9:46 AM
2178.9 Max
1936.8
1694.7
1452.6
1210.5
968.4
726.3
484.2
242.1
0 Min
ANSYS
R16.1
0
1.5e+004
3e+004 (mm)
7.5e+003
2.25e+004
Z
X
Y

- Abrasion Test

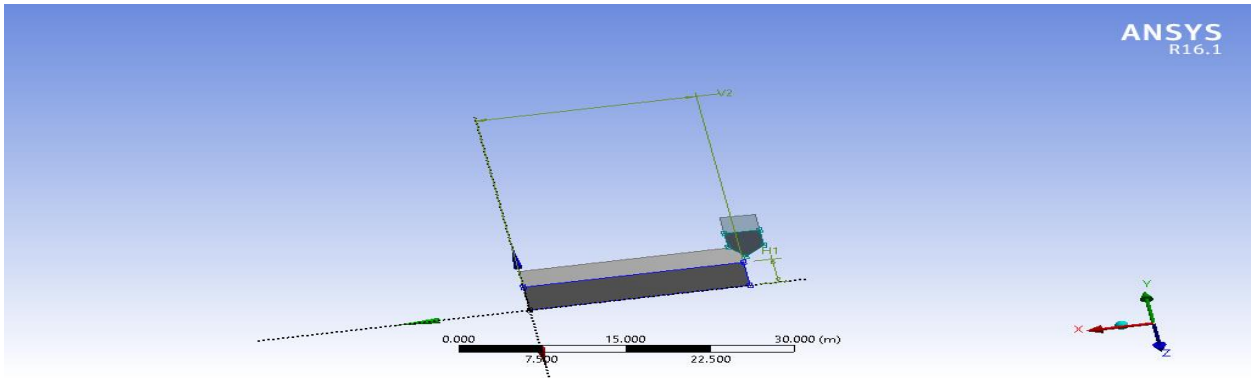

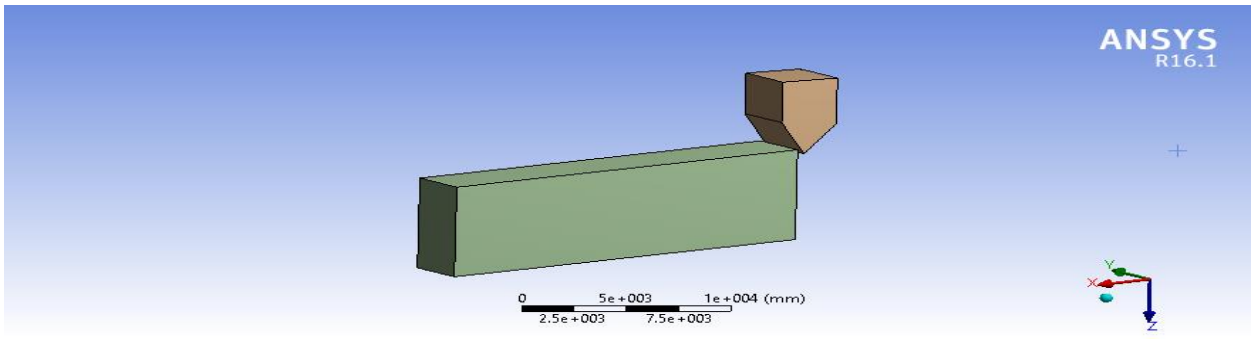

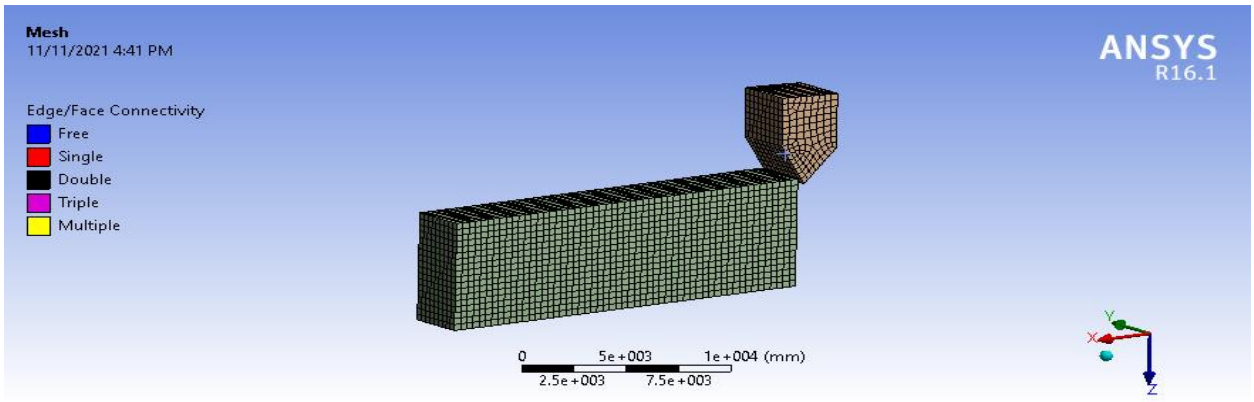

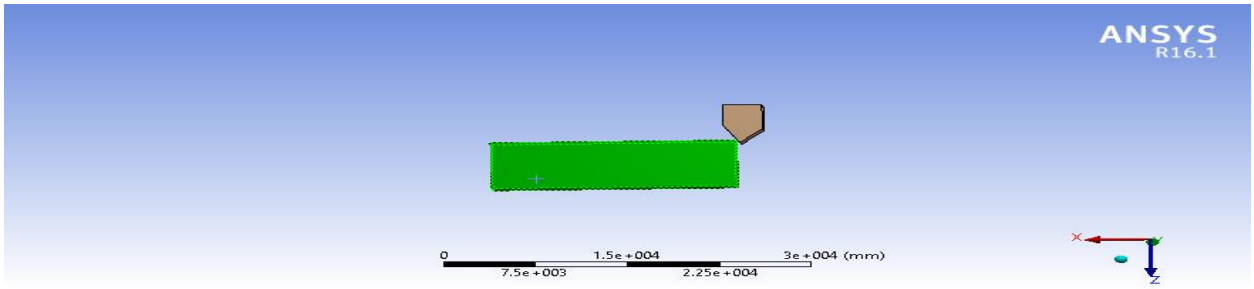

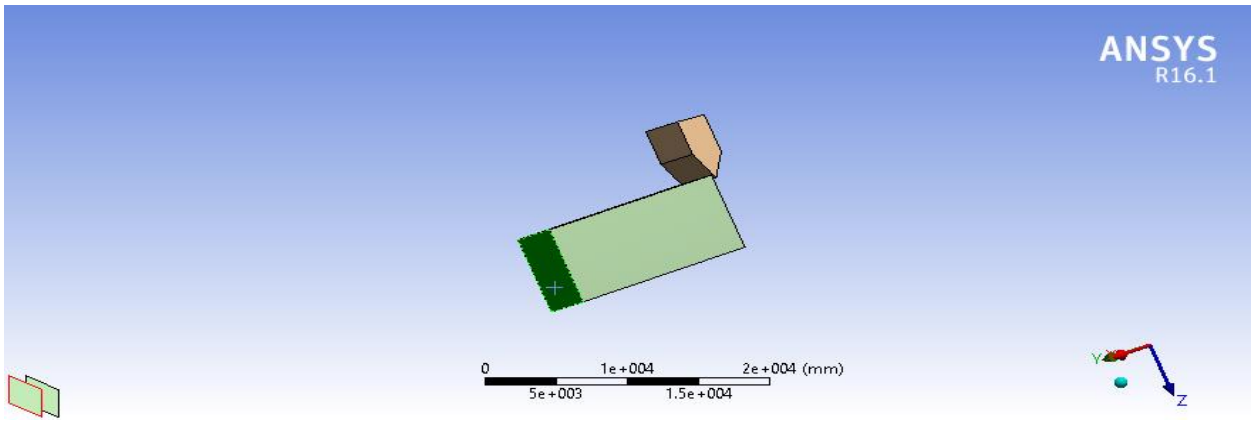
ANSYS
R16.1
0
1e+004
2e+004 (mm)
5e+003
1.5e+004
Y
Z

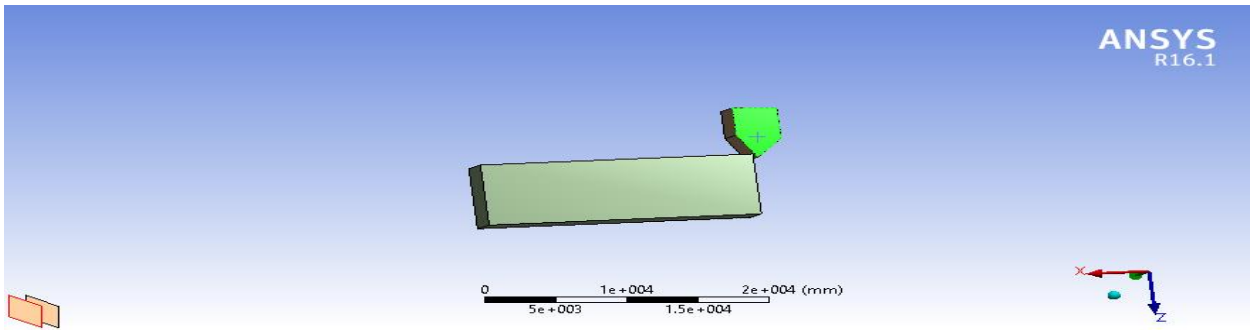
ANSYS
R16.1
0
1e+004
2e+004 (mm)
5e+003
1.5e+004
X
Z

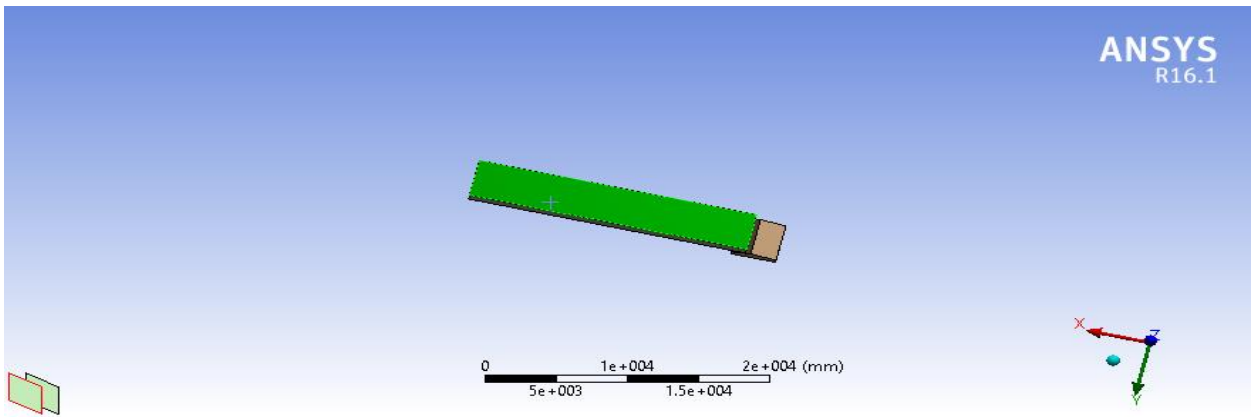
ANSYS
R16.1
0
1e+004
2e+004 (mm)
5e+003
1.5e+004
X
Z
Y

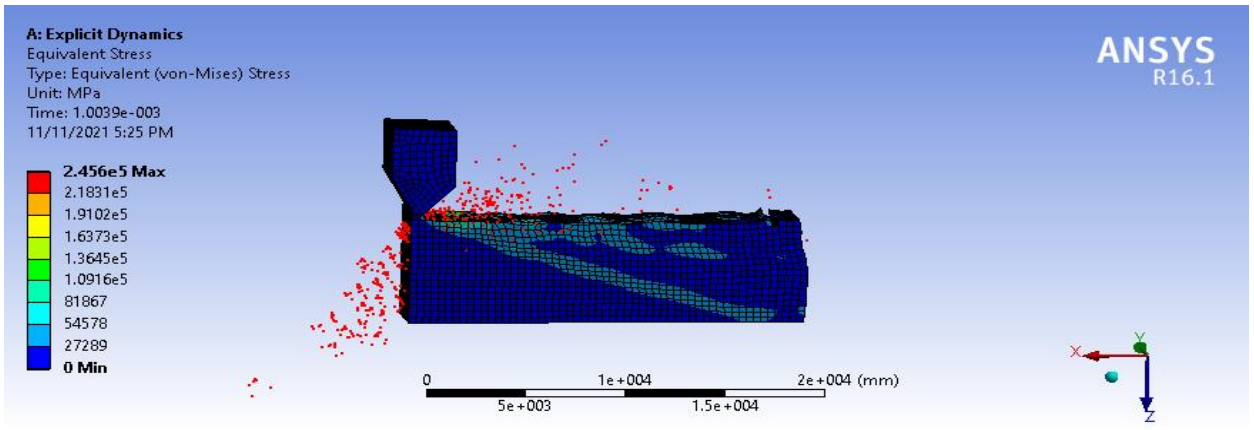
A: Explicit Dynamics
Equivalent Stress
Type: Equivalent (von-Mises) Stress
Unit: MPa
Time: 1.0039e-003
11/11/2021 5:25 PM
2.456e5 Max
2.1831e5
1.9102e5
1.6373e5
1.3645e5
1.0916e5
81867
54578
27289
0 Min
ANSYS
R16.1
0
1e+004
2e+004 (mm)
5e+003
1.5e+004
X
Y
Z

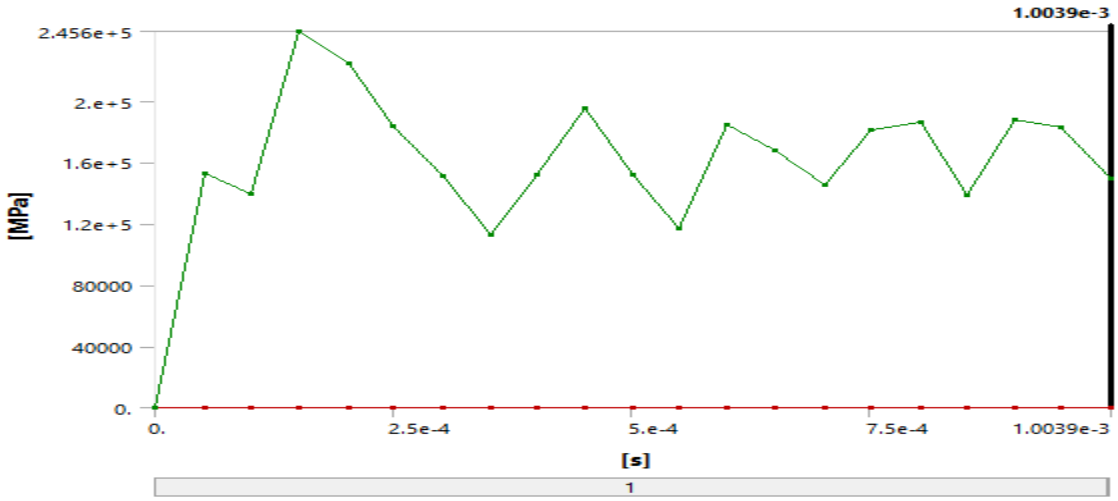

Model (A4) > Explicit Dynamics (A5) > Solution (A6) > Equivalent Stress

Model (A4) > Explicit Dynamics (A5) > Solution (A6) > Equivalent Stress

Time [s]	Minimum [MPa]	Maximum [MPa]
1.1755e-038		0.
5.2358e-005		1.5255e+005
1.0032e-004		1.3958e+005
1.5152e-004		2.456e+005
2.0349e-004		2.2486e+005
2.5004e-004		1.8363e+005
3.0227e-004		1.5115e+005
3.5269e-004		1.1287e+005
4.0131e-004		1.5191e+005
4.5081e-004		1.9533e+005
5.0203e-004		1.5193e+005
5.5109e-004		1.1687e+005
6.0094e-004		1.8499e+005
6.5011e-004		1.6793e+005
7.0337e-004		1.4552e+005
7.5193e-004		1.8152e+005
8.0358e-004		1.8654e+005
8.5237e-004		1.3876e+005
9.0252e-004		1.8765e+005
9.5049e-004		1.8321e+005
1.0039e-003		1.4925e+005

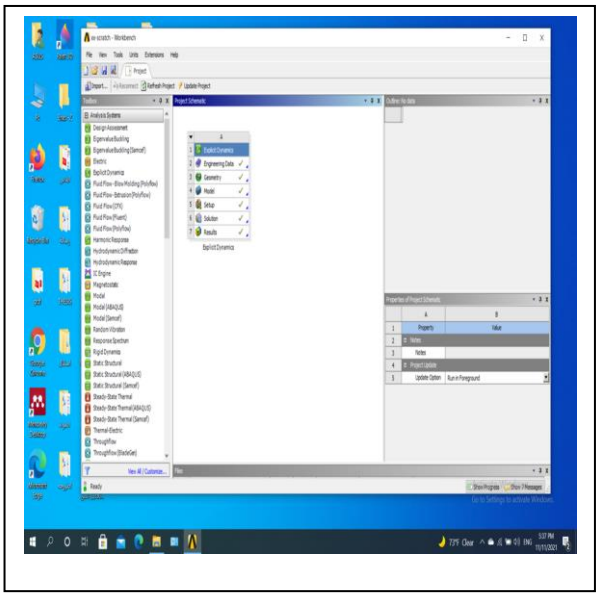

- Vickers Test

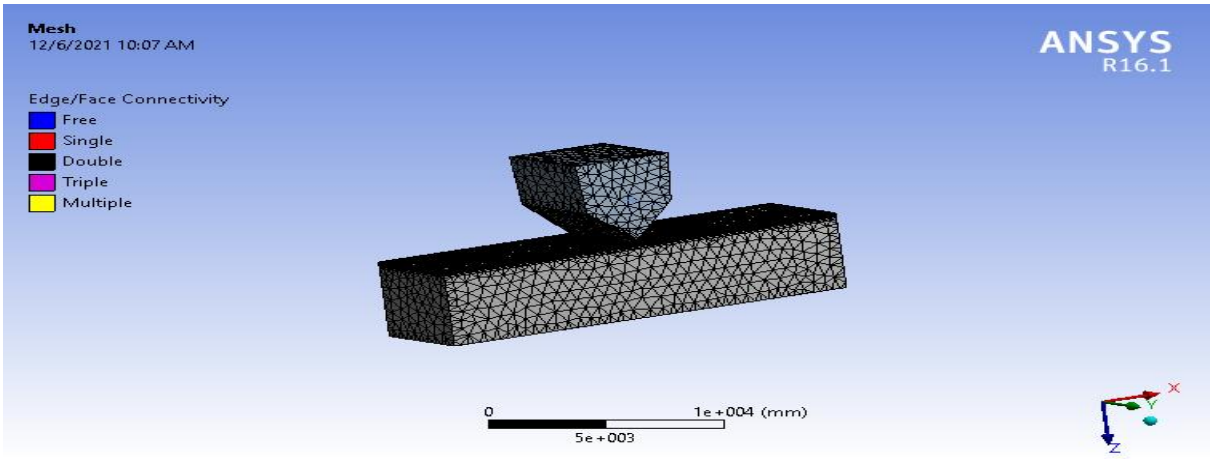

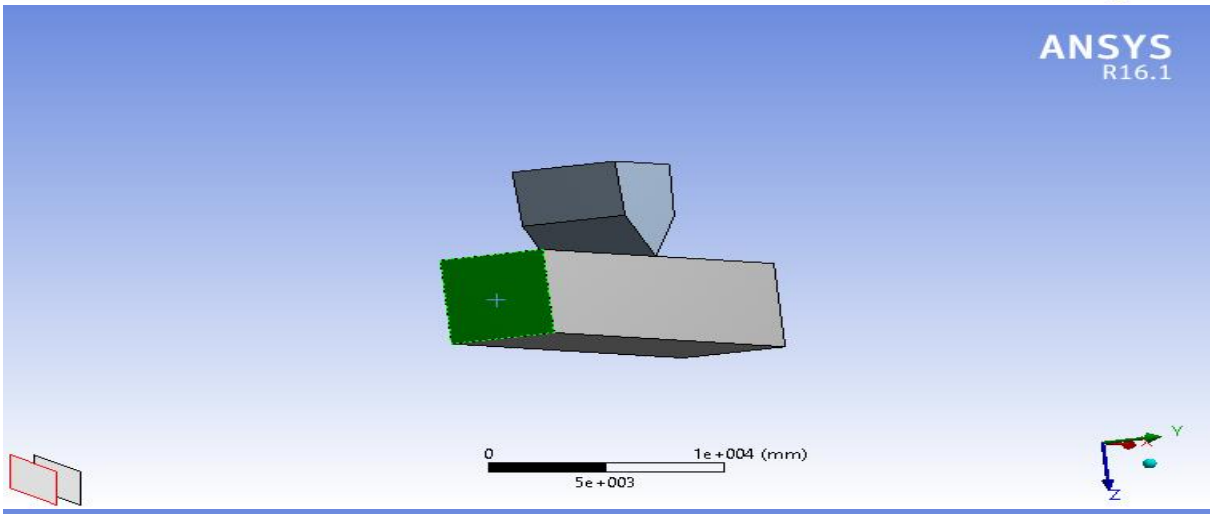

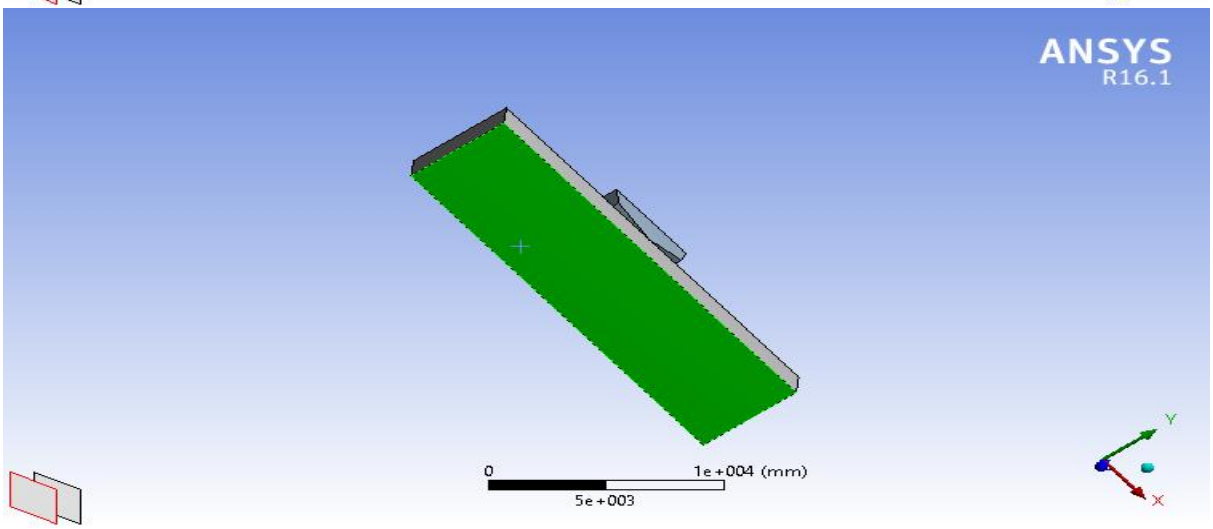

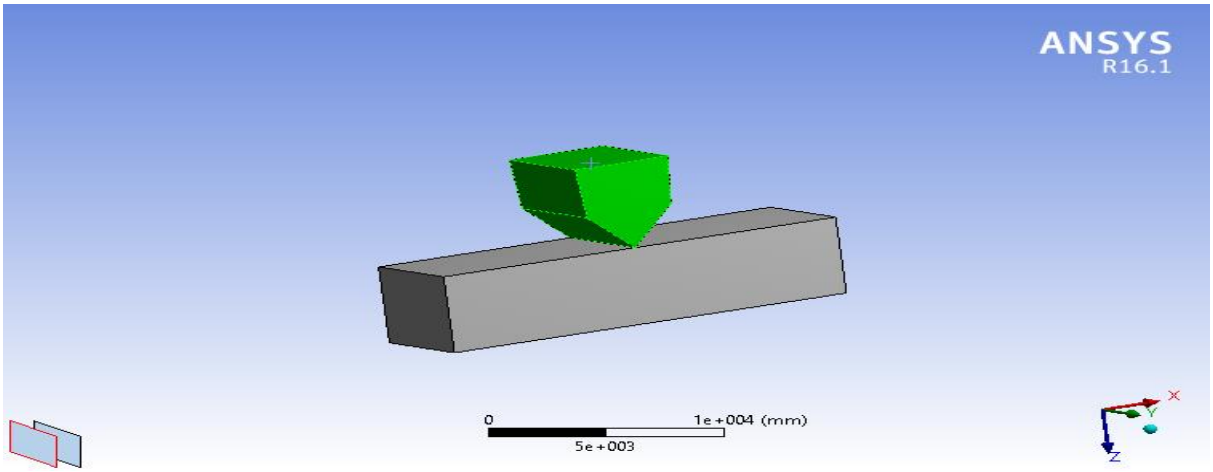
ANSYS
R16.1
0
1e+004 (mm)
5e+003
X
Y
Z

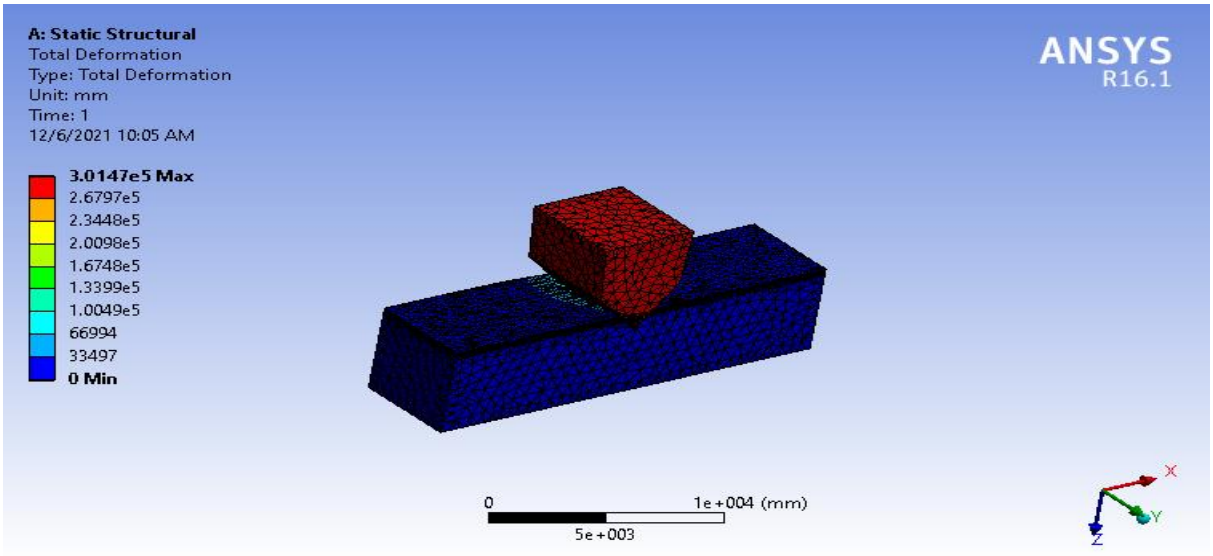
A: Static Structural
Total Deformation
Type: Total Deformation
Unit: mm
Time: 1
12/6/2021 10:05 AM
3.0147e5 Max
2.6797e5
2.3448e5
2.0098e5
1.6748e5
1.3399e5
1.0049e5
66994
33497
0 Min
ANSYS
R16.1
0
1e+004 (mm)
5e+003
X
Y
Z

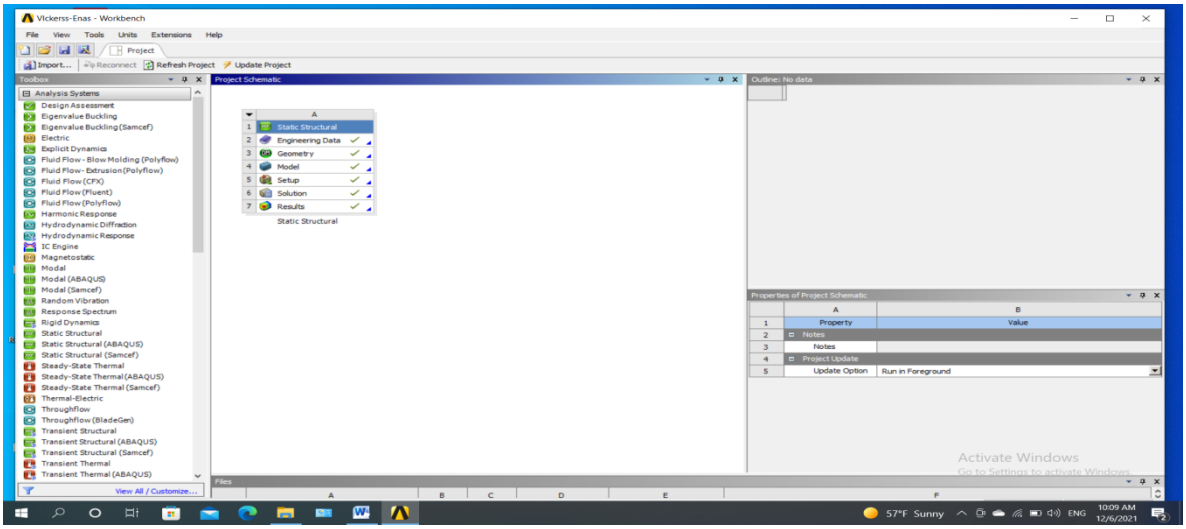
Vickerss-Enas - Workbench
File
View
Tools
Units
Extensions
Help
Project
Import...
Reconnect
Refresh Project
Update Project
Toolbox
Analysis Systems
Design Assessment
Eigenvalue Buckling
Eigenvalue Buckling (Samcef)
Electric
Explicit Dynamics
Fluid Flow - Blow Molding (Polyflow)
Fluid Flow - Extrusion (Polyflow)
Fluid Flow (CFX)
Fluid Flow (Fluent)
Fluid Flow (Polyflow)
Harmonic Response
Hydrodynamic Diffraction
Hydrodynamic Response
IC Engine
Magnetostatic
Modal
Modal (ABAQUS)
Modal (Samcef)
Random Vibration
Response Spectrum
Rigid Dynamics
Static Structural
Static Structural (ABAQUS)
Static Structural (Samcef)
Steady-State Thermal
Steady-State Thermal (ABAQUS)
Steady-State Thermal (Samcef)
Thermal-Electric
Throughflow
Throughflow (BladeGen)
Transient Structural
Transient Structural (ABAQUS)
Transient Structural (Samcef)
Transient Thermal
Transient Thermal (ABAQUS)
View All / Customize...
Project Schematic
Static Structural
Engineering Data
Geometry
Model
Setup
Solution
Results
Outline: No data
Properties of Project Schematic
Property
Value
Notes
Project Update
Update Option
Run in Foreground
Files
Activate Windows
57°F Sunny
ENG
10:09 AM
12/6/2021

Referance

[1] T. Larsen, T. L. Andersen, B. Thorning, and M. E. Vigild, "The effect of particle addition and fibrous reinforcement on epoxy-matrix composites for severe sliding conditions," *Wear*, vol. 264, no. 9–10, pp. 857–868, 2008.

[2] Y. Meng, J. Xu, Z. Jin, B. Prakash, and Y. Hu, A review of recent advances in tribology, vol. 8, no. 2. 2020.

[3] P. Dearnley, "COATINGS TRIBOLOGY," no. April, pp. 4–6, 2016, doi: 10.1179/sur.1994.10.4.264.

[4] I. Minami, "Molecular science of lubricant additives," *Appl. Sci.*, vol. 7, no. 5, p. 445, 2017.

[5] K. Friedrich, Z. Zhang, and A. K. Schlarb, "Effects of various fillers on the sliding wear of polymer composites," *Compos. Sci. Technol.*, vol. 65, no. 15–16, pp. 2329–2343, 2005.

[6] M. Turko, "Hexagonal boron nitride as a tablet lubricant and a comparison with conventional lubricants," vol. 353, pp. 45–51, 2008, doi: 10.1016/j.ijpharm.2007.11.018.

[7] A. N. Klein and C. Binder, "Development of Self-lubricating Composite Materials of Nickel with Molybdenum Disulfide , Graphite and Hexagonal Boron Nitride Processed by Powder Metallurgy : Preliminary Study Development of Self-lubricating Composite Materials of Nickel with Molybdenum," no. December 2012, 2014, doi: 10.1590/S1516-14392013005000185.

[8] E. Omrani, P. K. Rohatgi, and P. L. Menezes, *Tribology and applications of self-lubricating materials*. CRC Press, 2017.

[9] M. N. Gardos, "Self-lubricating composites for extreme environment applications," *Tribol. Int.*, vol. 15, no. 5, pp. 273–283, 1982.

[10] R. L. Fusaro, "Self-lubricating polymer composites and polymer transfer film lubrication for space applications," *Tribol. Int.*, vol. 23, no. 2, pp. 105–122, 1990.

[11] B. Bhushan, *Modern tribology handbook, two volume set*. CRC press, 2000.

[12] L. C. Seabra and A. M. Baptista, "Tribological behaviour of food grade polymers against stainless steel in dry sliding and with sugar," *Wear*, vol. 253, no. 3–4, pp. 394–402, 2002.

[13] D. L. Burris and W. G. Sawyer, "A low friction and ultra low wear rate PEEK/PTFE composite," *Wear*, vol. 261, no. 3–4, pp. 410–418, 2006.

[14] D. L. Burris and W. G. Sawyer, "Improved wear resistance in alumina-PTFE nanocomposites with irregular shaped nanoparticles," *Wear*, vol. 260, no. 7–8, pp. 915–918, 2006.

[15] N. L. McCook, B. Boesl, D. L. Burris, and W. G. Sawyer, "Epoxy, ZnO, and PTFE nanocomposite: friction and wear optimization," *Tribol. Lett.*, vol. 22, no. 3, pp. 253–257,

2006.

[16] J. Fox, “Analysis of Polymer Additives in the Packaging Industry,” *Packag. Sci.*, p. 3, 2008, [Online]. Available: https://www.iopp.org/files/public/FoxFloridaAdditives.pdf.

[17] T. M. Paulus, V. F. Medina, T. J. Keyser, B. T. Rundgren, M. K. Hess, and J. J. Sills, “Mechanical Equipment Lubrication,” no. March, 2018.

[18] C. Cusano and H. E. Sliney, “Dynamics of solid dispersions in oil during the lubrication of point contacts, Part I—Graphite,” *Asle Trans.*, vol. 25, no. 2, pp. 183–189, 1982.

[19] W. O. Winer, “Molybdenum disulfide as a lubricant: a review of the fundamental knowledge,” *Wear*, vol. 10, no. 6, pp. 422–452, 1967.

[20] P. C. H. Mitchell, “Oil-soluble Mo-S compounds as lubricant additives,” *Wear*, vol. 100, no. 1–3, pp. 281–300, 1984.

[21] S. C. Tung and M. L. McMillan, “Automotive tribology overview of current advances and challenges for the future,” *Tribol. Int.*, vol. 37, no. 7, pp. 517–536, 2004.

[22] H. E. Sliney, “Solid lubricant materials for high temperatures—a review,” *Tribol. Int.*, vol. 15, no. 5, pp. 303–315, 1982.

[23] E. R. Booser, *CRC Handbook of Lubrication and Tribology, Volume III: Monitoring, materials, synthetic lubricants, and applications*, vol. 3. CRC Press, 1993.

[24] I. Minami, “Molecular science of lubricant additives,” *Appl. Sci.*, vol. 7, no. 5, 2017, doi: 10.3390/app7050445.

[26] R. M. Atlas and R. Bartha, “Degradation and mineralization of petroleum in sea water: Limitation by nitrogen and phosphorous,” *Biotechnol. Bioeng.*, vol. 14, no. 3, pp. 309–318, 1972, doi: 10.1002/bit.260140304.

[27] T. S. Making, “Chapter 4 Solid Surfaces,” 1996.

[28] K. Friedrich and Z. Zhang, “Engineering Tribology — Second Edition: Gwidon W. Stachowiak and Andrew W. Batchelor; Butterworth-Heinemann, 2001, pp. 744, Price $79.95, ISBN 0750673044,” *Tribol. Int.*, vol. 34, no. 10, pp. 723–724, 2001.

[29] G. Boidi, S. Krenn, and S. J. Eder, “Identification of a Material–Lubricant Pairing and Operating Conditions That Lead to the Failure of Porous Journal Bearing Systems,” *Tribol. Lett.*, vol. 68, no. 4, pp. 1–14, 2020.

[30] A. Thesis, “Rheological measurements and coreflood data analysis in support of chemical enhanced oil recovery,” no. August, 2017.

[31] S. V. Dhanapal and P. Nanthagopalan, “Investigations on the Influence of Binders toward Rheological Behavior of Cementitious Pastes,” *J. Mater. Civ. Eng.*, vol. 32, no. 3, p. 4019374, 2020.

[32] Y. B. Liu, S. C. Lim, S. Ray, and P. K. Rohatgi, “Friction and wear of aluminium-graphite composites: the smearing process of graphite during sliding,” *Wear*, vol. 159, no. 2, pp. 201–205, 1992, doi: 10.1016/0043-1648(92)90303-P.

[33] P. K. Rohatgi, S. Ray, and Y. Liu, “Tribological properties of metal matrix-graphite particle composites,” *Int. Mater. Rev.*, vol. 37, no. 1, pp. 129–152, 1992, doi: 10.1179/imr.1992.37.1.129.

[34] I. V Kragelsky, “Friction and wear,” *Mashinostroenie, Moscow*, p. 480, 1968.

[35] K. Bhunia, S. S. Sablani, J. Tang, and B. Rasco, “Migration of Chemical Compounds from Packaging Polymers during Microwave , Conventional Heat Treatment , and Storage,” vol. 12, 2013, doi: 10.1111/1541-4337.12028.

[36] A. Spector, “The present application claims the benefit of United States Patent Application,” vol. 2009, no. April, 2009.

[37] G. Wypych, *Release , and Slip Additives*. 2005.

[38] H. Yuan, Q. Hao, R. Su, W. Qi, and Z. He, “Migration of phthalates from polyvinyl chloride film to fatty food simulants: Experimental studies and model application,” *J. Consum. Prot. Food Saf.*, vol. 15, no. 2, pp. 135–143, 2020.

[39] M. Bahiraei, “Particle migration in nanofluids: a critical review,” *Int. J. Therm. Sci.*, vol. 109, pp. 90–113, 2016.

[40] “j 37 4,” pp. 37–47, 2011.

[41] T. W. Scharf and S. V Prasad, “Solid lubricants: a review,” *J. Mater. Sci.*, vol. 48, no. 2, pp. 511–531, 2013.

[42] A. M. Bakry *et al.*, “Microencapsulation of oils: A comprehensive review of benefits, techniques, and applications,” *Compr. Rev. food Sci. food Saf.*, vol. 15, no. 1, pp. 143–182, 2016.

[43] L. Nordstierna, A. A. Abdalla, M. Nordin, and M. Nydén, “Comparison of release behaviour from microcapsules and microspheres,” *Prog. Org. Coatings*, vol. 69, no. 1, pp. 49–51, 2010.

[44] W. Li, C. Kumara, H. M. Meyer III, H. Luo, and J. Qu, “Compatibility between various ionic liquids and an organic friction modifier as lubricant additives,” *Langmuir*, vol. 34, no. 36, pp. 10711–10720, 2018.

[45] Q. Yu *et al.*, “Task-Specific Oil-Miscible Ionic Liquids Lubricate Steel/Light Metal Alloy: A Tribochemistry Study,” *Adv. Mater. Interfaces*, vol. 5, no. 19, p. 1800791, 2018.

[46] G. Huang, Q. Yu, Z. Ma, M. Cai, F. Zhou, and W. Liu, “Oil-soluble ionic liquids as antiwear and extreme pressure additives in poly-α-olefin for steel/steel contacts,” *Friction*, vol. 7, no. 1, pp. 18–31, 2019.

[47] M. Dašić, I. Stanković, and K. Gkagkas, “Influence of confinement on flow and lubrication properties of a salt model ionic liquid investigated with molecular dynamics,” *Eur. Phys. J. E*, vol. 41, no. 11, pp. 1–12, 2018.

[48] Z.-W. Guo, C.-Q. Yuan, X.-Q. Bai, and X.-P. Yan, “Experimental study on wear performance and oil film characteristics of surface textured cylinder liner in marine diesel engine,” *Chinese J. Mech. Eng.*, vol. 31, no. 1, pp. 1–10, 2018.

[49] F. J. Kolb and E. M. Weigel, “Lubrication of Motion-Picture Film: A Tutorial Paper,” J. SMPTE, vol. 74, no. 4, pp. 297–307, 1965.

[50] S. Naderizadeh *et al.*, “Superhydrophobic Coatings from Beeswax-in-Water Emulsions with Latent Heat Storage Capability,” *Adv. Mater. Interfaces*, vol. 6, no. 5, p. 1801782, 2019.

[51] V. N. Bakunin, A. Y. Suslov, G. N. Kuzmina, O. P. Parenago, and A. V Topchiev, “Synthesis and application of inorganic nanoparticles as lubricant components–a review,” *J. Nanoparticle Res.*, vol. 6, no. 2, pp. 273–284, 2004.

[52] V. S. Jatti and T. P. Singh, “Copper oxide nano-particles as friction-reduction and anti-wear additives in lubricating oil †,” vol. 29, no. 2, pp. 793–798, 2015, doi: 10.1007/s12206-015-0141-y.

[53] M. Z. Baykara, M. R. Vazirisereshk, and A. Martini, “Emerging superlubricity: A review of the state of the art and perspectives on future research,” *Appl. Phys. Rev.*, vol. 5, no. 4, p. 41102, 2018.

[54] L. Liu *et al.*, “Recent advances in friction and lubrication of graphene and other 2D materials: Mechanisms and applications,” *Friction*, vol. 7, no. 3, pp. 199–216, 2019, doi: 10.1007/s40544-019-0268-4.

[55] T. Onodera *et al.*, “Effect of tribochemical reaction on transfer-film formation by poly (tetrafluoroethylene),” *J. Phys. Chem. C*, vol. 118, no. 22, pp. 11820–11826, 2014.

[56] T. Onodera *et al.*, “Chemical reaction mechanism of polytetrafluoroethylene on aluminum surface under friction condition,” *J. Phys. Chem. C*, vol. 118, no. 10, pp. 5390–5396, 2014.

[57] A. A. Pitenis, K. L. Harris, C. P. Junk, G. S. Blackman, W. G. Sawyer, and B. A. Krick, “Ultralow wear PTFE and alumina composites: it is all about tribochemistry,” *Tribol. Lett.*, vol. 57, no. 1, pp. 1–8, 2015.

[58] J. N. Panda, J. Bijwe, and R. K. Pandey, “Particulate PTFE as a super-efficient secondary solid lubricant in PAEK composites for exceptional performance in adhesive wear mode,” *Compos. Part C Open Access*, vol. 4, p. 100110, 2021.

[59] J. Sahu, K. Panda, B. Gupta, N. Kumar, P. A. Manojkumar, and M. Kamruddin, “Enhanced tribo-chemical properties of oxygen functionalized mechanically exfoliated hexagonal boron nitride nanolubricant additives,” *Mater. Chem. Phys.*, vol. 207, pp. 412–422, 2018.

[60] P.-R. Wu, W. Li, Y.-M. Feng, T. Ge, Z. Liu, and Z.-L. Cheng, “Fabrication and tribological properties of oil-soluble MoS2 nanosheets decorated by oleic diethanolamide borate,” *J. Alloys Compd.*, vol. 770, pp. 441–450, 2019.

[61] W. Wang, G. Xie, and J. Luo, “Black phosphorus as a new lubricant,” *Friction*, vol. 6, no. 1, pp. 116–142, 2018.

[62] J. Ran, H. Xie, X. Lai, H. Li, and X. Zeng, “Significant improvement of tribological performances of polyamide 46/polyphenylene oxide alloy by functionalized zirconium

phosphate," *Tribol. Int.*, vol. 128, pp. 204–213, 2018.

[63] H. Wang *et al.*, "Tribological behavior of NiAl-layered double hydroxide nanoplatelets as oil-based lubricant additives," *ACS Appl. Mater. Interfaces*, vol. 9, no. 36, pp. 30891–30899, 2017.

[64] P. Bai, S. Li, D. Tao, W. Jia, Y. Meng, and Y. Tian, "Tribological properties of liquid-metal galinstan as novel additive in lithium grease," *Tribol. Int.*, vol. 128, pp. 181–189, 2018.

[65] W. Shang *et al.*, "Tuning of the hydrophilicity and hydrophobicity of nitrogen doped carbon dots: A facile approach towards high efficient lubricant nanoadditives," *J. Mol. Liq.*, vol. 266, pp. 65–74, 2018.

[66] K. Gao, Q. Chang, B. Wang, N. Zhou, and T. Qing, "The purification and tribological property of the synthetic magnesium silicate hydroxide modified by oleic acid," *Lubr. Sci.*, vol. 30, no. 7, pp. 377–385, 2018.

[67] W. Xia *et al.*, "Effects of oil-in-water based nanolubricant containing TiO2 nanoparticles in hot rolling of 304 stainless steel," *J. Mater. Process. Technol.*, vol. 262, pp. 149–156, 2018.

[68] Y. Meng, F. Su, and Y. Chen, "Nickel/multi-walled carbon nanotube nanocomposite synthesized in supercritical fluid as efficient lubricant additive for mineral oil," *Tribol. Lett.*, vol. 66, no. 4, pp. 1–11, 2018.

[69] P. K. Kannan, D. J. Late, H. Morgan, and C. S. Rout, "Recent developments in 2D layered inorganic nanomaterials for sensing," *Nanoscale*, vol. 7, no. 32, pp. 13293–13312, 2015.

[70] M. R. M. Jamir, M. S. A. Majid, and A. Khasri, *Natural lightweight hybrid composites for aircraft structural applications*. Elsevier Ltd, 2018.

[71] W. L. Rasmussen, "Novel Carbazole Based Methacrylates, Acrylates, and Dimethacrylates to Produce High Refractive Index Polymers," pp. 28–47, 2002, [Online]. Available: http://scholar.lib.vt.edu/theses/available/etd-12202001-135708/.

[72] C. Serra, "Free Radical Polymerization," *Micro Process Eng. A Compr. Handb.*, vol. 2, pp. 197–212, 2013, doi: 10.1002/9783527631445.ch29.

[73] A. Jabbarzadeh, J. D. Atkinson, and R. I. Tanner, "Effect of the wall roughness on slip and rheological properties of hexadecane in molecular dynamics simulation of Couette shear flow between two sinusoidal walls," *Phys. Rev. E - Stat. Physics, Plasmas, Fluids, Relat. Interdiscip. Top.*, vol. 61, no. 1, pp. 690–699, 2000, doi: 10.1103/PhysRevE.61.690.

[74] U. S. Tewari, S. K. Sharma, and P. Vasudevan, *Polymer tribology*, vol. C29, no. 1. 1989.

[75] P. Dašić, F. Franek, E. Assenova, and M. Radovanović, "logInternational standardization and organizations in the field of triboy," *Ind. Lubr. Tribol.*, 2003.

[76] A. Dasari, Z.-Z. Yu, and Y.-W. Mai, "Fundamental aspects and recent progress on wear/scratch damage in polymer nanocomposites," *Mater. Sci. Eng. R Reports*, vol. 63, no. 2, pp. 31–80, 2009.

[77] M. S. Lee and N. J. Jo, “Coating of methyltriethoxysilane—modified colloidal silica on polymer substrates for abrasion resistance,” *J. Sol-Gel Sci. Technol.*, vol. 24, no. 2, pp. 175–180, 2002.

[78] X. Dangsheng, “Friction and wear properties of UHMWPE composites reinforced with carbon fiber,” *Mater. Lett.*, vol. 59, no. 2–3, pp. 175–179, 2005.

[79] N. P. Suh and D. Tabor, “Tribophysics,” 1987.

[80] S. Jahanmir, N. P. Suh, and E. P. Abrahamson Ii, “The delamination theory of wear and the wear of a composite surface,” *Wear*, vol. 32, no. 1, pp. 33–49, 1975.

[81] J. van Kuilenburg, “A mechanistic approach to tactile friction.” Citeseer, 2013.

[82] H. A. Badr, “Experimental Study and Finite Element Modeling for the Flexural Behavior of Self-Compacting Reinforced Concrete T-Beams Strengthened with Carbon Fiber Reinforced Polymer,” 2012.

[83] K. Januchta and M. M. Smedskjaer, “Indentation deformation in oxide glasses: Quantification, structural changes, and relation to cracking,” *J. Non-Crystalline Solids X*, vol. 1, p. 100007, 2019.

[84] E. P. Abrahamson, S. Jahanmir, and N. P. Suh, “The effect of surface finish on the wear of sliding surfaces,” *Ann. CIRP*, vol. 24, pp. 513–514, 1975.

[85] C. Kowandy, C. Richard, and Y. M. Chen, “Characterization of wear particles for comprehension of wear mechanisms: Case of PTFE against cast iron,” *Wear*, vol. 265, no. 11–12, pp. 1714–1719, 2008.

[86] Y. Yamaguchi, *Tribology of plastic materials: their characteristics and applications to sliding components*, vol. 16. Elsevier, 1990.

[87] V. A. Smurugov, A. I. Senatrev, V. G. Savkin, V. V Biran, and A. I. Sviridyonok, “On PTFE transfer and thermoactivation mechanism of wear,” *Wear*, vol. 158, no. 1–2, pp. 61–69, 1992.

[88] S. Bahadur, D. Gong, and J. W. Anderegg, “The investigation of the action of fillers by XPS studies of the transfer films of PEEK and its composites containing CuS and CuF2,” *Wear*, vol. 160, no. 1, pp. 131–138, 1993.

[89] S. Bahadur and D. Gong, “The role of copper compounds as fillers in the transfer and wear behavior of polyetheretherketone,” *Wear*, vol. 154, no. 1, pp. 151–165, 1992.

[90] D. Tabor, “Friction-The Present State of Our,” vol. 1031169, no. April, 1981.

[91] F. P. Bowden, F. P. Bowden, and D. Tabor, *The friction and lubrication of solids*, vol. 1. Oxford university press, 2001.

[92] G. Crosa and I. J. R. Baumvol, *Tribology of Polymer Composites Used as Frictional Materials*, 1st ed., vol. 8. Elsevier Science Publishers B.V., 1993.

[93] K. Friedrich, Z. Lu, and A. M. Hager, “Recent advances in polymer composites’ tribology,” *Wear*, vol. 190, no. 2, pp. 139–144, 1995.

[94] A. S. M. HANDBOOK, “ASM Metals Handbook, Vol. 18,” *Frict. Lubr. wear Technol.*, 1992.

[95] A. Zmitrowicz, “Wear patterns and laws of wear–a review,” *J. Theor. Appl. Mech.*, vol. 44, no. 2, pp. 219–253, 2006.

[96] H. A. Ameen, K. S. Hassan, E. M. M. Mubarak, H. A. Ameen, K. S. Hassan, and E. M. M. Mubarak, “Effect of loads, sliding speeds and times on the wear rate for different materials,” *Am. J. Sci. Ind. Res.*, vol. 2, no. 1, pp. 99–106, 2011.

[97] K. Liu, H. Yan, P. Zhang, J. Zhao, Z. Yu, and Q. Lu, “Wear Behaviors of TiN/WS2+ hBN/NiCrBSi Self-Lubricating Composite Coatings on TC4 Alloy by Laser Cladding,” *Coatings*, vol. 10, no. 8, p. 747, 2020.

[98] S. Lafaye, C. Gauthier, and R. Schirrer, “Analysis of the apparent friction of polymeric surfaces,” *J. Mater. Sci.*, vol. 41, no. 19, pp. 6441–6452, 2006.

[99] C. Gauthier, S. Lafaye, and R. Schirrer, “Elastic recovery of a scratch in a polymeric surface: experiments and analysis,” *Tribol. Int.*, vol. 34, no. 7, pp. 469–479, 2001.

[100] C. Xiang, H. Sue, J. Chu, and B. Coleman, “Scratch behavior and material property relationship in polymers,” *Scratch Behav. Mater. Prop. Relatsh. Polym. J. Polym. Sci. Part B*, vol. 39, no. 1, pp. 47–59, 2001.

[101] B. J. Briscoe, P. D. Evans, E. Pellilo, and S. K. Sinha, “Scratching maps for polymers,” *Wear*, vol. 200, no. 1–2, pp. 137–147, 1996.

[102] A. M. S. Hamouda, “The influence of humidity on the deformation and fracture behaviour of PMMA,” *J. Mater. Process. Technol.*, vol. 124, no. 1–2, pp. 238–243, 2002.

[103] C. Gauthier and R. Schirrer, “Time and temperature dependence of the scratch properties of poly (methylmethacrylate) surfaces,” *J. Mater. Sci.*, vol. 35, no. 9, pp. 2121–2130, 2000.

[104] S. K. Sinha and D. B. J. Lim, “Effects of normal load on single-pass scratching of polymer surfaces,” *Wear*, vol. 260, no. 7–8, pp. 751–765, 2006.

[105] V. Jardret and P. Morel, “Viscoelastic effects on the scratch resistance of polymers: relationship between mechanical properties and scratch properties at various temperatures,” *Prog. Org. coatings*, vol. 48, no. 2–4, pp. 322–331, 2003.

[106] S. Kitova, M. Minchev, and G. Danev, “Soft plasma treatment of polymer surfaces,” *J. Optoelectron. Adv. Mater.*, vol. 7, no. 1, pp. 249–252, 2005.

[107] V. Jardret, H. Zahouani, J.-L. Loubet, and T. G. Mathia, “Understanding and quantification of elastic and plastic deformation during a scratch test,” *Wear*, vol. 218, no. 1, pp. 8–14, 1998.

[108] B. J. Briscoe and S. K. Sinha, “Scratch resistance and localised damage characteristics of polymer surfaces–a review,” *Mater. und Werkstofftechnik Entwicklung, Fert. Prüfung, Eig. und Anwendungen Tech. Werkstoffe*, vol. 34, no. 10-11, pp. 989–1002, 2003.

[109] G. Subhash and W. Zhang, “Investigation of the overall friction coefficient in single-pass

scratch test," *Wear*, vol. 252, no. 1–2, pp. 123–134, 2002.

[110] S. Lafaye, C. Gauthier, and R. Schirrer, "A surface flow line model of a scratching tip: apparent and true local friction coefficients," *Tribol. Int.*, vol. 38, no. 2, pp. 113–127, 2005.

[111] C. Gauthier, A.-L. Durier, C. Fond, and R. Schirrer, "Scratching of a coated polymer and mechanical analysis of a scratch resistance solution," *Tribol. Int.*, vol. 39, no. 2, pp. 88–98, 2006.

[112] M. P. Scott, M. Rahman, and C. S. Brazel, "Application of ionic liquids as low-volatility plasticizers for PMMA," *Eur. Polym. J.*, vol. 39, no. 10, pp. 1947–1953, 2003.

[113] J. M. PigŁowski and M. Bryjak, "Surface studies of poly (methyl methacrylate)/poly (styrene-co-acrylonitrile) blends," *Eur. Polym. J.*, vol. 34, no. 11, pp. 1669–1673, 1998.

[114] G. Bracco and B. Holst, *Surface science techniques*, vol. 51, no. 1. 2013.

[115] B. Doshi, M. Sillanpää, and S. Kalliola, "A review of bio-based materials for oil spill treatment," *Water Res.*, vol. 135, pp. 262–277, 2018.

[116] D. ASTM, "3835–Standard Test Method for Determination of Properties of Polymeric Materials by Means of a Capillary Rheometer," *ASTM, West Conshohocken, PA*, 1996.

[117] N. Zhang, *Characterization of micro injection moulding process for replication of micro/nano features and micro components*. University College Dublin (Ireland), 2013.

[118] Z. Tadmor and C. G. Gogos, *Principles of polymer processing*. John Wiley & Sons, 2013.

[119] L. J. Muntz, "Rheometer Market Analysis." WORCESTER POLYTECHNIC INSTITUTE, 2017.

[120] E. B. Bagley, "End corrections in the capillary flow of polyethylene," *J. Appl. Phys.*, vol. 28, no. 5, pp. 624–627, 1957.

[121] The Polymer Technology Group, "Capillary Rheometer," 2007, [Online]. Available: http://www.polymertechnology.it/bacheca/fluid/Esercitazione081105b.pdf.

[122] F. N. Cogswell, "Converging flow of polymer melts in extrusion dies," *Polym. Eng. Sci.*, vol. 12, no. 1, pp. 64–73, 1972.

[123] G. Schramm, A practical approach to rheology and rheometry. Haake Karlsruhe, 1994.

[124] N. J. Hadi, MSc. Abd Alhussein, and T. L. Rydzkowski, "EXPERIMENTAL AND NUMERICAL SIMULATUON OF NON-NEWTONIAN IN CAPILLARY RHEOMETER." Journal of Engineering Science and Technology Review, Material A 2019 (1); 64-87 Orginal Article

[125] D. G. Thomas, "Significant Aspects of Non-Newtonian Technology," *Prog. Int. Res. Thermodyn. Transp. Prop.*, pp. 669–686, 1962.

[126] R. Alfani, N. Grizzuti, G. L. Guerrini, and G. Lezzi, "The use of the capillary rheometer for the rheological evaluation of extrudable cement-based materials," *Rheol. Acta*, vol. 46, no. 5, pp. 703–709, 2007, doi: 10.1007/s00397-007-0164-0.

[127] F. T. Trouton, “On the coefficient of viscous traction and its relation to that of viscosity,” *Proc. R. Soc. London. Ser. A, Contain. Pap. a Math. Phys. Character*, vol. 77, no. 519, pp. 426–440, 1906.

[128] A. Standard, “D445: standard test method for kinematic viscosity of transparent and opaque liquids (and calculation of dynamic viscosity),” *Am. Soc. Test. Mater. West Conshohocken, PA*, 2006.

[129] R. B. Bird, “Rheology and kinetic theory of polymeric liquids,” *Annu. Rev. Phys. Chem.*, vol. 28, no. 1, pp. 185–206, 1977.

[130] J. R. Fried, *Polymer science and technology*. Pearson Education, 2014.

[131] G. Barra, “PhD thesis The rheology of caramel By Giuseppina Barra Thesis submitted to the University of Nottingham for the degree of Doctor of Philosophy February 2004 Division of Food Sciences University of Nottingham,” no. June, 2014.

[132] D. Kay, P. J. Carreau, P. G. Lafleur, L. Robert, and B. Vergnes, “A study of the stick-slip phenomenon in single-screw extrusion of linear polyethylene,” *Polym. Eng. Sci.*, vol. 43, no. 1, pp. 78–90, 2003.

[133] H. P. Schreiber, E. B. Bagley, and A. M. Birks, “Filament distortion and die entry angle effects in polyethylene extrusion,” *J. Appl. Polym. Sci.*, vol. 4, no. 12, pp. 362–363, 1960.

[134] P. U. Manual, “ver. 3.10, Fluent Inc,” *Centerra Resour. Park*, vol. 10.

[135] B. Vergnes, “Extrusion defects and flow instabilities of molten polymers,” *Int. Polym. Process.*, vol. 30, no. 1, pp. 3–28, 2015.

[136] R. Ahmed, R. F. Liang, and M. R. Mackley, “The experimental observation and numerical prediction of planar entry flow and die swell for molten polyethylenes,” *J. Nonnewton. Fluid Mech.*, vol. 59, no. 2–3, pp. 129–153, 1995.

[137] K. Choi, S. Min, and K. Yeon, “Setting Shrinkage Characteristics of Methyl Methacrylate-Modified Vinyl Ester Polymer Concrete,” 2016, doi: 10.3844/ajassp.2016.586.592.

[138] H. Klenk, P. H. Gotz, R. Siegmeier, and W. Mayr, “Peroxy compounds, organic. Ullmann’s encyclopedia of industrial chemistry.” Wiley-VCH, Weinheim, 2000.

[139] M. Šupová, G. S. Martynková, and K. Barabaszová, “Effect of Nanofillers Dispersion in Polymer Matrices : A Review Effect of Nanofillers Dispersion in Polymer Matrices : A Review,” no. February 2014, 2011, doi: 10.1166/sam.2011.1136.

[140] K. Mögenburg, “Konservering av Irma Salo Jægers nonfigurative maleri’SIRR’fra 1963-Med fokus på kunstnerintervju og behandling av ufernissert malerioverflate.” 2020.

[141] S. Bogdanov and B. P. Science, “Beeswax: Production, Properties, Composition, Control,” no. June, 2016.

[142] E. Summary, “Calcium Stearate,” vol. 2119, no. m, pp. 1–11.

[143] L. Ren, T. Wang, Z. Chen, Y. Li, and L. Qian, “Self-lubricating PEO–PTFE composite coating on titanium,” *Metals (Basel).*, vol. 9, no. 2, pp. 1–11, 2019, doi:

10.3390/met9020170.

[144] K. D. Behler, A. Stravato, V. Mochalin, G. Korneva, G. Yushin, and Y. Gogotsi, "Nanodiamond-polymer composite fibers and coatings," *ACS Nano*, vol. 3, no. 2, pp. 363–369, 2009, doi: 10.1021/nn800445z.

[145] K. Ishihara, "Highly lubricated polymer interfaces for advanced artificial hip joints through biomimetic design," *Polym. J.*, vol. 47, no. 9, pp. 585–597, 2015, doi: 10.1038/pj.2015.45.

[146] T. Murakami *et al.*, "Evaluation of a superior lubrication mechanism with biphasic hydrogels for artificial cartilage," *Tribol. Int.*, vol. 89, pp. 19–26, 2015, doi: 10.1016/j.triboint.2014.12.013.

[147] M. Liu, X. Zhang, J. Zhang, Q. Zheng, and B. Liu, "Study on Antibacterial Property of PMMA Denture Base Materials with Negative Ion Powder," *IOP Conf. Ser. Mater. Sci. Eng.*, vol. 301, no. 1, pp. 10–16, 2018, doi: 10.1088/1757-899X/301/1/012034.

[148] A. Graziano, C. Garcia, S. Jaffer, J. Tjong, and M. Sain, "Novel functional graphene and its thermodynamic interfacial localization in biphasic polyolefin systems for advanced lightweight applications," *Compos. Sci. Technol.*, vol. 188, 2020, doi: 10.1016/j.compscitech.2019.107958.

[149] K. Palanikumar, R. AshokGandhi, B. K. Raghunath, and V. Jayaseelan, "Role of calcium carbonate(CaCO3) in improving wear resistance of polypropylene(PP) components used in automobiles," *Mater. Today Proc.*, vol. 16, pp. 1363–1371, 2019, doi: 10.1016/j.matpr.2019.05.237.

[150] W. Wang, G. Xie, and J. Luo, "Superlubricity of black phosphorus as lubricant additive," *ACS Appl. Mater. Interfaces*, vol. 10, no. 49, pp. 43203–43210, 2018.

[151] N. Deep and P. Mishra, "Evaluation of mechanical properties of functionalized carbon nanotube reinforced PMMA polymer nanocomposite," *Karbala Int. J. Mod. Sci.*, vol. 4, no. 2, pp. 207–215, 2018, doi: 10.1016/j.kijoms.2018.02.001.

[152] H. Li, Y. Ma, Z. Li, Y. Cui, and H. Wang, "Synthesis of novel multilayer composite microcapsules and their application in self-lubricating polymer composites," *Compos. Sci. Technol.*, vol. 164, no. February, pp. 120–128, 2018, doi: 10.1016/j.compscitech.2018.05.042.

[153] H. Li, Y. Ma, Z. Li, J. Ji, Y. Zhu, and H. Wang, "High temperature resistant polysulfone/silica double-wall microcapsules and their application in self-lubricating polypropylene," *RSC Adv.*, vol. 7, no. 79, pp. 50328–50335, 2017, doi: 10.1039/c7ra06851d.

[154] H. Li, Y. Cui, Z. Li, Y. Zhu, and H. Wang, "Fabrication of microcapsules containing dual-functional tung oil and properties suitable for self-healing and self-lubricating coatings," *Prog. Org. Coatings*, vol. 115, no. October 2017, pp. 164–171, 2018, doi: 10.1016/j.porgcoat.2017.11.019.

[155] M. M. Rueda *et al.*, "Rheology and applications of highly filled polymers: A review of current understanding," *Prog. Polym. Sci.*, vol. 66, no. November 2017, pp. 22–53, 2017,

doi: 10.1016/j.progpolymsci.2016.12.007.

[156] R. Gunes, K. Arslan, M. K. Apalak, and J. N. Reddy, “Ballistic performance of honeycomb sandwich structures reinforced by functionally graded face plates,” *J. Sandw. Struct. Mater.*, vol. 21, no. 1, pp. 211–229, 2019, doi: 10.1177/1099636216689462.

[157] B. Shen, S. Chen, Y. Chen, and F. Sun, “Enhancement on the tribological performance of diamond films by utilizing graphene coating as a solid lubricant,” *Surf. Coatings Technol.*, vol. 311, pp. 35–45, 2017, doi: 10.1016/j.surfcoat.2016.12.094.

[158] N. Saurín, T. Espinosa, J. Sanes, F. J. Carrión, and M. D. Bermúdez, “Ionic nanofluids in tribology,” *Lubricants*, vol. 3, no. 4, pp. 650–663, 2015, doi: 10.3390/lubricants3040650.

[159] G. Styles, R. Rahmani, H. Rahnejat, and B. Fitzsimons, “In-cycle and life-time friction transience in piston ring-liner conjunction under mixed regime of lubrication,” *Int. J. Engine Res.*, vol. 15, no. 7, pp. 862–876, 2014, doi: 10.1177/1468087413519783.

[160] D. Y. Zhang, P. B. Zhang, P. Lin, G. N. Dong, and Q. F. Zeng, “Tribological properties of self-lubricating polymer-steel laminated composites,” *Tribol. Trans.*, vol. 56, no. 6, pp. 908–918, 2013, doi: 10.1080/10402004.2013.805348.

[161] N. Espallargas, L. Vitoux, and S. Armada, “The wear and lubrication performance of liquid-solid self-lubricated coatings,” *Surf. Coatings Technol.*, vol. 235, pp. 342–353, 2013, doi: 10.1016/j.surfcoat.2013.07.063.

[162] M. Mansha, C. Gauthier, P. Gerard, and R. Schirrer, “The effect of plasticization by fatty acid amides on the scratch resistance of PMMA,” *Wear*, vol. 271, no. 5–6, pp. 671–679, 2011, doi: 10.1016/j.wear.2010.12.089.

[163] R. A. Ibrahim and W. Y. Ali, “Tribological performance of polyester composites filled by vegetable oils,” *Materwiss. Werksttech.*, vol. 41, no. 5, pp. 287–292, 2010, doi: 10.1002/mawe.201000599.

[164] O. Kulikov, K. Hornung, and M. Wagner, “Low Viscous Hydrophilic Processing Additives for Extrusion of Polyethylene at Reduced Temperatures,” no. Mi, 2010, doi: 10.1002/pen.

[165] M. Sangermano and M. Messori, “Scratch resistance enhancement of polymer coatings,” *Macromol. Mater. Eng.*, vol. 295, no. 7, pp. 603–612, 2010, doi: 10.1002/mame.201000025.

[166] L. P. Sung *et al.*, “Scratch behavior of nano-alumina/polyurethane coatings,” *J. Coatings Technol. Res.*, vol. 5, no. 4, pp. 419–430, 2008, doi: 10.1007/s11998-008-9110-z.

[167] M. Stefanov, A. N. Enyashin, T. Heine, and G. Seifert, “Nanolubrication: How do MoS2-based nanostructures lubricate?,” *J. Phys. Chem. C*, vol. 112, no. 46, pp. 17764–17767, 2008, doi: 10.1021/jp808204n.

[168] Q. Cao, Q. Yu, D. W. Connell, and G. Yu, “Titania/carbon nanotube composite (TiO 2/CNT) and its application for removal of organic pollutants,” *Clean Technol. Environ. Policy*, vol. 15, no. 6, pp. 871–880, 2013.

[170] A. Standard, “Standard Practice for General techniques for Obtaining Infrared Spectra for Qualitative Analysis,” *Annu. B. ASTM Stand. E*, vol. 1252, no. 98, pp. 1–11, 2002.

[171] C. Schick, “Differential scanning calorimetry (DSC) of semicrystalline polymers,” *Anal. Bioanal. Chem.*, vol. 395, no. 6, pp. 1589–1611, 2009.

[172] A. S. for T. and Materials, *Standard test method for wear testing with a pin-on-disk apparatus*. ASTM International, 2010.

[173] S. T. Gonczy and N. Randall, “An ASTM standard for quantitative scratch adhesion testing of thin, hard ceramic coatings,” *Int. J. Appl. Ceram. Technol.*, vol. 2, no. 5, pp. 422–428, 2005.

[174] I. ASTM, “Standard test methods for flexural properties of unreinforced and reinforced plastics and electrical insulating materials,” *ASTM D790-07*, 2007.

[175] D. W. Hetzner, “Microindentation hardness testing of materials using ASTM e384,” *Microsc. Microanal.*, vol. 9, no. S02, pp. 708–709, 2003.

[176] E. Hodová, Š. Mašová, K. Rosíková, M. P. Vanhove, and I. Hodová, “Microscopic techniques in the study of African parasitic nematodes,” 2017.

[177] G. Products and C. Properties, “Standard Test Method for Hydrophobic Contamination on Glass by Contact Angle,” *Annu. B. ASTM Stand.*, vol. 90, no. Reapproved, pp. 1–3, 2004.

[178] ASTM Int., “Standard Test Method for Determination of Properties of Polymeric Materials by Means of a Capillary Rheometer,” *Annu. B. ASTM Stand.*, vol. i, no. C, pp. 1–11, 2010.

[179] M. B. Pérez-Gago and J. M. Krochta, “Lipid particle size effect on water vapor permeability and mechanical properties of whey protein/beeswax emulsion films,” *J. Agric. Food Chem.*, vol. 49, no. 2, pp. 996–1002, 2001.

[180] M. M. Shokrieh, A. Saeedi, and M. Chitsazzadeh, “Mechanical properties of multi-walled carbon nanotube/polyester nanocomposites,” *J. Nanostructure Chem.*, vol. 3, no. 1, pp. 1–5, 2013.

[181] P. Cai, T. Wang, and Q. Wang, “Effect of several solid lubricants on the mechanical and tribological properties of phenolic resin-based composites,” *Polym. Compos.*, vol. 36, no. 12, pp. 2203–2211, 2015, doi: 10.1002/pc.23132.

[182] P. Kurkcu, L. Andena, and A. Pavan, “An experimental investigation of the scratch behaviour of polymers: 1. Influence of rate-dependent bulk mechanical properties,” *Wear*, vol. 290, pp. 86–93, 2012.

[183] B. H. Stuart, “Surface plasticisation of poly (ether ether ketone) by chloroform,” *Polym. Test.*, vol. 16, no. 1, pp. 49–57, 1997.

[184] S. Jahanmir, A. Z. Hunsberger, and H. Heshmat, “Load capacity and durability of H-DLC coated hydrodynamic thrust bearings,” *J. Tribol.*, vol. 133, no. 3, 2011, doi: 10.1115/1.4003997.

[185] C. V Panin, L. A. Kornienko, T. N. Suan, L. R. Ivanova, and M. A. Poltaranin, “The effect

of adding calcium stearate on wear-resistance of ultra-high molecular weight polyethylene," *Procedia Eng.*, vol. 113, pp. 490–498, 2015.

[186] S. Chen, W. Shen, G. Wu, D. Chen, and M. Jiang, "A new approach to the functionalization of single-walled carbon nanotubes with both alkyl and carboxyl groups," *Chem. Phys. Lett.*, vol. 402, no. 4–6, pp. 312–317, 2005.

[187] S.-Y. Lee and S.-J. Park, "Hydrogen adsorption of acid-treated multi-walled carbon nanotubes at low temperature," *Bull. Korean Chem. Soc.*, vol. 31, no. 6, pp. 1596–1600, 2010.

[188] R. Yudianti, H. Onggo, Y. Saito, T. Iwata, and J. Azuma, "Analysis of functional group sited on multi-wall carbon nanotube surface," *Open Mater. Sci. J.*, vol. 5, no. 1, 2011.

Websites:

[25] **https://wiki.anton-paar.com/co-es/basics-of-tribology/**

الخلاصة:

من أجل توفير عمر تشحيم طويل، يجب التأكد من أن البوليمر الصلب أو مركب البوليمر يوفر تزييتًا ذاتيًا وفي نفس الوقت، يجب أن يوفر ضغط تلامس مناسب للواجهة، وهو العامل الأكثر أهمية مع مركبات التشحيم الذاتي بحيث يكون المركب البوليمري قادرًا على دعم الضغوط الديناميكية للحمل والضغوط المطبقة.

في هذه الدراسة تم تصنيع مركب تزييت ذاتي متعدد الميثيل ميثاكريلات (PMMA) مع مواد تشحيم صلبة وأنبوب نانو كربوني متعدد الجدران وتم اختياره كطريقة للتشحيم الذاتي. تم اختيار ستيرات الكالسيوم وشمع البولي إيثيلين وشمع العسل كمواد تشحيم صلبة لها القدرة على الانتقال إلى سطح البوليمر خلال فترة خدمتها. استخدام البلمرة في الموقع للجذور الحرة مع المعلمات التالية:

PMMA(٪wt 0.9 BPO + 100MMA٪) / مادة تشحيم صلبة (0.05 ، 0.1 ، 0.2 ، 0.5 وزناً٪) PMMA / MWCNT (0.05 ، 0.1 ، 0.2 ،0.5 وزناً% عن طريق الصوتنة) ، مركب هجين ((50٪ PMMA: 50٪ شمع عسل) (0.05 ، 0.1 ، 0.2 ، 0.5 وزن٪) + PMMA) .

تم استخدام تحويل فوريه للأشعة تحت الحمراء (FTIR) للتحقق من هوية مواد التشحيم الصلبة بعد بلمرة الجذور الحرة والجسيمات النانوية الكربونية متعددة الجدران في الموقع. فيما يتعلق بالسلوك الترايبولوجي لسطح البوليمرات المقواة بمواد تشحيم صلبة وحشو نانوي بعد اختبار التآكل ، باستخدام الفحص المجهري البصري (OM) ، يتم التحقق من التدفق باستخدام مقياس ضغط شعري (SR20) وأجري اختبار زاوية التلامس للتحقق من الفعالية من مواد التشحيم الصلبة وحشوات النانو في زيادة قابلية البوليمر المقاوم للماء. تتميز صفائح PMMA المنتجة بأشكال دائرية نسبيًا ، يبلغ متوسط قطرها 15 سم وسمكها حوالي 2 مم. أثبتت نتائج الاختبارات لكل من الاحتكاك والتآكل كفاءة أعلى تصل إلى (9.4٪) ومعامل احتكاك (0.8٪) للعينة المملوءة بشمع العسل أكثر بكثير من باقي المزلقات الصلبة مما

يؤكد انتقال الجزيئات. على السطح ويقلل من مقدار إجهاد القص البيني أثناء الاحتكاك الجاف ، وبزيادة مع مرور الوقت والأحمال المطبقة بسرعة ثابتة ، يؤثر الاحتكاك سلبًا على معدلات التآكل الكلية ويضعف الهيكل الداخلي وبالتالي الخصائص الميكانيكية. يعمل نظام التزييت الذاتي بنجاح وهذا ما تؤكده نتائج اختبار الخدش للعينات التي أظهرت سلوك التشوه للبلاستيك البوليمر النقي والتشوه المرن للبوليمر المملوء بشمع العسل وكانت النتائج متوافقة مع نتائج الاحتكاك والتآكل. كان هذا واضحًا من التأثير المتبقي بعد الخدش، والذي يتميز بمنطقة ناعمة جدًا في منطقة التلامس مع القليل من إجهاد التلامس ومرونة خدش السطح ويلعب دورًا مهمًا في تقليل إجهاد القص السطحي حتى (0.8٪). أظهرت نتائج ريوميتر التدفق الشعري للبوليمر الاساس مع مواد تشحيم صلبة وحشوات تقوية أن لزوجة القص تتناقص مع زيادة معدل القص ويزيد إجهاد القص مع زيادة معدل القص. تؤدي زيادة إجهاد القص إلى قطع السلسلة البوليمرية وتقليل اللزوجة مع زيادة درجة الحرارة، وزيادة الهجرة إلى السطح، مما ساعد على تأجيل عملية البثق وتقليل مقدار كسر الانصهار الكلي. يلعب إجهاد القص دورًا مهمًا في الإشارة إلى جودة السطح، فمن الواضح أن تحديد المنطقة الحرجة ضروري لتتمكن من تغيير جودة السطح وعلاقته بالضغط وإجهاد القص ومعدل القص.

جمهورية العراق
وزارة التعليم العالي والبحث العلمي
جامعة بابل
كلية هندسة المواد
قسم هندسة صناعات البوليمر والبتروكيماوي

تقصي الخصائص الترايبولوجية والريولوجية لمركب بوليمري ذاتي التشحيم

رسالة

مقدمة إلى كلية هندسة المواد / جامعة بابل وهي جزء من متطلبات نيل درجة الماجستير في هندسة المواد / البوليمر

من قبل الباحثة

إيناس طالب صاحب عودة

(بكالوريوس هندسة مواد / بوليمر ، 2017)

بإشراف

أ.م.د. عمار عماد الكواز

1442هـ **2021 م**